The use of fungal mycelium for the production of bio-based materials

Freek Appels

The use of fungal mycelium for the production of bio-based materials

Freek Vincentius Wilhelmus Appels

PhD thesis Utrecht University, Utrecht, NL (2020)

The research described in this report was performed within the Microbiology group of Utrecht University, Padualaan 8, 3584 CH Utrecht, The Netherlands.

Dit proefschrift werd mede mogelijk gemaakt met financiële steun van de J.E. Jurriaanse Stichting.

Printing of this thesis was financially supported by the Netherlands Society of Medical Microbiology (NVMM) and the Royal Netherlands Society for Microbiology (KNVM).

Cover design: Faranak Nourbakhsh
Printed by: ProefschrifMaken| www.proefschriftmaken.nl
ISBN: 978-94-6380-683-1

The use of fungal mycelium for the production of bio-based materials

Het gebruik van mycelium van schimmels voor de productie van biobased materialen

(met een samenvatting in het Nederlands)

Proefschrift

ter verkrijging van de graad van doctor aan de Universiteit Utrecht op gezag van de rector magnificus, prof. dr. H.R.B.M. Kummeling, ingevolge het besluit van het college voor promoties in het openbaar te verdedigen op woensdag 5 februari 2020 des middags te 4.15 uur

door

Freek Vincentius Wilhelmus Appels

geboren op 15 september 1989
te Veldhoven

Promotor: Prof. dr. H.A.B. Wösten

“*Wat je bezit is op weg naar anderen*”

Jan Verhallen

Contents

Chapter 1	General introduction	1
Chapter 2	Fabrication factors influencing mechanical, moisture- and water-related properties of mycelium-based composites	17
Chapter 3	Growth assessment and mechanical analysis of mycelium-based materials of nine mushroom forming fungi	37
Chapter 4	Hydrophobin gene deletion and environmental growth conditions impact mechanical properties of mycelium by affecting the density of the material	49
Chapter 5	Mechanical properties of pure mycelium materials resulting from *Schizophyllum commune* liquid shaken cultures	63
Chapter 6	Characterization of the cell wall of a mushroom forming fungus at atomic resolution using solid-state NMR	77
Chapter 7	Summary and General discussion	101
	References	113
	Nederlandse samenvatting	127
	Curriculum vitae	132
	List of publications	135
	Acknowledgements	137

Chapter 1

General introduction

Appels, F. V. W., Salueña Martín, J. & Wösten, H. A. B.

A non-sustainable economy

Resource management in current socio-economic systems is often based on a “take-produce-consume-discard” model. This model assumes abundance of resources and unlimited waste disposal with no negative side effects (Jurgilevich et al., 2016). However, natural resource consumption is higher than its regeneration rate and discharged waste streams outpace the remediation capacity of ecosystems. Environmental consequences of this extractive model are resource depletion and waste accumulation in the biosphere leading to environmental problems such as climate change and desertification (Watson et al., 2016). Due to the intrinsic unsustainability of linear industrial processes, it is imperative to look for alternatives.

Biomimicry is an important strategy in the transition towards a sustainable economy. This strategy is inspired by biological forms, processes and systems in order to solve human challenges (Kennedy and Marting, 2016). As Earth can be considered a closed system, resource management in nature largely depends on cyclic processes. Achieving a sustainable industrial system asks for the implementation of such cyclic processes (Greyson, 2007). A circular economy is a restorative system where resources are processed in cycles, either by society or by biogeochemical processes (Greyson, 2007). It mirrors natural principles such as production from waste, resilience through diversity and use of renewable energy sources. Circular economy focuses on closing the loop of materials and reducing resource consumption and waste entering the environment. This is achieved by reusing, repairing, refurbishing and recycling existing materials and products (Jurgilevich et al., 2016). This changes the concept of *waste*; used products become resources for the biocycle or the technocycle (Nemethy & Kőmíves, 2016). China is an example of a large economy starting to implement circularity by putting specific circularity indicators on the public agenda (Geng, Fu, Sarkis, & Xue, 2012). Reliable indicators for circularity that have been developed target aspects such as resource conservation and waste production. Plastic accumulation is a clear example of a waste problem resulting from our extractive economy. Therefore, the life cycle of plastics is such a circularity indicator (Huysman, de Schaepmeester, Ragaert, Dewulf, & de Meester, 2017).

The plastic revolution

Commercial development of plastics started in the 1940's and has led to great societal impact. Life standards improved greatly due to the wide applicability of these versatile polymers and gave rise to the term 'plastic age' (Thompson, Swan, Moore, & Vom Saal, 2009). The use of plastics was a driver of innovation in various industries like electronics, healthcare, construction and packaging. This versatile and inexpensive material rendered products that are resistant to corrosion, are water-impermeable and can be used for instance to insulate electrical conductors (Thompson, Moore, Saal, & Swan, 2009).

Despite the numerous benefits provided by plastics, their environmental impact is large. In 2015 alone, 380 million metric tons of plastics were produced worldwide (Geyer, Jambeck, & Law, 2017). Production of plastics is energy-consuming and large volumes of greenhouse gasses are emitted. Moreover, this petro-based material causes economic dependence on use of fossil fuels. In total, 8% of global crude oil is used for the production of plastics, thereby competing for feedstock for energy production (Harding, Dennis, von Blottnitz, & Harrison, 2007). Plastics are mainly used to produce disposables with a life span of less than a year. It is estimated that 42% of the plastics produced in 2015 was used as packaging, while 54% of total plastic waste that year originated from packaging (Geyer et al., 2017). From these disposed plastics, less than one-third is recycled. This is partly caused by the mixing of different polymers that hampers separation and purification of plastic waste (Hopewell, Dvorak, & Kosior, 2009). Most plastics end in landfills where they accumulate or from which they disperse into nature. This plastic waste fragments by sunlight with a rate depending on environmental conditions such as humidity, temperature, light and oxygen availability (Albertsson & Hakkarainen, 2017). The resulting microplastics affect wildlife and human health (Geyer et al., 2017; Hermabessiere et al., 2017; Revel, Châtel, & Mouneyrac, 2018).

Oil-based plastics are only one example of materials that have a negative footprint. Other industries that have proven to be unsustainable are the textile and building industry. The textile industry uses up to 200 liters of water per kg fabric and causes major pollutions as a result of dyeing practices (Parisi, Fatarella, Spinelli, Pogni, & Basosi, 2015). On the other hand, the building industry consumes vast amounts of

energy. Consumption of energy is estimated up to 40% of total energy consumption in the EU and is responsible for up to 50% of total greenhouse gas emissions (Asif, Muneer, & Kelley, 2007; Zabalza Bribián, Aranda Usón, & Scarpellini, 2009).

Circular economy

Two important factors in circular production of materials are renewable feedstocks and biodegradability. Renewable feedstocks refer to raw materials that are being extracted from nature and are replenishable, such as biomass used for producing biofuels (Melero, Iglesias, & Garcia, 2012). Biodegradability refers to the capability of being degraded by biological activity (Vert et al., 2012). The relation between bio-based, biodegradable and sustainability is complex. Bio-based materials are materials that are synthesized by living organisms like plants, fungi and bacteria. Therefore, renewability is guaranteed. Bio-based is not per definition sustainable. For instance, current production of palm oil or usage of tropical hardwood as feedstock is bio-based but not sustainable. There not per definition a relation between bio-based and biodegradability. Biodegradability of bio-plastics refers to, according to the American Society for Testing and Materials (ASTM) standards, the possibility "*to degrade by the action of naturally occurring microorganisms such as bacteria, fungi, and algae*" whereas compostability of bio-plastics refers to "*a bio-plastic that undergoes degradation by biological processes during composting to yield carbon dioxide, water, inorganic compounds, and biomass at a rate consistent with other known compostable materials leaving no visually distinguishable or toxic residues."* (Kale, Auras, Singh, & Narayan, 2007; Song, Murphy, Narayan, & Davies, 2009).

There is an inituitive believe that materials produced from bio-based feedstocks are biodegradable (Garrison et al., 2016). This is however not an origin-dependent property but relies on the chemical composition of the material and the metabolic capacity of the environment (Song et al., 2009). Examples of bio-based and biodegradable materials are polylactic acid (PLA) and polyhydroxyalkanoates (PHA), whereas non-biodegradable bio-based polymers are bio-polyethylene (bio-PE) and bio-poly(ethylene terephthalate)(bio-PET) (Iwata, 2015). For these reasons, biodegradability of bio-based materials needs to be regarded as an important factor when using renewable resources as feedstock.

Bio-based materials are applied in an increasing range of applications (Álvarez-Chávez, Edwards, Moure-Eraso, & Geiser, 2012). They may result from the use of the whole organism (e.g. wood) or from extraction and/or purification of its components (e.g. starch). The latter strategy is also used in the production of bioplastics. Examples are PLA and PHA that are studied for use as water-resistant coatings and food packaging purposes (Arrieta, Fortunati, Dominici, López, & Kenny, 2015) and for use in the pharmaceutical and food industry (Chen, 2010), respectively. These bioplastics result from bacterial fermentation of agricultural products (Tokiwa et al., 2009). Apart from bacteria-derived bioplastics there are plant-based bioplastics that can be composed of e.g. cellulosic- or starch-based polymers (Mohanty, Misra, & Drzal, 2002). Another resource for bio-based polymeric materials may be fungal mycelium. So far, the whole organism is used to produce materials (see below).

The fungal kingdom

Fungi are ubiquitous microorganisms that play an important role in nature and for mankind (Baxi et al., 2016). The fungal kingdom is diverse with 120.000 identified species and an estimated total number of up to 3.8 million species (Hawksworth & Lücking, 2017). The two major phyla are the Ascomycota and Basidiomycota. Most yeast- and mold-like fungi are ascomycetes, while most mushroom forming fungi belong to the Basidiomycota. Fungi need organic compounds for their energy and carbon source. To this end, they degrade dead organic matter or establish a pathogenic, neutral or mutual beneficial symbiosis with plants, animals or other microbes. For instance, part of the mushroom forming fungi feed on plant or animal waste, while others establish pathogenic or mutual beneficial interactions such as mycorrhizal interactions.

Besides the role of fungi in biogeochemical cycles, they have a major economic and societal relevance. Ascomycetes and basidiomycetes are used for the production of food, pharmaceuticals, enzymes, chemicals and energy (Berends, Scholtmeijer, Wösten, Bosch, & Lugones, 2009; Grimm & Wösten, 2018; Jansen et al., 2017; Johnson, 2013; Kothe, 2001; Kues & Liu, 2000; Sarrouh, 2012). On the other hand, fungi cause severe infections especially in patients with a compromised immune system. Over 300 million people have been estimated to suffer from serious fungal-related diseases with *Candida*, *Aspergillus*, *Pneumocystis* and *Cryptococcus*

collectively killing over 1.6 million people annually (“Stop neglecting fungi,” 2017). Besides causing human diseases, fungi infect all major crops (e.g. corn, wheat and rice) and cause major postharvest losses of food (Oerke, 2006).

The fungal kingdom encompasses unicellular and multicellular forms. The unicellular forms are known as yeasts. They multiply by budding or by fission. Multicellular fungi colonize substrates by means of filaments. These mm- to cm-long hyphae have generally a width between 1-10 µm. By growing at their tips and branching subapically, a 3D network of hyphae is formed. The diameter of such a mycelium can vary in size ranging from millimeter to kilometer dimensions. Representatives of the fungal kingdom are able to degrade lignocellulose. This complex is found in cell walls of plants and consists of lignin, cellulose and hemicellulose. It is highly recalcitrant due to the heterogeneous and polyphenolic composition of lignin. It is produced by plants by dehydrogenative polymerization of coniferyl alcohol, sinapyl alcohol and coumaryl alcohol, which corresponds to guaiacyl (G), syringyl (S) and p-hydroxyphenyl (H) structures of lignin, respectively (Sannigrahi, Pu, & Ragauskas, 2010). By shielding cellulose and hemicellulose it also protects these polymers from degradation. Many agricultural waste streams such as straw and sawdust mainly consist of lignocellulose. Due to its low nutritional value it cannot be used to feed animals. This explains why 250 million tons of straw was burned in China alone in 2009 (Grimm & Wösten, 2018). Fungi can upgrade these waste streams by making cellulose available to animals or by transforming these into materials (see below).

Wood degrading fungi are mainly found in the phylum of the Basidiomycota (Ohm et al., 2014; Riley et al., 2014). The wood degrading fungi are generally classified as white- and brown-rot fungi based on the ability to degrade lignin, cellulose and hemicellulose (Floudas et al., 2012; Horwath, 2015; Ohm et al., 2014). Brown-rot fungi degrade cellulose and hemicellulose but are not able to depolymerize lignin. As a result, the undigested plant material is rich in lignin, which explains its brown appearance (Zhu et al., 2016). On the other hand, white rot fungi depolymerize lignin, cellulose and hemicellulose leaving residues with a bleached appearance. Brown- and white rots use the breakdown products of cellulose and hemicellulose for energy and as carbon source, while very little lignin carbon is used for metabolic processes (Horwath, 2015). The current white/brown rot paradigm is however a subject of

discussion as genetic research revealed inconsistencies regarding enzymatic capacities described to these groups of fungi (Riley et al., 2014). More detailed information about biodegradation and bioconversion of lignocellulosic residues can be found in a review by Sánchez (2008).

Mycelium materials

Mycelium-based materials can be made of pure mycelium or a combination of mycelium and another material such as the substrate (Figure 1). Pure mycelium can be used as leather or textile replacement, while composite materials have been developed for use as packaging, insulation and construction materials.

Figure 1 Insulation panels (A), floor tiles (B) and multi-purpose pots (C) obtained by fungal colonization of plant-based substrates and pure mycelium leather (D). Pictures obtained with permission from Mogu (Varese, Italy).

Pure mycelium is obtained by growing a fungus on a substrate in static growth conditions (Haneef et al., 2017; Lugones et al., 2004; Chapter 4) or as a liquid shaken culture (Chapter 5). The fungus is grown until the waste stream or a more easily digestible substrate such as glucose is completely consumed. The pure mycelium can be used to produce a pure mycelium material or can be mixed with other materials

such as fibers to form a composite material. Alternatively, composite materials can be obtained by inactivating the fungus before it has fully consumed its substrate. In this case one makes use of the property of hyphae to bind organic fibers or particles together while colonizing the substrate (Jones et al., 2018). Fungal growth can be stopped by drying and/or heating the colonized substrate. Heating will kill the fungus, while drying will preserve the fungus in a 'hibernated' state. In the latter case, growth can be reinitiated by wetting the colonized substrate.

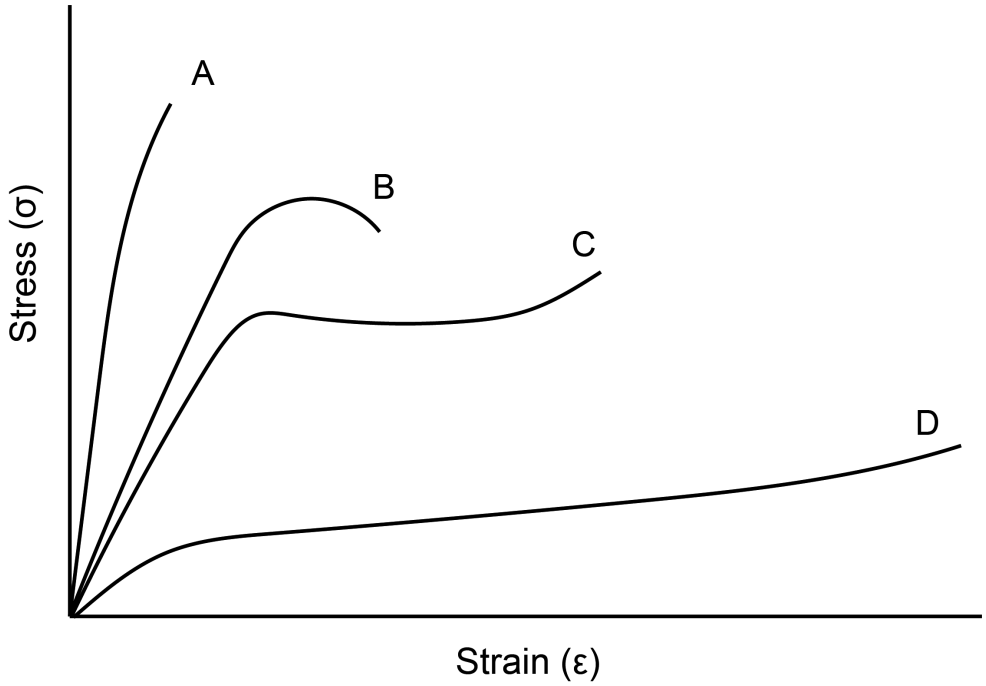

Figure 2 Stress-strain curves of strong and brittle material (A), strong and non-ductile material (B), ductile material (C) and plastic material (D).

Material properties are defined as a set of attributes of a material. Density (ρ, kg m^{-3}) and price ($ kg^{-1}) are examples of general properties, while examples of mechanical properties are the Young's modulus (E, GPa), ultimate tensile strength (σ, MPa) and elongation at breaking (ε, %) (Ashby, 2005). The Young's modulus, that combines stress with strain, indicates the degree of elasticity (Figure 2). Elastic materials have a lower E than rigid materials. For example, rubber has an E between 0.01–0.1 GPa, while polyvinyl chloride (PVC) has an E of around 4 GPa (Ashby *et al.*, 2010). Ultimate tensile strength is defined as the nominal stress at which a material, loaded in tension,

separates (Ashby, 2005), opposite of compression strength. Brittle materials like glass and ceramics separate without significant deformation, whereas ductile materials like rubber show significant deformation before separation. Brittleness and ductility are material properties that are often associated with respectively high and low Young's moduli and can be deduced from stress/strain curves (Figure 2).

The material properties together with their ability to be shaped or moulded are important factors for the applicability of a material (Ashby, 1993). Metals, polymers, elastomers, ceramics, glasses and hybrids are the main classes of materials (Figure 3). Hybrid materials include composites such as reinforced plastics and aluminium, foams and natural materials such as wood, bone and skin (Ashby, 2005). Based on their properties fungal materials have foam, natural material and polymer-like properties (Appels et al., 2018, 2019; Jones, Huynh, Dekiwadia, Daver, & John, 2017; Chapters 2–5).

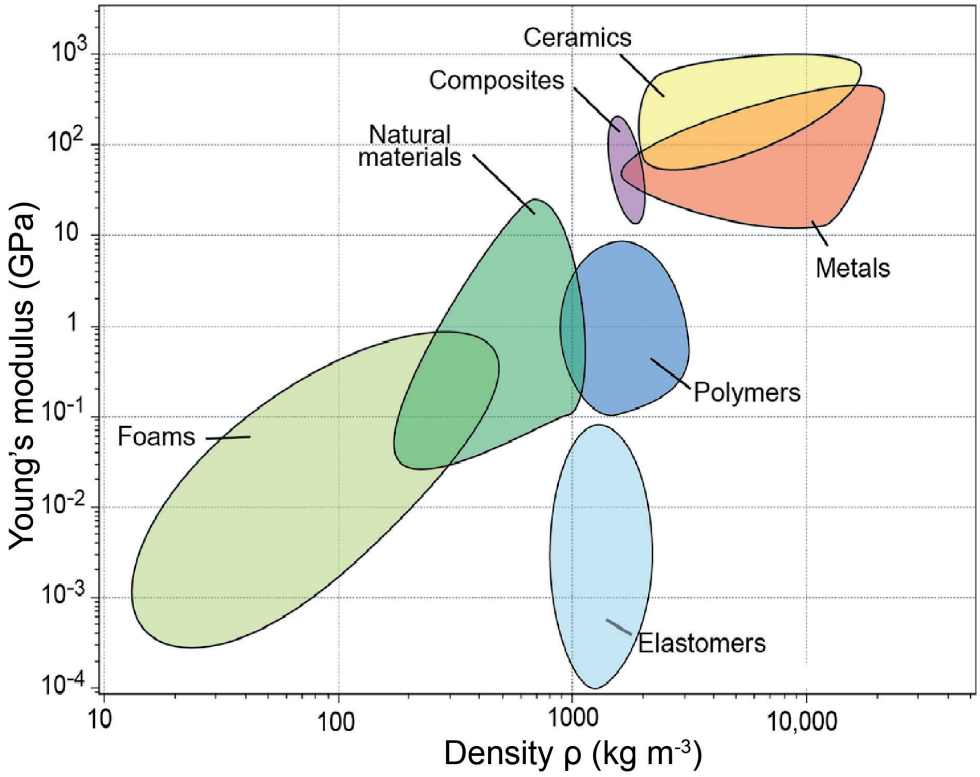

Figure 3 Relation between the E-modulus (GPa) and density (kg m^{-3}) of material families (Ashby, 2005).

The properties of pure mycelium materials are the result of the substrate, the type of fungus and its growth conditions (Appels et al., 2018; Haneef et al., 2017; Chapters 4 & 5) as well as its post-processing. For instance, *Pleurotus ostreatus* grown on cellulose forms a stiffer mycelium material when compared to *Ganoderma lucidum,* while supplementing the cellulose based substrate with dextrose makes both fungal materials more elastic (Haneef et al., 2017). Pure mycelial sheets obtained with *S. commune* showed comparable rigidity and ultimate tensile strength as leather (Chapter 5). Elasticity was increased by treatment with glycerol. Increasing glycerol concentrations led to a shift of mechanical properties resembling natural materials to elastomer-like materials such as rubber.

Mycelium composite materials have been developed that exhibit properties similar to expanded polystyrene and other foams (Appels et al., 2019; Islam, Tudryn, Bucinell, Schadler, & Picu, 2018; Pelletier et al., 2017; Yang, Zhang, Still, White, & Amstislavski, 2017; Ziegler, Bajwa, Holt, McIntyre, & Bajwa, 2016, Chapter 2). The mycelium dominates the soft compression at small strain, while the organic substrate particles cause rapid stiffening at higher strain. Like pure mycelium materials, properties of the mycelium composites depend on the fungus, substrate, growth conditions and processing of the material (Appels et al., 2018, 2019; Jones et al., 2017, Chapters 2 & 4). Differences in acoustic properties are an example of the impact of the type of substrate on mycelium composite material (Pelletier et al., 2017). Cotton bur fiber is a relatively low performing acoustic material when compared to other substrates. Yet, it still absorbs 70–75% of the sound at a peak frequency of 1000 Hz. This suggests that the source of the feedstock is quite flexible when implementing a design for mycelium based acoustic absorption panels. The impact of growth conditions on the properties of mycelium material composites is illustrated by the finding that densely packed substrate results in higher elastic moduli and compressive strength when compared to loosely packed substrate (Yang et al., 2017). In the next sections a more detailed composition of the cell wall of fungi is described, in particular that of the mushroom forming fungus *Schizophyllum commune,* as well as the impact of physical and chemical treatment on mycelium materials.

Cell wall composition of *S. commune*

Cell walls of fungi play an essential role in interactions of fungi with their (a)biotic environment and are important for morphogenesis and mechanical strength of hyphae (Gow, Latge, & Munro, 2017). The latter implies that the hyphal cell wall also plays an important role in determining the properties of mycelium materials. Despite their importance, relatively little is known about the fungal cell wall. The composition of fungal cell walls is dynamic and varies between species, strains, environmental conditions and developmental stage (Bowman & Free, 2006; Erwig & Gow, 2016). The composition of the cell wall of *S. commune* has been studied by enzymatic and chemical treatment (Sietsma, Rast, & Wessels, 1977; Sietsma & Wessels, 1979; Sonnenberg, Sietsma, & Wessels, 1982; van Wetter, Wösten, Sietsma, & Wessels, 2000). Cell walls of the vegetative mycelium of *S. commune* consist of glucose (67.6%), N-acetylglucosamine (12.5%), mannose (3.4%), xylose (0.2%), amino acids (6.4%) and lipids (3.0%) (Sietsma & Wessels, 1977). Glucose and N-acetylglucosamine are contained in glucans and chitin, respectively, that form different layers in the cell wall. The outer layer of the *S. commune* cell wall consists of a water-soluble mucilage of (1-3)(1-6)-β-glucan (Sietsma & Wessels, 1979). This so-called schizophyllan is also secreted into the culture medium (van Wetter et al., 2000; Zhang, Cui, Cheung, & Wang, 2007). An alkali-soluble (1,3)-α-linked glucan is located beneath the mucilage, while the inner layer of the cell wall consists of chitin cross-linked to a highly branched (1,3)(1,6)-β-glucan (Sietsma & Wessels, 1979, 1981). This forms the alkali-insoluble backbone of the cell wall. How the lipids and xylose contribute to the cell wall is not known. The amino acids and at least part of the mannose form (glyco)proteins. SC3 is such a glycoprotein (de Vocht et al., 1998). This amphipathic protein is one of the most abundant proteins in cell walls of aerial hyphae of *S. commune*, while it also occurs at lower levels in cell walls of substrate hyphae. The amount of schizophyllan is increased in a Δ*sc3* strain, while the amount of glucan cross-linked to chitin is reduced (van Wetter et al., 2000). SC3 also attaches hyphae to hydrophobic surfaces (Wösten, Schuren, & Wessels, 1994) (Wösten, Schuren, et al., 1994), mediates escape of hyphae from the aqueous environment into the air (Wösten et al., 1999), and makes aerial structures hydrophobic (Wösten, de Vries, & Wessels, 1993; Wösten, Asgeirsdóttir, Krook, Drenth, & Wessels, 1994). The latter is illustrated by the fact that the water contact angle of a wild-type mycelium with aerial hyphae is 115 degrees, similar to the hydrophobic surface of Teflon, while water

immediately soaks into the mycelium of a Δ*sc3* strain (van Wetter et al., 2000; Wösten et al., 1999).

Physical treatment of mycelium materials

Hot-pressing impacts material properties of mycelium materials. High temperature increases the incidence of the Maillard reaction. This complex non-enzymatic reaction known to be responsible for browning of food and flavor formation (Van Boekel, 2006) links amino acids and reducing sugars (Martins, Jongen, & van Boekel, 2000). Incidence of the Maillard reaction is also affected by other environmental conditions such as pH and water activity (Eichner & Karel, 1972; Jousse, Jongen, Agterof, Russell, & Braat, 2002; Martins et al., 2000). Pressure increases the density of the material thus changing its properties. Pressure, or other forms of mechanical stress, can also lower the activation energy of chemical reactions (Beyer & Clausen-Schaumann, 2005).

Chemical treatment of mycelium materials

Plasticizers and crosslinking agents are commonly used chemicals to alter material properties. Plasticizers increase plasticity of a material by lowering the glass transition temperature T_g (Cowie & Caleria, 2007). The plasticizer acts like a lubricant by improving the capacity of polymers to move. Plasticizers such as glycerol and water do so by filling the space between polymer chains, thereby increasing their distance (Cowie & Caleria, 2007). As such, plasticizers are being used to make materials more suitable for injection moulding. (Vieira, Da Silva, Dos Santos, & Beppu, 2011). Crosslinkers are the opposite of plasticizers and reduce mobility of a polymer structure. Crosslinking enhances specific mechanical properties such as ultimate tensile strength and at the same time reduce elasticity (Azeredo & Waldron, 2016). Ionic and hydrophobic interactions are examples of non-covalent crosslinks. On the other hand, chemical crosslinking involves formation of covalent bonds (Azeredo & Waldron, 2016). For instance, dialdehydes such as glutaraldehyde and glyoxal link the reactive amino or hydroxyl groups in polysaccharides (Crini, 2005). Chemical crosslinks can also be the result of for instance gamma-, or photoirradiation and sulfur vulcanization (Bhattacharya, Rawlins, & Ray, 2009). Properties of biological materials, such as fungal mycelium, can be changed by introducing both non-covalent and covalent crosslinks with proteins and polysaccharides (Yang, Dou, Liang, & Shen, 2005).

Aim of this Thesis

At the start of the project described in this Thesis only 3 publications on mycelium materials were available in peer reviewed journals. A search in Google Scholar on December 15, 2019 for 'Mycelium Materials' shows the growing interest in materials produced with fungal mycelium. The number of articles on this topic grew from 2 in 2016, 7 in 2017, 12 in 2018 and 18 in 2019. This illustrates the novelty of the field and, as a consequence, the need for systematic studies on the impact of fungal strains, substrates, growth conditions and physical and chemical treatments on material properties of mycelium materials. Moreover, it was not yet clear which type of materials can be produced with mycelium. At the start of the project only foam like materials had been described.

Chapter 2 shows that morphology, density, tensile and flexural strength, as well as moisture- and water-uptake properties of mycelium composite materials depends on the type of substrate (straw, sawdust, cotton), fungal species (*Pleurotus ostreatus* vs. *Trametes multicolor*) and processing technique (no-, cold- or heat-pressing). The fungal species impacted colonization level and the thickness of the air-exposed mycelium called fungal skin. This, together with the type of substrate determined the stiffness and water resistance of the materials. It was also shown that heat pressing improved homogeneity, strength and stiffness of the materials shifting their performance from foam-like to cork- and wood-like materials. These results show that a palette of mycelium composite materials can be formed. In fact, it is the first time mycelium composites have been described with natural material properties.

Growth of natural isolates of mushroom forming fungi was screened for the production of bio-based materials in **Chapter 3**. A method was developed to quantify growth using CO_2 production resulting from growth as a proxy. CO_2 production was monitored for 28 days and corresponded to visual monitoring of mycelium growth. *Trametes hirsuta* and *Lenzites betulina* showed most dense mycelium when grown on rapeseed straw and also produced most CO_2. *Bjerkandera adusta* produced less CO_2 after 28 days of growth. Yet, mechanical properties after pressing were similar to those of *T. hirsuta* and *L. betulina* being similar to the class of natural materials. As CO_2 is one of the most important greenhouse gases causing climate change and the fact that it grew faster

when compared to *T. hirsuta* and *L. betulina, B. adusta* seems to have most potential for the production of bio-based fungal materials.

The impact of environmental growth conditions and deletion of the hydrophobin gene *sc3* on mycelium material properties of *S. commune* was studied in **Chapter 4**. The Δ*sc3* mycelium retained more water with increasing temperature when compared to the wild type. The Young's modulus and the ultimate tensile strength of the Δ*sc3* mycelium were 3–4-fold higher when compared to the wild-type mycelium. This correlated with mycelium density, while no differences in chemical composition of the wild-type and Δ*sc3* mycelia were observed by ATR-FTIR. Together, mechanical properties of wild type mycelium were like those of natural materials, while those of Δ*sc3* were more similar to thermoplastics.

Chapter 5 describes the properties of pure mycelium resulting from liquid shaken cultures of *S. commune* 4-39. Treating mycelial films with the plasticizing agent glycerol impacted material properties. The largest effect was observed after treatment with 32% glycerol causing a 2.4-fold increase in density, a 150-fold lower E, a 2.8-fold lower ultimate tensile strength and a 20-fold higher elongation at break. These values cause the material to shift from performing as natural-like materials to elastomer-like materials. Moreover, glycerol treatment changed the surface of mycelium films from hydrophobic to hydrophilic and made the hyphal matrix less permeable for water.

Previously, cell wall composition and architecture were studied using destructive techniques such as chemical extraction. **Chapter 6** describes for the first time the composition of intact cell walls of a basidiomycete using solid state NMR. This non-destructive technique indicates that cell walls are composed of a flexible part consisting of β-(1,3)-glucan, β-(1,3-1,6)-glucan, α-(1,4)-glucan and homo- or heteropolymeric mannose, and a rigid part composed of chitin, β-(1,3)-glucan, β-(1,3-1,6)-glucan, α-(1,3)-glucan and homo- or heteropolymeric fucose. The presence of not only chitin, β-(1,3)-glucan and β-(1,3-1,6)-glucan in the rigid part but also α-(1,3)-glucan and homo- or heteropolymeric fucose changes the paradigm of the structural organization of the cell wall of the model basidiomycete *S. commune*.

Results presented in this Thesis are summarized and discussed in **Chapter 7.**

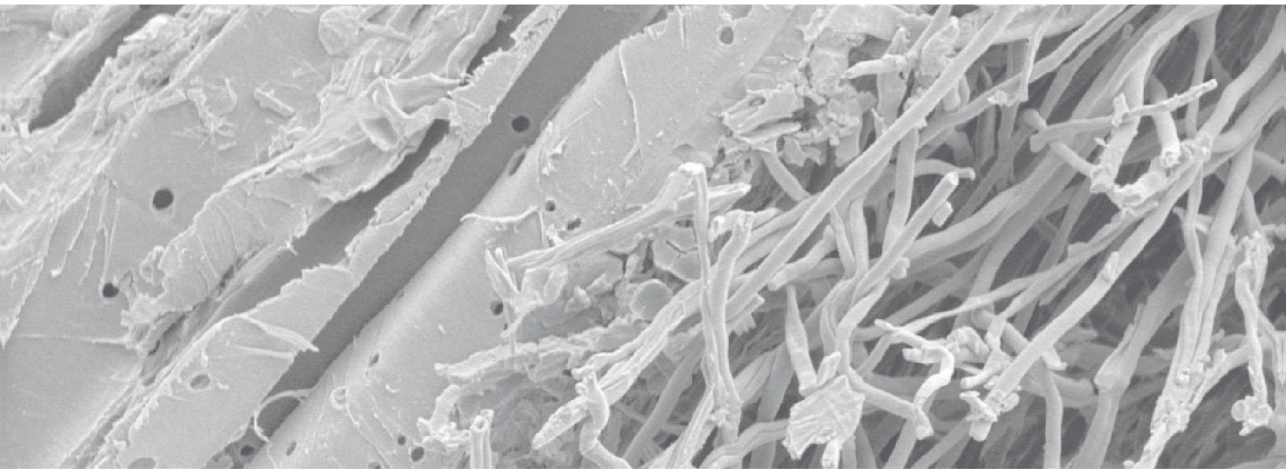

Chapter 2

Fabrication factors influencing mechanical, moisture- and water-related properties of mycelium-based composites

Appels, F. V. W., Camere, S., Montalti, M., Karana, E., Jansen, K. M. B., Dijksterhuis, J., Krijgsheld, P., & Wösten, H. A. B.

This chapter has been published as:

Appels, F. V. W., Camere, S., Montalti, M., Karana, E., Jansen, K. M. B, Dijksterhuis, J., Krijgsheld, P. & Wösten, H. A. B. (2019). Fabrication factors influencing mechanical, moisture- and water-related properties of mycelium-based composites. *Materials & Design*, *161*, 64-71.

Abstract

Mycelium-based composites result from the growth of filamentous fungi on organic materials such as agricultural waste streams. These novel biomaterials represent a promising alternative for product design and manufacturing both in terms of sustainable manufacturing processes and circular lifespan. This study shows that their morphology, density, tensile and flexural strength, as well as their moisture- and water-uptake properties can be tuned by varying type of substrate (straw, sawdust, cotton), fungal species (*Pleurotus ostreatus* vs. *Trametes multicolor*) and processing technique (no pressing or cold or heat pressing). The fungal species impacts colonization level and the thickness of the air-exposed mycelium called fungal skin. Colonization level and skin thickness as well as the type of substrate determine the stiffness and water resistance of the materials. Moreover, it is shown that heat pressing improves homogeneity, strength and stiffness of the materials shifting their performance from foam-like to cork- and wood-like. Together, these results demonstrate that by changing the fabrication process, differences in performance of mycelium materials can be achieved. This highlights the possibility to produce a range of mycelium-based composites. In fact, it is the first time mycelium composites have been described with natural material properties.

Introduction

One of the challenges of our society is the transition towards a sustainable economy. To this end, the use of non-renewable resources has to be reduced for the production of materials and consumer products (Ashby, 2012; Geiser, 2001; Hislop & Hill, 2011; Vezzoli, 2013). Renewable mycelium-based materials have the potential to contribute to the new economy by replacing petroleum-based products such as plastics. These bio-based products could for instance be used as thermal and acoustic insulation (Pelletier et al., 2013; Yang, Zhang, Still, White, & Amstislavski, 2017) and packaging (Holt et al., 2012).

So far, mycelium-based materials have been produced mainly from mushroom forming fungi. These fungi are known for their ability to colonize large areas in nature. For example, single individuals of the genus *Armillaria* have been identified that had colonized ≥1000 hectares of soil, making them the largest organisms on earth

(Ferguson, Dreisbach, Parks, Filip, & Schmitt, 2003; Smith, Bruhn, & Anderson, 1992). Moreover, mushroom forming fungi are known for their ability to degrade lignocellulosic waste streams such as sawdust and straw. Like other fungi, they colonize their substrate by means of 1–10 µm-wide filamentous cells called hyphae. These hyphae form a three-dimensional network by growing at their tips and by branching subapically. This mycelium secretes enzymes that convert polymers in the substrate into breakdown products that can be taken up to serve as nutrients. As a result, the organic material is being degraded in time, while being replaced by fungal biomass on and within substrate particles. At a certain moment, hyphae grow out of the substrate into the air creating a fluffy or compact layer covering the substrate. This compact layer is also known as fungal skin.

Pure and composite fungal materials are distinguished (Grimm & Wösten, 2018). Pure fungal materials are the result of complete degradation of the substrate or are obtained by removing the fungal skin from the substrate. The properties of pure mycelium materials depend on the substrate, the type of fungus and its growth conditions (Appels et al., 2018; Haneef et al., 2017; Islam, Tudryn, Bucinell, Schadler, & Picu, 2017; Chapter 4) as well as post-processing. *Pleurotus ostreatus* mycelium material grown on cellulose is more stiff when compared to that of *Ganoderma lucidum,* while addition of dextrose to the cellulose based substrate makes both fungal materials more elastic (Haneef et al., 2017). Even a single gene can affect the material properties of the mycelium. The mycelium of a *Schizophyllum commune* strain in which the hydrophobin gene *sc3* is inactivated (van Wetter, Wösten, Sietsma, & Wessels, 2000) has a 3–4-fold higher maximum tensile strength when compared to the wild-type (Appels et al., 2018; Chapter 4). This is caused by increased mycelium density. On top of this, the mycelium of the Δ*sc3* deletion strain retains more water when compared to the wild type strain (Appels et al., 2018, Chapter 4). This is explained by the fact that the encoded protein coats aerial hyphae with a hydrophobic coating (Wösten, 2001). Environmental growth conditions also impact *S. commune* mycelium properties (Appels et al., 2018, Chapter 4). Its maximum tensile strength ranges between 5.1–9.6 MPa depending whether this fungus is grown in the light or in the dark at ambient or 7% CO_2. Together, mechanical properties of wild type and Δ*sc3* mycelium of *S. commune* are similar to those of natural materials and thermoplastics, respectively.

During colonization of the substrate, fungal growth can be stopped by drying and/or heating the material. By drying, the fungus is preserved in a 'hibernated' state, allowing the fungus to restart growth when moisture conditions become favourable again. Instead, heating will kill the fungus. Drying and/or heating of the substrate at some stage during colonization will result in mycelium-based composites. So far, composite materials have been shown to exhibit properties similar to expanded polystyrene or other foams (Islam, Tudryn, Bucinell, Schadler, & Picu, 2018; Pelletier et al., 2013; Yang et al., 2017; Ziegler, Bajwa, Holt, McIntyre, & Bajwa, 2016). The mycelium matrix in the composite dominates the soft compression at small strain, while the organic substrate particles cause rapid stiffening at higher strain. The mycelium composite shows the Mullins effect under cyclic conditions (i.e. the stress–strain curve depends on the maximum loading previously encountered) (Islam et al., 2018). Studies indicate that, like pure mycelium, properties of the mycelium composites depend on the fungus, substrate, growth conditions and processing of the material (Jones, Huynh, Dekiwadia, Daver, & John, 2017). The effect of the substrate on mycelium composite material is illustrated by differences in acoustic properties (Pelletier et al., 2013). For instance, cotton bur fiber was a relatively low performer when compared to other feedstocks. Still, it showed 70–75% acoustic absorption at a peak frequency of 1000 Hz, suggesting that the source of the feedstock is quite flexible when implementing a design for mycelium based acoustic absorption panels. The impact of growth conditions was reported by Yang et al. (2017). Densely packed substrate resulted in higher density, elastic moduli and compressive strength when compared to loosely packed substrate. Time of inactivation of the fungus had a small impact on the material density and thermal conductivity, but showed a negative impact on the elastic moduli and a positive impact on the compressive strength. On the other hand, addition of natural fiber improved both the elastic moduli and compressive strength.

Here, we addressed whether non-foam type of mycelium composite materials can be obtained by varying the type of fungus, substrate and processing of the material. Heat pressing resulted in mycelium composite material with density, elastic modulus and flexural strength similar to that of natural materials like wood and cork.

Materials and Methods

Strains and culture conditions

Trametes multicolor (Mycelia BVBA M9915) and *Pleurotus ostreatus* (SPOPO Sylvan 195) were grown for 14 days by CNC Exotic Mushrooms (Gennep, The Netherlands) on beech sawdust and 1–3 cm rapeseed straw (Gedizo trading BV, Netherlands) and on non-woven low-quality cotton fiber (proprietary information of Mogu, Lombardy, Italy). Rapeseed straw and beech sawdust were supplemented with bran (CNC Exotic Mushrooms) and had a final humidity of 65–70%, while non-woven low-quality cotton fibers had a final humidity of 55%. In all cases, autoclavable bags (SacO2, Belgium) with filter size XL were filled with 3 kg substrate, sterilized and inoculated with spawn of *T. multicolor* or *P. ostreatus* (Mycelia, Belgium).

Fabrication conditions

Plastic thermo-formed moulds (34x34x4 cm, PET-G) were filled with pre-grown substrate. The material was hand-pressed to distribute the substrate as uniform as possible and covered with perforated cellophane foil (0.35 µm, standard commercial PPI). The fungus was allowed to grow further at 25°C for 14 days in the dark. In order to achieve a homogeneous colonization at both sides, plates were demoulded and kept at the same conditions for 10 more days in opposite orientation to extend the growth on the side that had previously been in contact with the mould. Heat (150°C) or cold (20°C) pressing was performed with a CE-certified mechanical multi-plate press (Vigevano, Italy) for 20 minutes at F<30 kN. Materials exposed to heat pressing were cooled at room temperature, whereas non-pressed or cold-pressed materials were dried at environmental conditions for 24–48 hours.

Specimen preparation

Specimens were cut from two different plates by manual vertical sawing. They were cut in dog-bone shape for tensile tests (155x35 mm, neck 75x22 mm), in rectangular shape for flexural testing (155x34 mm) and as square specimens (45x45 mm) for moisture and water absorption tests. Specimen dimensions were measured before testing, showing minimal dimensional variation (e.g. 155.5±0.85 mm x 28±0.9 mm x 13±0.75 mm for TRN). Prior to testing, materials were dried at 80°C for 24 hours. Tests were performed within 30 minutes after the drying treatment at 22°C and 50% humidity.

Morphological analysis

All samples were analyzed by visual inspection, while TRN, TRH and PCH materials were also subjected to light microscopy (Nikon SMZ25, Japan) and cryo scanning electron microscopy (cryo-SEM). In the latter case, materials were cut into small squares (5 x 5 mm) with a scalpel and attached to a 10 mm ø copper cup with a 2 mm piece of Scotch tape. Samples were snap-frozen with liquid nitrogen and transferred to an Oxford CT1500 Cryostation attached to a JEOL 5600LV scanning electron microscope (JEOL, Tokyo, Japan). Specimens were sublimated at −85°C to remove ice and sputter-coated with gold for 2 minutes before acquiring micrographs at an acceleration voltage of 5 kV.

Density measurements

Density was calculated from the weight after drying and the volume of each specimen prepared for tensile and flexural tests.

Mechanical tests

Ten specimens of each material were tested for tensile and bending behaviour. Tests were performed with a Zwick/Roell Z010 universal testing machine (Ulm, Germany) using an elongation rate of 2 mm min^{-1} and a maximum force of 1 kN. Flexural tests were performed in a three-point bending setup with the same machine using a cross-head speed of 2 mm min^{-1} and clamp support distance of 80 mm. Data were analysed to obtain stress-strain plots, tensile and flexural strength, and the elastic and flexural modulus.

Moisture exposure

Five square specimens were tested for each material to determine water uptake at 40°C at a relative humidity (RH) of 60% and 80%. After drying until constant mass (m_0) and measuring thickness at three different points, specimens were placed on a grid in a moisture chamber (Espec SH-660, Hudsonville, MI, USA) exposing both sides of the material to the selected temperature and moisture conditions. Weight was measured every 10 minutes within the first hour of testing and after 2, 4, 24, 48, 96 and 192 hours. Weight increase was plotted against the square root of time. Thickness of specimens was measured at the start of the experiment and after 4 and 192 hours to record expansion of volume.

Water absorption

Square specimens were tested in triplo to determine the water uptake when placed on top of water. Specimens were placed in containers filled with distilled water maintained at 23±1°C and weight was measured after 1, 2, 4, 24, 48, 96 and 192 hours. For each measurement, samples were removed from the water surface, manually removing the superficial water with filter paper and weighed within 1 minute after removal from the water.

Thermogravimetric analysis

Thermogravimetric analysis was performed with a TGA Q50 (TA Instruments, New Castle, DE, USA). Measurements were performed with biological duplicates of 25 mg of mycelium in a platinum pan using an air flow of 100 mL min^{-1}. Temperature increased from 20 to 600°C with a rate of 10°C min^{-1}.

Statistical analysis

Statistical analysis was performed with the software package IBM SPSS statistics 22.0 (IBM Corporation, Armonk, New York). Welch's unequal variances t-tests were performed followed by a Games-Howell post hoc test ($p \leq 0.05$) for tensile and flexural strength experiments and for density and water absorption experiments. Final weight increase of a given material after exposure to 60% and 80% RH was analysed using independent sample t-tests ($p \leq 0.05$).

Results and Discussion

Morphological analysis

The nine materials that were produced (Table 1) presented different visual characteristics (Figure 1). The non-pressed (TRN, TBN, PCN, PRN) and cold-pressed (PCC, PRC) materials showed the same colour and texture. However, the non-pressed TRN, PCN and PRN materials looked soft and foamy and appeared flexible, while the non-pressed material TBN and the cold-pressed materials PCC and PRC appeared tougher at visual inspection. Thus, sawdust resulted in a more dense appearance when compared to straw and cotton fibers in the case of non-pressed materials. *T. multicolor* grown on rapeseed straw (TRN) formed a soft, velvety skin at the substrate surface and had an elastic, foam-like appearance. The equivalent material of

Table 1 Fungal species, substrate and postprocessing technique used to produce the materials tested in this study.

Material type[1]	Fungus	Substrate	Pressing
TRN	*T. multicolor*	Rapeseed straw	Non-pressed
TBN	*T. multicolor*	Beech sawdust	Non-pressed
TRH	*T. multicolor*	Rapeseed straw	Heat-pressed
PRN	*P. ostreatus*	Rapeseed straw	Non-pressed
PRC	*P. ostreatus*	Rapeseed straw	Cold-pressed
PRH	*P. ostreatus*	Rapeseed straw	Heat-pressed
PCN	*P. ostreatus*	Cotton	Non-pressed
PCC	*P. ostreatus*	Cotton	Cold-pressed
PCH	*P. ostreatus*	Cotton	Heat-pressed

[1]The material types are coded using the initials of each fabrication variable, e.g. **TRN** represents ***T****rametes*, **R**apeseed straw, **N**on-pressed.

P. ostreatus (PRN) showed a rough skin and more rigid appearance. Light microscopy of cross sections of TRN showed that fungal colonization was more dense close to air-exposed sides of the material when compared to the material centre (Figure 2B). Hyphae had fully colonized the space in between the straw particles at the outer part of the material but they had not extensively penetrated the organic material as shown by cryo-SEM (Figure 2CD).

Heat-pressed *T. multicolor* and *P. ostreatus* materials (TRH, PCH and PRH) resembled natural composites like fiberboard by sight (Figure 1). These samples showed chromatic variation, ranging from white to brown. The browning of the material is most likely caused by Maillard reactions involving sugars and proteins present in the fungal cell walls and the plant material. Alternatively, it may be caused by caramelization of plant and fungal sugars or by pyrolysis of organic material (Powrie, Wu, & Molund, 1986). Light microscopy showed that browning of TRH had mainly occurred in the fungal skin (Figure 2F), possibly explained by the low water content of this part of the material (Powrie et al., 1986).

In all cases, individual hyphae within the mycelium were less clearly visible after heat pressing (Figure 2C,D versus Figure 2G,H,K,L), probably due to glueing of hyphae and substrate together.

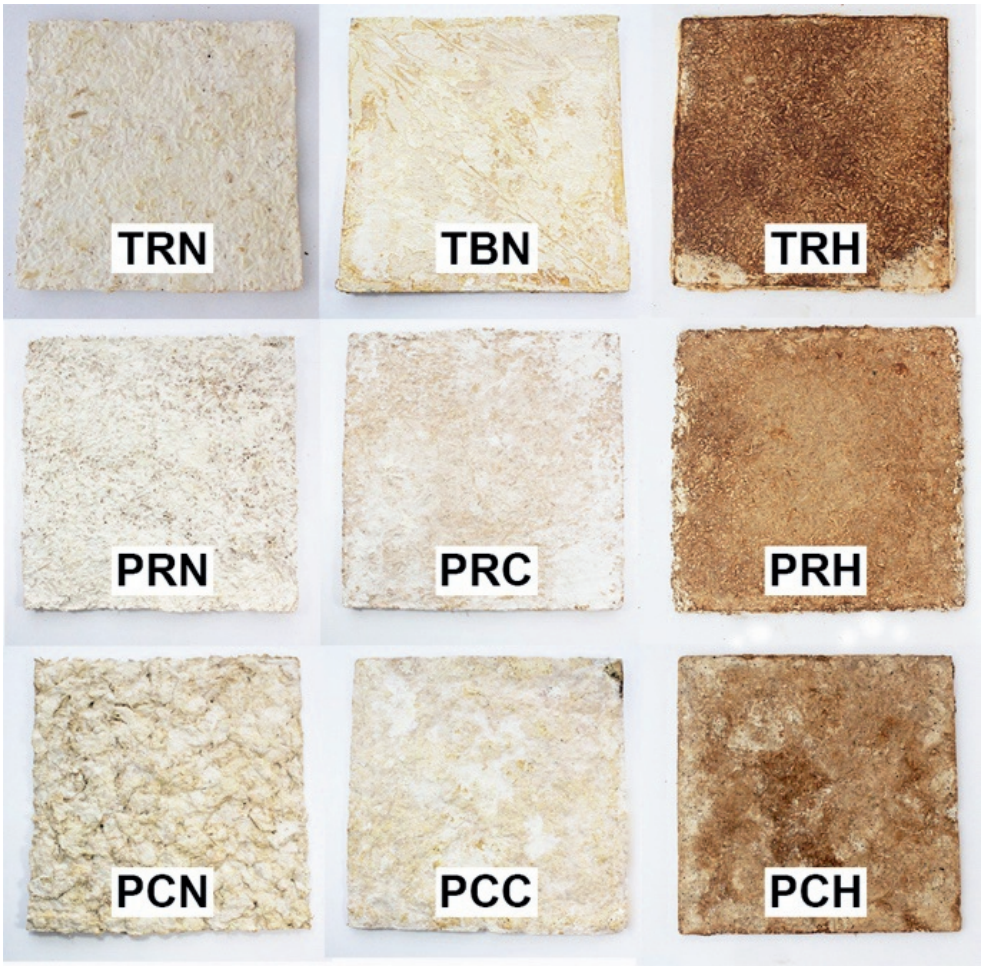

Figure 1 Materials resulting from growth of *T. multicolor* on sawdust (TBN) and straw with (TRH) or without (TRN) heat pressing and growth of *P. ostreatus* on cotton with heat pressing (PCH), cold pressing (PCC) and without pressing (PCN) and on straw with heat pressing (PRH), cold pressing (PRC) and without pressing (PRN).

Heat-treated materials appeared also more dense when compared to the non-pressed materials but still hyphae were less numerous in the material centre. The reduced presence of hyphae in the centre of the materials, even after heat pressing, is expected to impact the strength of the material. Hyphal abundance in the centre of the materials may be improved by forced airflow through the substrate during colonization, thus increasing oxygen levels in the material centre. Alternatively, the time of colonization may be increased.

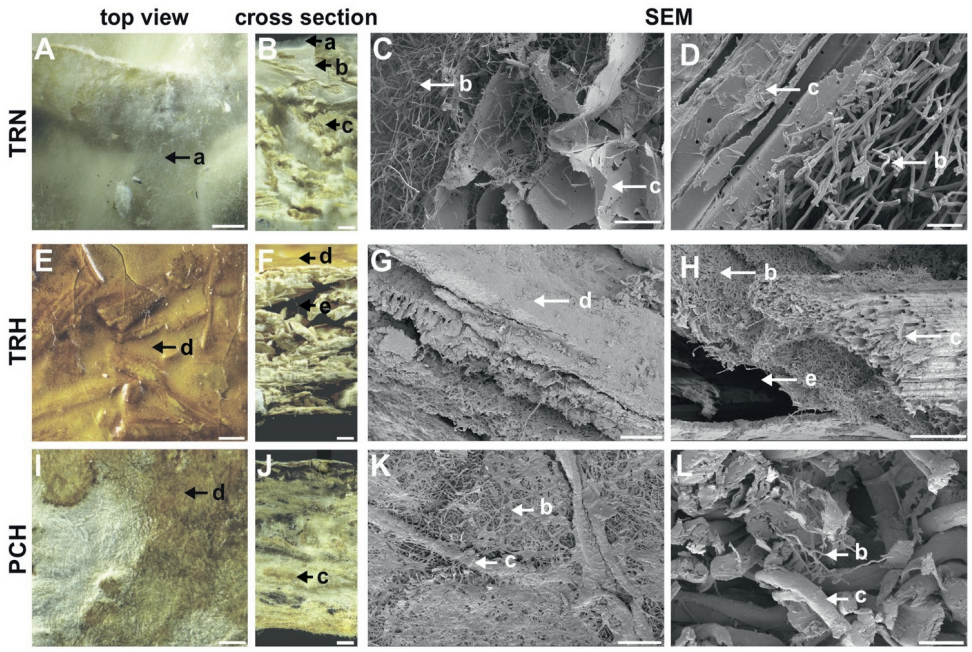

Figure 2 Stereomicroscopy and cryo-SEM images of TRN (A-D), TRH (E-H) and PCH (I-L). Arrows indicate aerial hyphae (a), mycelium (b), substrate (c), fused hyphae (d) and air-voids (e). Scale bars represent 1 mm (A,B,E,F,I,J) 100 µm (H), 50 µm (C, G, K), 20 µm (L) and 10 µm (D).

In all cases, individual hyphae within the mycelium were less clearly visible after heat-pressing (Figure 2C,D versus Figure 2G,H,K,L), probably due to glueing of hyphae and substrate together. Heat-treated materials appeared also more dense when compared to the non-pressed materials but still hyphae were less numerous in the material centre. The reduced presence of hyphae in the centre of the materials, even after heat-pressing, is expected to impact the strength of the material. Hyphal abundance in the centre of the materials may be improved by forced airflow through the substrate during colonization, thus increasing oxygen levels in the material centre. Alternatively, the time of colonization may be increased.

Density

Density of the mycelium composite materials ranged from 0.10 to 0.39 g cm^{-3} (Table 2). Non-pressed materials (TRN, TBN, PCN, PRN) had a density of 0.10 to 0.17 g

cm^{-3}, similar to those (0.06 to 0.22 g cm^{-3}) of other non-pressed mycelium composites (Holt et al., 2012).

Table 2 Properties (±SEM) of mycelium-based composites. Letters indicate statistically significant differences with the materials with the same lettering (Games-Howell, p≤0.05, n≥4).

Material	Density (g cm^{-3})	Thickness (mm)	Tensile strength (MPa)	Elastic modulus (MPa)	Elongation at break (%)	Flexural strength (MPa)	Flexural modulus (MPa)
TRN (a)	0.10±0.01$^{b,c,e-i}$	13.9±0.4^{g,h}	0.04±0.01$^{d,g-i}$	4±0.4^{a-i}	4.7±0.9$^{b,e-i}$	0.22±0.07^{g}	3±1.6^{f-i}
TBN (b)	0.17±0.01^{a-i}	15.2±0.3^{g-i}	0.05±0.01$^{d,f-i}$	13±0.5$^{a-e,g,i}$	1.5±0.3^{a}	0.29±0.02^{c,d,g}	9±1.4$^{c,d,f-i}$
PCN*(c)	0.13±0.01$^{a,b,e-i}$	11.5±0.3^{h}	n/a*	n/a*	n/a*	0.05±0.01$^{b,e-i}$	1±0.2$^{b,f-i}$
PRN (d)	0.13±0.01$^{b,e-i}$	11.2±0.1^{g,h}	0.01±0.00^{a-i}	2±0.3^{a-i}	2.8±0.4^{f,g,i}	0.06±0.01$^{b,e-i}$	1±0.4$^{b,f-i}$
PCC (e)	0.24±0.01$^{a-d,g-i}$	11.7±0.1^{g-i}	0.03±0.00$^{d,g-i}$	6±0.3$^{a-d,g-i}$	1.4±0.2^{a,i}	0.24±0.03^{c,d,g}	12±3.3^{g,i}
PRC (f)	0.24±0.01$^{a-d,g-i}$	11.6±0.1^{g-i}	0.03±0.00$^{b,d,g-i}$	9±1.2$^{a,d,g-i}$	0.8±0.1^{a,d}	0.21±0.01^{c,d,g}	15±1.1$^{a-d,g,i}$
TRH (g)	0.35±0.01^{a-f}	8.8±0.1$^{a,b,d-h}$	0.15±0.01^{a-f}	59±6.8^{a-f}	0.9±0.1^{a,d}	0.86±0.06^{a-f}	80±7.9^{a-h}
PCH (h)	0.35±0.02^{a-f}	8.0±0.0^{a-i}	0.13±0.02^{a-f}	35±6.5$^{a,c-f,i}$	1.6±0.3^{a}	0.62±0.11^{c,d}	34±5.5$^{a-d,g}$
PRH (i)	0.39±0.01^{a-f}	9.5±0.0^{b,e,f,h}	0.24±0.03^{a-f}	97±9.0$^{a-f,h}$	0.7±0.1^{a,d,e}	0.87±0.14^{d}	72±6.6^{a-f}

*Properties of material PCN could not be determined, as specimens failed at clamping.

The sawdust-based material (TBN) had the highest density among the non-pressed samples (Table 2). Cold pressing (PCC, PRC) increased density 2-fold, while heat pressing (TRH, PCH, PRH) resulted in a >3-fold density increase. Moreover, heat pressing resulted in a lower density variation across specimens with a standard error of 5–7.5% contrasting 10–18% in the case of non-pressed and cold-pressed materials. Heat-pressing also resulted in more even thickness within the same specimen. For instance, variation decreased from 4.5% (PCN) to 2.3% (PCC) to 0.5% (PCH). Together, mycelium-based materials are lighter when compared to other wood composites such as medium-density fiberboard (0.50–1.00 g cm^{-3}) and oriented strand board (OSB) wood composite (0.55–0.70 g cm^{-3}) (Ashby & Johnson, 2014).

Mechanical properties

The nine mycelium composites showed different behaviour when subjected to tensile stress, particularly depending on the pressing treatment but not on substrate or fungus used (Table 2). Heat-pressed samples had significant higher tensile strength and elastic modulus when compared to their corresponding cold-pressed

and non-pressed samples, while also cold-pressed *Pleurotus* rapeseed (PRC) samples had higher tensile strength and elastic moduli compared to non-pressed *Pleurotus* rapeseed material (PRN). Heat-pressed *P. ostreatus* rapeseed straw material (PRH) was stiff and strong but brittle, as shown by its steep curve, high tensile strength (0.24 MPa) and relatively low rupture strain (0.7%)(Table 2; Figure 3A). Cold pressing of the same substrate-fungus combination (PRC) resulted in a material with much lower stiffness and tensile stress, but similar rupture strain. The non-pressed sample (PRN) on the other hand had a very low stiffness (2 MPa) and tensile strength (0.01 MPa) but took ±4.7% strain before failing completely (Table 2; Figure 3A).

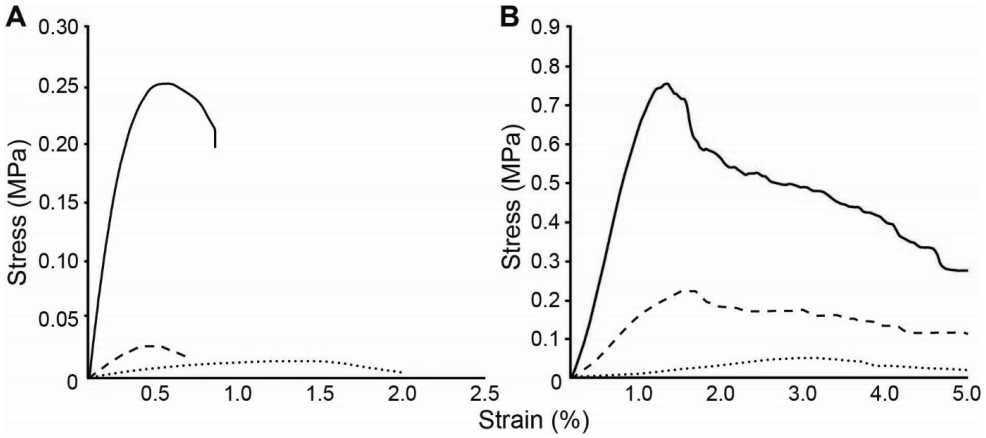

Figure 3 Tensile (**A**) and bending (**B**) tests of *P. ostreatus* grown on rapeseed straw without pressing (dotted line) and cold (striped line) or hot (solid line) pressing.

Elongation at break decreased to a similar extent after pressing *P. ostreatus* material with or without heat, irrespective of the substrate. However, cold- and heat-pressed *P. ostreatus* materials grown on cotton (PCC, PCH) showed a higher elongation at break than straw-based materials (PRC, PRH). Together, the density and the Young's modulus of mycelium materials are similar to those of natural materials and foams (Figure 4).

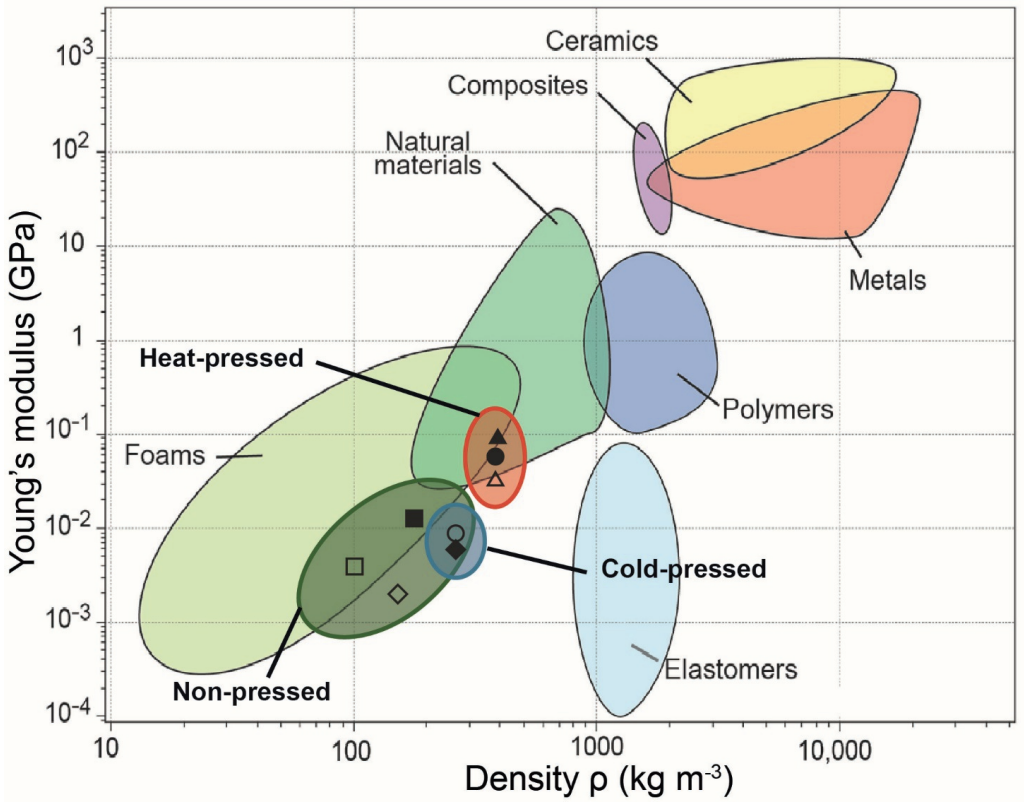

Figure 4 Material family chart of the Young's modulus (GPa) vs density (kg m^{-3}). Non-, cold- and heat-pressed materials form clusters within foam- (TRN □ , TBN ■ , PRN ◇ , PCC ◆ , PRC ○) and natural-like materials (TRH ● , PCH △ , PRH ▲). Figure adapted from Ashby (2005).

Similar trends in stiffness and maximum stress were seen during three-point bending. The flexural strength increased from non-pressed to cold-pressed and hot-pressed. The non-pressed materials presented flexural strengths varying from 0.05 to 0.29 MPa (Table 2) and flexural moduli from 1 to 9 MPa (Table 2). The ultimate rupture strain upon bending was larger for all three processing conditions when compared to those obtained with the tensile measurements (Figure 3). This is explained by the fact that the fungal skin of the materials was more resistant to bending when compared to the substrate part (Figure 5).

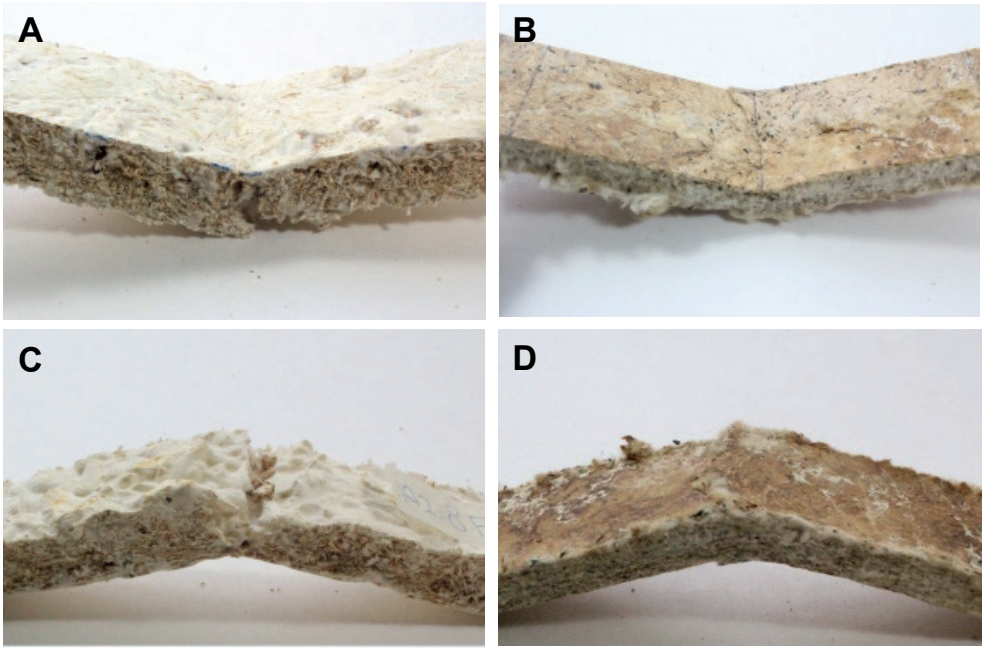

Figure 5 Non-pressed *T. multicolor*-straw material (TRN) (**A,C**) and heat-pressed *P. ostreatus*-cotton material (PCH) (**B,D**) under flexural stress leaves the top side (i.e. the fungal skin) intact while the bottom side is broken.

Together, our data extend the range in flexural strengths and moduli that can be obtained with non-pressed fungal materials. Non-pressed *Ganoderma*-cotton plant biomass materials were reported to have bending strengths in the range of 7–26 kPa (Holt et al., 2012), while flexural moduli of 66–72 MPa were found in the case of cotton or hemp based mycelium materials (Ziegler et al., 2016).

Moisture exposure and water immersion

Weight and thickness of mycelial materials was measured before and after exposure to 60% and 80% RH. Statistical analysis showed no general increase in weight except for PRC and PRH placed at 80% RH. However, a trend was observed with all mycelium materials gaining most weight within the first 2 hours of moisture exposure and reaching saturation (M∞) in approximately 12 hours. Saturation time and overall weight increase of all mycelium materials was higher in samples exposed to 80% RH compared to 60% RH. They showed a 7.57–11.63% and a 3.15–8.22% final weight increase at 40°C, respectively. Overall, cotton-based materials showed a lower final

weight increase (3.15–5.80% [60% RH] and 7.57–8.12% [80% RH]) compared to rapeseed straw based materials (3.87–8.22% [60% RH] and 10.00–10.96% [80% RH]) (Table 3).

TRH and PRH materials showed an increase in thickness at 80% RH but not 60% RH (Table 3). Conversely, thickness of PRN, PCC and PRC had increased at 60% RH but not at 80% RH. The latter may be due to collapse of material due to higher water content. The expansion analysis is particularly relevant for the choice of mycelium-based composites for applications where the materials should be sandwiched between others, as for example is the case with insulation materials in the building industry.

Table 3 Weight increase and thickness expansion at saturation of mycelium-based composites when exposed to RH 60% and 80% at 40°C and after placing the material on water for 192 h. Asterisks indicate statistical significant differences (t-test, p≤0.05, n≥3) and letters indicate statistical significant differences with corresponding materials (Games-Howell, p≤0.05, n=3).

Material	Weight increase 60% RH (%)	Weight increase 80% RH (%)	Thickness expansion 60% RH (%)	Thickness expansion 80% RH (%)	Weight increase after placing material on water (%)
TRN (a)	8.22±0.25	10.44±0.17	0.29±1.19	5.43±1.38	436±73
TBN (b)	5.71±0.12	11.63±0.10	6.72±2.81	-0.47±1.21	43±5[d-i]
PCN (c)	3.15±0.14	7.57±0.14	18.74±4.16	0.57±2.62	508±76
PRN (d)	3.87±0.32	10.26±0.31	24.24±4.61*	-5.13±1.64	279±2[b,e,i]
PCC (e)	3.74±0.18	7.84±0.20	22.12±1.07*	-2.96±1.08	238±1[b,d,h]
PRC (f)	4.94±0.30	10.00±0.10*	21.06±1.68*	0.96±0.26	262±8[b]
TRH (g)	7.26±0.09	10.96±0.20	0.93±0.41	1.98±0.78*	246±8[b]
PCH (h)	5.80±0.11	8.12±0.30	-1.93±2.12	-0.14±1.64	281±5[b,e,i]
PRH (i)	7.09±0.27	10.92±0.26*	0.97±0.57	2.5±0.56*	239±3[b,d,h]

Placing materials on top of water resulted in increased weight for all mycelial materials. TBN showed the lowest water uptake when the mycelium materials were placed on water (Table 3). This is likely explained by the water repellent fungal skin of *T. multicolor* formed under this condition. In contrast, TRN and PCN showed the highest water uptake. Thus, there was no relation between water absorption and the type of fungus, substrate, or pressing condition used. Other *Pleurotus*-based mycelium composites grown on grain fibers were reported to absorb up to 278% water over a maximum of 24 hours (López Nava, Méndez González, Ruelas Chacón, & Nájera

Luna, 2016), while cotton-based mycelium composites from an undocumented fungus absorbed 198% water after 168 h immersion.

Thermogravimetric analysis of mycelial materials

Thermogravimetric analysis showed similar degradation patterns for mycelial materials grown on rapeseed straw, cotton or beech sawdust as substrate. Water content was higher for samples grown on rapeseed straw (7.6–9.6%) than on cotton (5.8–7.2%) as shown by the weight loss at 100°C (Figure 6). Initial degradation temperature was ±225°C for rapeseed straw and ±242°C for cotton materials. Pressing or the type of fungus did not impact the degradation profiles. Yet, uncolonized substrates had a slower decrease in weight when compared to the colonized substrates. Possibly, fungal colonization makes the substrate more accessible for thermal degradation.

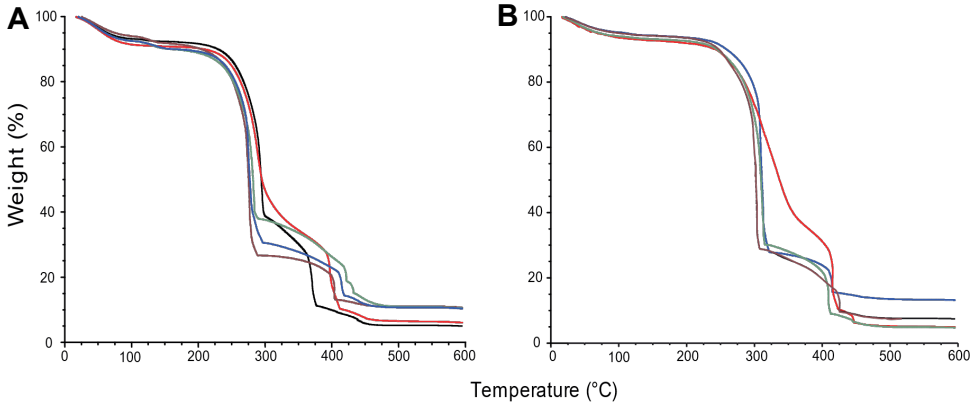

Figure 6 TGA Analysis of mycelial materials with rapeseed straw as substrate (**A**) or cotton as substrate (**B**). Decrease in weight% was measured while increasing temperature. The line in blue, green, brown and black represent PRH, TRH, TRN and PRC, respectively (**A**), while the lines in blue, green and brown represent PCN, PCH and PCC, respectively (**B**). Red lines represent the uncolonized substrates.

Conclusions

Visual appearance, density, mechanical properties and water-absorbing behaviour was assessed of a range of mycelium based composites that were obtained by varying the type of fungus, substrate and pressing conditions. *P. ostreatus* and *T. multicolor* colonized the substrate but also formed a fungal skin at the substrate-air interface. The

skin of *T. multicolor* was thicker than that of *P. ostreatus*. In general, the non-pressed and cold-pressed materials had a whitish, velvety appearance with a foam like structure. In contrast, the heat-pressed materials were compact and had a brown appearance. The latter is probably due to Maillard reactions, caramelization and/or pyrolysis of organic material (Powrie et al., 1986). The mycelium materials had a density of 0.10 to 0.39 g cm^{-3} being lighter than for instance medium-density fiberboard (0.50–1.00 g cm^{-3}) and oriented strand board (OSB) (0.55–0.70 g cm^{-3}) wood composites (Ashby & Johnson, 2014). Saw dust resulted in a higher density than cotton fibers or straw as a substrate, while cold- and heat-pressing increased density 2- and >3-fold, respectively. Moreover, heat pressing reduced density and thickness variation between and within the samples.

Pressing, but not the type of substrate or fungus, impacted the tensile strength and elasticity modulus of the mycelium materials. Tensile strength and elasticity modulus of heat-pressed materials were higher when compared to the corresponding cold-pressed and non-pressed materials. A similar trend was observed during three-point bending. The flexural strength increased from non-pressed to cold-pressed and hot-pressed. The flexural strain needed to break the samples was higher than those needed during the tensile measurements. This is explained by the fact that the fungal skin is more elastic than the colonized substrate and therefore breaks at higher strain when compared to the substrate part of the material.

There was no overall relation between water absorption and the type of fungus, substrate, or pressing condition used to produce the material. TRH and PRH materials showed an increase in thickness at 80% RH but not 60% RH, while thickness of PRN, PCC and PRC had increased at 60% RH but not 80% RH. The latter may be due to collapse of material due to higher water content. Saturation time of mycelium materials as well as their overall weight increase was higher in samples exposed to 80% RH. They showed a 3.15–8.22% and a 7.57–11.63% final weight increase at 40°C when exposed to 60% and 80% RH, respectively.

Thermogravimetric analysis showed similar degradation patterns for mycelial materials grown on rapeseed straw, cotton or beech sawdust as substrate. Moreover, pressing or the type of fungus did not impact the degradation profiles. Yet, uncolonized

substrates showed slower decrease in weight when compared to colonized substrates. Possibly, fungal colonization makes the substrate more accessible for thermal degradation. In addition we found that the water content of samples grown on rapeseed straw (7.6–9.6%) was higher than on cotton (5.8–7.2%) and that the initial degradation temperature of rapeseed straw based materials was lower (± 225°C) than that of cotton based materials (±242°C).

Based on density and elastic modulus, mycelium-based composites produced in this study qualify as foam-like and natural materials (Ashby, 2005) (Figure 4). Heat pressing shifted mycelium composites from foam-like performance to cork and wood-like performance. Further improvement of the mycelium materials may be obtained by promoting colonization in the central part of the substrate. It was shown that colonization by *P. ostreatus* and *T. multicolor* was much higher at the outer parts of the substrates. Improved colonization in the central part of the materials may be accomplished by forcing air through the feedstock during colonization, thus increasing oxygen levels in the material centre. Alternatively, the time of colonization may be increased.

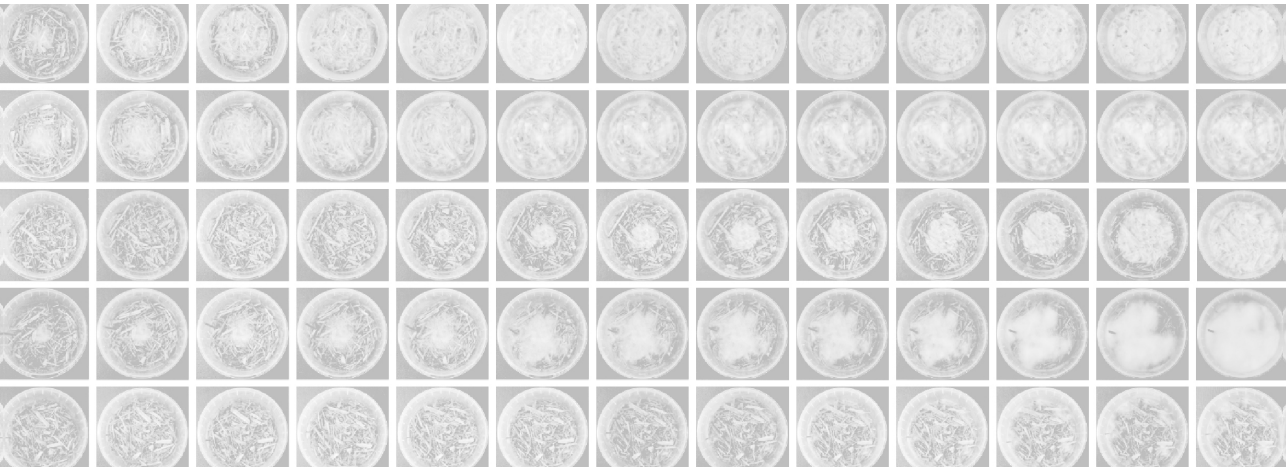

Chapter 3

Growth assessment and mechanical analysis of mycelium-based materials of nine mushroom forming fungi

Appels, F. V. W., Broeze, S. I., & Wösten, H. A. B.

Abstract

Conversion to a sustainable economy requires the development of recyclable materials that are produced from renewable feedstocks. Composite materials resulting from fungal colonization of lignocellulose waste represent such materials. In this study, nine wood degrading fungi were screened for growth on rapeseed straw. Growth was monitored visually and by a newly developed system in which CO_2 was used as a proxy for mycelium activity of *Trametes hirsuta, Schizophyllum commune, Kuehneromyces mutabilis, Bjerkandera adusta, Gloeophyllum odoratum, Lenzites betulina, Xylaria hypoxylon, Daedalopsis configrosa,* and *Coprinellus micaceus*. *Schizophyllum commune* and *Bjerkandera adusta* produced high CO_2 levels early during colonization of rapeseed straw, while *Trametes hirsuta* and *Lenzites betulina* showed a lower initial CO_2 production but a higher overall release of CO_2. The latter two strains also showed most dense colonization of the substrate when inspected visually. Among six selected species, the three highest cumulative CO_2 producers (i.e. *T. hirsuta, L. betulina* and *B. adusta*) performed best mechanically after heat pressing. Young's moduli of these materials ranged between 1.16 and 1.52 GPa, ultimate tensile strength between 0.62 and 1.08 MPa, flexural modulus between 0.30 and 0.62 GPa and ultimate flexural strength between 0.13 and 0.24 MPa. Together, the mechanical properties of these mycelium materials place them in the class of natural materials. Moreover, results show that *B. adusta* has high potential for production of mycelium materials because of its fast growth, its relatively low CO_2 release and its mechanical properties.

Introduction

Contemporary resource management in our socio-economic system causes a growing interest in the use and development of bio-based materials. The current system is too often based on a linear "take-produce-consume-discard" model, demanding a shift towards a system that focuses on sustainability. In a sustainable economy there is no assumption of abundance of resources and unlimited waste disposal but a focus on circularity. In a circular economy resources are processed in cycles, mimicking natural principles developed out of necessity as our planet can be considered a closed system to matter. To achieve circularity biomimicry can be a key strategy. In this approach inspiration is taken from biological forms, processes and systems to solve human

challenges. An example of such an approach is the use of fungal mycelium for the production of mycelium-based materials.

Fungi play an important role in nutrient recycling in nature. The two largest phyla within the fungal kingdom are the Ascomycota and the Basidiomycota. The latter contains 16 classes, 52 orders, 177 families, 1589 genera and more than 30,000 species (Hibbett et al., 2007). Thus, about 30% of the described fungal taxa belongs to this phylum (Dai et al., 2015). Members of the Basidiomycota include mushroom forming fungi. Some of these fungi can colonize large areas in nature, exemplified by individuals of the genus *Armillaria* that were shown to have colonized ≥1000 hectares of soil (Ferguson, Dreisbach, Parks, Filip, & Schmitt, 2003; Smith et al., A1992). This makes these species the largest organisms on earth. Within the soil, many mushroom forming fungi feed on lignocellulosic waste from plants. These substrates are colonized by means of 2–10 µm-wide filamentous cells called hyphae. These hyphae secrete enzymes that degrade the lignocellulose into molecules that can be taken up to serve as a source for energy and biomass production. Thus, the organic material is converted in time in fungal biomass.

Pure and composite mycelium materials are distinguished (Appels et al., 2018, 2019; Haneef et al., 2017; Jones, Huynh, Dekiwadia, Daver, & John, 2017; Chapters 2, 4 & 5). Composite mycelium materials can be produced by killing the fungus before the organic substrate (e.g. saw dust or straw) is totally degraded by the fungus. Within this material, the mycelium acts as a binder resulting in an end product with the properties of foams like polystyrene (Appels et al., 2019; Jones et al., 2017; Chapter 2). By pressing, more strong materials are obtained that resemble natural materials like wood and cork (Appels et al., 2019; Ashby, 2005; Chapter 2). A more artificial fungal composite material was grown by Haneef et al. (2017) where cellulose fibers were added to a liquid synthetic medium during growth. As a result, the cellulose fibers were incorporated in the material. Apart from the substrate, the environmental growth conditions and post-processing, the fungal species impacts the properties of the mycelium material. For instance, Haneef and colleagues (2017) showed that *Ganoderma lucidum* and *Pleurotus ostreatus* grown on cellulose had Young's moduli of respectively 12 MPa and Appels and colleagues (2019, Chapter 2) showed *Trametes versicolor* had a 2-fold increase of Young's modulus compared to *P.*

ostreatus (4 MPa vs 2 MPa). Here, 9 wood-degrading mushroom forming fungi were screened for fast colonization and material properties. *B. adusta* has high potential for mycelium material production based on its fast substrate colonization, its relatively low total CO_2 release and its mechanical performance.

Material and Methods

Strains and growth conditions

Strains of *Trametes hirsuta, Schizophyllum commune, Kuehneromyces mutabilis, Bjerkandera adusta, Gloeophyllum odoratum, Lenzites betulina, Xylaria hypoxylon, Daedalopsis configrosa, Coprinellus micaceus* were isolated from a forest (Utrecht, The Netherlands) and identified based on phenotypic traits. The strains were purified by growing pieces from the inside of the mushroom caps on potato dextrose agar (PDA) that contained 15 µg ml^{-1} tetracycline, 30 µg ml^{-1} kanamycin, 50 µg ml^{-1} ampicillin, 50 µg ml^{-1} streptomycin, 180 µg ml^{-1} cefotaxime and 1.5 µg ml^{-1} benomyl to prevent growth of bacteria and ascomycetes. Cultures were grown at 25°C in the dark for 7–10 days. Subsequently, mycelium was placed in the centre of fresh PDA plates without antibiotics and growth was continued at 25°C in the dark until the plates were fully covered (4 to 6 days). Spawn was produced at 25°C by inoculating 75 g sorghum seeds with 10 pieces of mycelium of these cultures (0.25 cm^2 each). When the sorghum seeds were fully colonized with mycelium, cultures were stored for a maximum of 6 weeks at 4°C in the dark.

Mycelium was grown at 25°C in the dark in closed micro boxes (Ø95 mm) with a micro filter placed in the lid (Micro box, Nevele, Belgium). To this end, one colonized sorghum seed was placed in the middle of a mixture of 7.8 rapeseed straw (1–3 cm fiber length) (Gedizo, the Netherlands), 0.3 g $CaCO_3$, 0.9 g starch from potato (Sigma-Aldrich, MO, USA) and 21 g water.

CO_2-measurements of growing mycelium

CO_2-production was measured for 10 min using Cozir Wide Range CO_2 sensors (CO2meter, Ormond Beach, FL, USA). Micro boxes were placed in a tin can with a volume of 628 cm^3 (HEMA, the Netherlands) with a CO_2-sensor inside. The sensor measured the CO_2-production in parts per million (ppm) every 5 seconds. The software program Gaslab was used to visualize CO_2-production in a graph. The cans were

closed with a solid lid and a silicon glove was placed over the lid to increase air tightness. After each measurement, CO_2 was allowed to diffuse out of the sensors before next measurements were performed. Total CO_2 production was calculated by assuming a similar CO_2 production as the last measurement at days when release of this gas was not quantified.

Post treatment: harvesting, pressing and cutting

Mycelium composites were removed from the microbox, dried for 4 days at room temperature and placed in a metal mould (Ø72 mm). A lab size heat-press Carver 3889 (Carver Inc., Wabash, Indiana, USA) was used to press samples for 6 minutes at 130°C with 28 MPa. After pressing, samples were cut, using a laser cutter LaserPro X (GCC, New Taipei, Taiwan). A dog bone shape (60.9 mm x 15.3 mm) was used for tensile tests, while flexural tests were done with a rectangular shape (60.0 mm x 9.8 mm). Paper tape was glued on the sample to make the cut sharper and cleaner and to protect samples from blackening during laser cutting. Different settings of the laser cutter (i.e. between 50 W and 4.0 IPS and 85 W and 2.0 IPS) were needed for cutting the different samples to prevent burning of some samples.

Tensile and flexural tests of fungal materials of wild type fungi

Thickness of the samples was measured on 3 random places in every specimen using a Heidenhain MT1281 electronic calliper (Heidenhain Corporation, Illinois, USA), while weight was assessed using a Kern EMB 100-3 (Kern & Sohn, Germany). Tensile and flexural measurements were performed at room temperature with an AllroundLine Z010 TH (ZwickRoell, Kennesaw, GA, USA) at ramp displacement of 0.5 mm min^{-1}. Data was analyzed TestXpert (ZwickRoell, Kennesaw, GA, USA).

Statistical analysis

Statistical analysis was performed using the software package SPSS, version 25 (SPSS Inc., Chicago, IL, USA). Young's modulus (both tensile and flexural), ultimate strength (both tensile and flexural), weight, thickness, density and CO_2 production were analysed using a one-way ANOVA followed by a Tukey's HSD post hoc test when data met ($p \leq 0.05$). The Games-Howell post hoc test was used when data did not show variance homogeneity.

Results

T. hirsuta, S. commune, K. mutabilis, B. adusta, G. odoratum, L. betulina, X. hypoxylon, D. configrosa and *C. micaceus* were grown for 28 days on rapeseed straw. Some species fully colonized the substrate (*T. hirsuta*, *B. adusta, S. commune* and *L. betulina*), whereas some did not (*K. mutabilis*, *G. odoratum, X. hypoxylon* and *D. configrosa, C. micaceus*) (Figure 1).

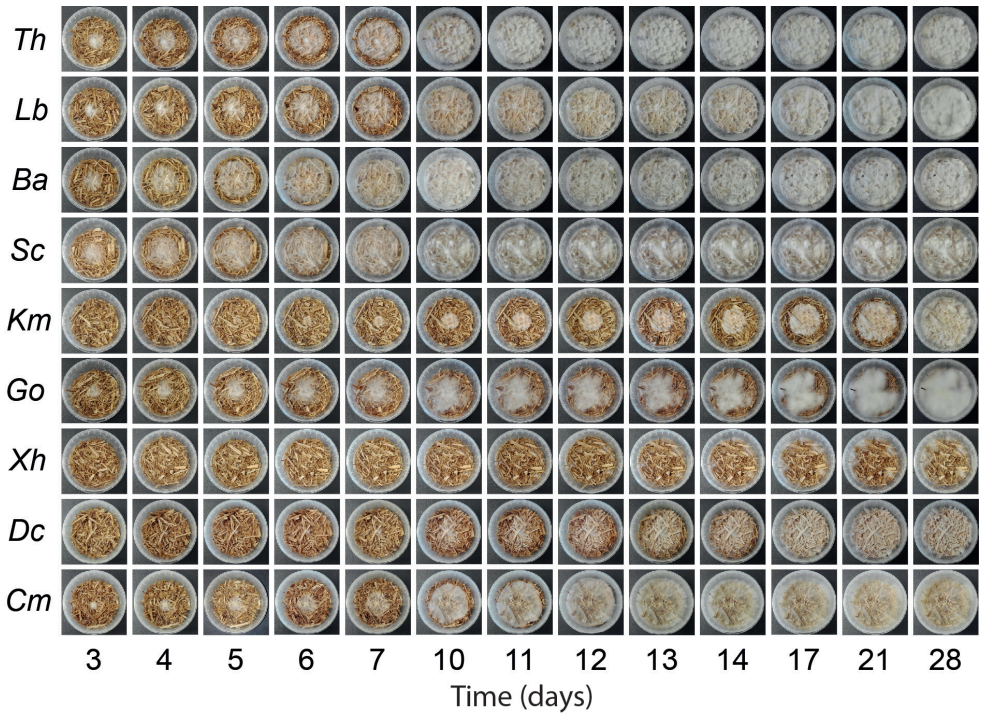

Figure 1 Colonization of rapeseed straw by *T. hirsuta*, *L. betulina*, *B. adusta*, *S. commune*, *K. mutabilis*, *G. odoratum*, *X. hypoxylon*, *D. configrosa*, *C. micaceus* after 28 days of growth.

S. commune and *B. adusta* showed most rapid colonization of the substrate; almost fully covering the substrate with mycelium at day 6. On the other hand, *T. hirsuta* and *L. betulina* showed densest colonization of the substrate at day 28. Colonization by *B. adusta* at day 28 was similar to *T. hirsuta* and *L. betulina* when viewed from the top. However, when looking at the side a less dense mycelium was observed (Figure 2). The morphology of the mycelium also differed as exemplified by *G. odoratum* that produced a wool-like mycelium, whereas *C. micaceus* produced a thinner film of mycelium covering the substrate.

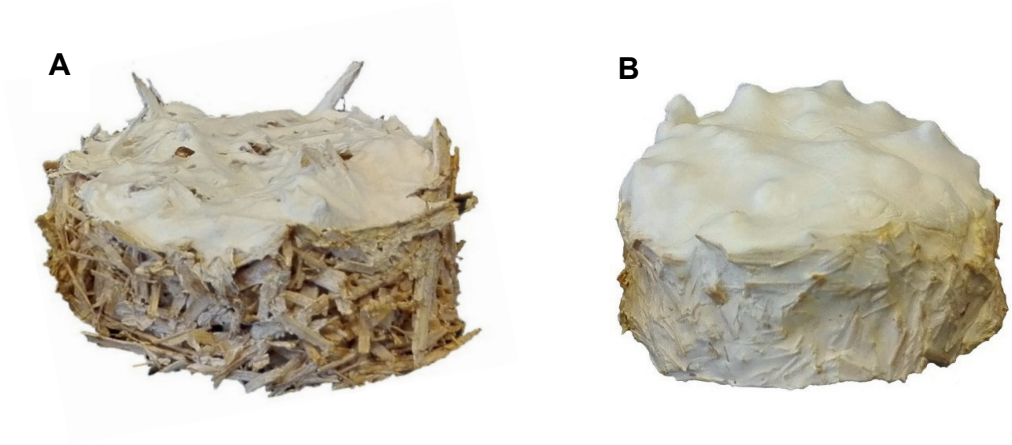

Figure 2 Side and top view of dried samples of *B. adusta* (**A**) and *T. hirsuta* (**B**) that had colonized rapeseed straw for 28 days.

CO_2 production was measured to quantify colonization of the substrate. *S. commune*, *B. adusta* and *G. odoratum* showed a peak in CO_2-production at day 6 or 7 (Figure 3A). On the other hand, *L. betulina*, *T. hirsuta*, *C. micaceus* and *X. hypoxylon* showed the peak at day 12, and *K. mutabilis* and *D. configrosa* at day 21. Peak CO_2-production varied between 543±34 ppm min^{-1} (*B. adusta*, day 7) and 177±18 ppm min^{-1} (*D. configrosa*, day 21).

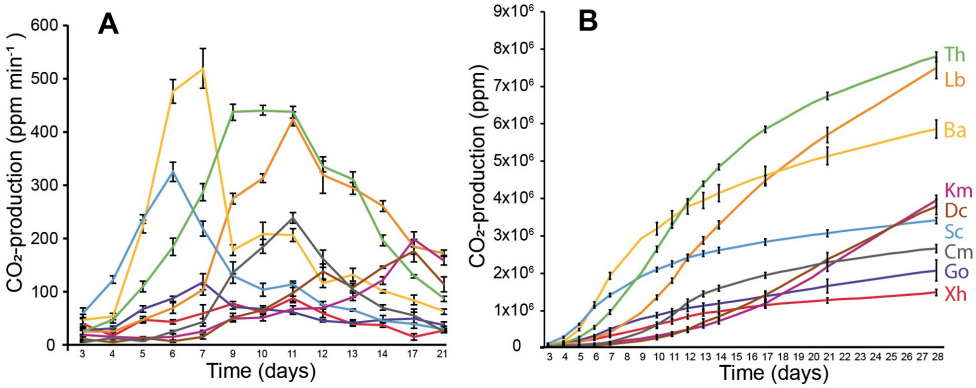

Figure 3 CO_2-production per minute (ppm) (**A**) and cumulative CO_2-production (ppm) (**B**) of different fungal species over a period of 28 days. Species used were *T. hirsuta* (green), *L. betulina* (orange), *B. adusta* (yellow), *K. mutabilis* (purple), *D. configrosa* (brown), *S. commune* (light blue), *C. micaceus* (grey), *G. odoratum* (dark blue), *X. hypoxylon* (red).

Peak CO_2-production varied between 543±34 ppm min^{-1} (*B. adusta*, day 7) and 177±18 ppm min^{-1} (*D. configrosa*, day 21). Total CO_2-production after 28 days of growth ranged

between 1.5x10^6±0.1 x10^6 ppm for *X. hypoxylon* to 7.8 x10^6±0.1 x10^6 ppm for *T. hirsuta* (Figure 3B). Notably, *S. commune* and *B. adusta* produced high CO_2 levels early during colonization but were not the species with highest overall CO_2 production.

Mycelium material properties

The colonized substrate of the 6 species releasing most CO_2 during the 28-day-period (Table 1) were subjected to heat-pressing followed by mechanical characterization. Tensile tests showed higher E-moduli for *L. betulina*, *B. adusta* and *T. hirsuta* than for *D. configrosa*, *K. mutabilis* and *S. commune* (Tukey post hoc, p<0.05). Values ranged between 0.28±0.04 GPa for *K. mutabilis* and 1.52±0.19 GPa for *T. hirsuta*. Ultimate tensile strength ranged between 0.18±0.03 MPa (*K. mutabilis* and *S. commune*) up to 1.08±0.11 MPa for *T. hirsuta* (Tukey post hoc, p<0.05). For flexural tests, E-moduli ranged between 0.08±0.04 GPa for *K. mutabilis* and 0.62±0.09 GPa for *T. hirsuta* (Tukey post hoc, p<0.05), while ultimate flexural strength ranged between 0.04±0.01 MPa for *K. mutabilis* to 0.24±0.07 MPa for *T. hirsuta* (Games Howell post hoc, p<0.05). Weight ranged from 0.93±0.01 g (*L. betulina*) to 1.22±0.03 g (*S. commune*) (Tukey post hoc, p<0.05), while material thickness ranged between 3.20±0.03 mm (*L. betulina*) and 4.70±0.10 mm (*S. commune*) (Tukey post hoc, p<0.05). This was accompanied with differences in density ranging from 418±18 kg m^{-3} (*K. mutabilis*) to 554±2 kg m^{-3} (*D. configrosa*) (Games Howell post hoc, p<0.05).

Table 1 Tensile modulus (E_t), ultimate tensile strength (σ_t), flexural modulus (E_f), ultimate flexural strength (σ_f), weight of rectangular shape, thickness and density (ρ) of *T. hirsuta*, *L. betulina*, *B. adusta*, *S. commune*, *K. mutabilis* and *D. configrosa*. Significant differences are indicated with corresponding letters.

	Et (GPa)	σt (MPa)	Ef (GPa)	σf (MPa)	Weight (g)	Thickness (mm)	ρ (kg m^{-3})
***Th* (a)**	1.52±0.19^{d-f}	1.08±0.11^{b-f}	0.62±0.09$^{b,d-f}$	0.24±0.07	1.01±0.01^{d}	3.41±0.14^{c-e}	538±29
***Lb* (b)**	1.16±0.08^{d-f}	0.63±0.04^{a,d,e}	0.30±0.09^{a}	0.13±0.01^{d,e}	0.93±0.01^{c-f}	3.20±0.03^{c-e}	495±12
***Ba* (c)**	1.23±0.13^{d-f}	0.62±0.06^{a,d,e}	0.44±0.06^{d-f}	0.17±0.02^{e}	1.04±0.02^{b,d}	3.95±0.05$^{a,b,d-f}$	453±11^{f}
***Sc* (d)**	0.38±0.09^{a-c}	0.18±0.03^{a-c}	0.08±0.01^{a,c}	0.06±0.01^{b}	1.22±0.03$^{a-c,e,f}$	4.70±0.10$^{a-c,f}$	445±15^{f}
***Km* (e)**	0.28±0.04^{a-c}	0.18±0.03^{a-c}	0.08±0.04^{a,c}	0.04±0.01^{b,c}	1.09±0.03^{b,d}	4.49±0.11$^{a-c,f}$	418±18^{f}
***Dc* (f)**	0.49±0.11^{a-c}	0.46±0.09^{a}	0.13±0.06^{a,c}	0.08±0.02	1.07±0.02^{b,d}	3.29±0.07^{c-e}	554±2^{c-e}

Discussion

Here, 9 wild type wood-degrading mushroom forming fungi were screened for fast and homogeneous growth of mycelium on rapeseed straw. Visual inspection and CO_2 production as ways to assess growth correlated. Total CO_2 production at the end of the experiment (day 28) was highest for *B. adusta* ($5.9x10^6 \pm 0.2x10^6$ ppm), *T. hirsuta* ($7.8x10^6 \pm 0.1x10^6$ ppm) and *L. betulina* ($7.5x10^6 \pm 0.3x10^6$ ppm). Besides showing highest mycelium activity and most dense mycelial growth, these isolates performed best in flexural and tensile tests. This indicates a correlation between the extent of colonization and the strength of the material (see also Figure 4). This poses the question whether colonization longer than 28 days will result in higher E values.

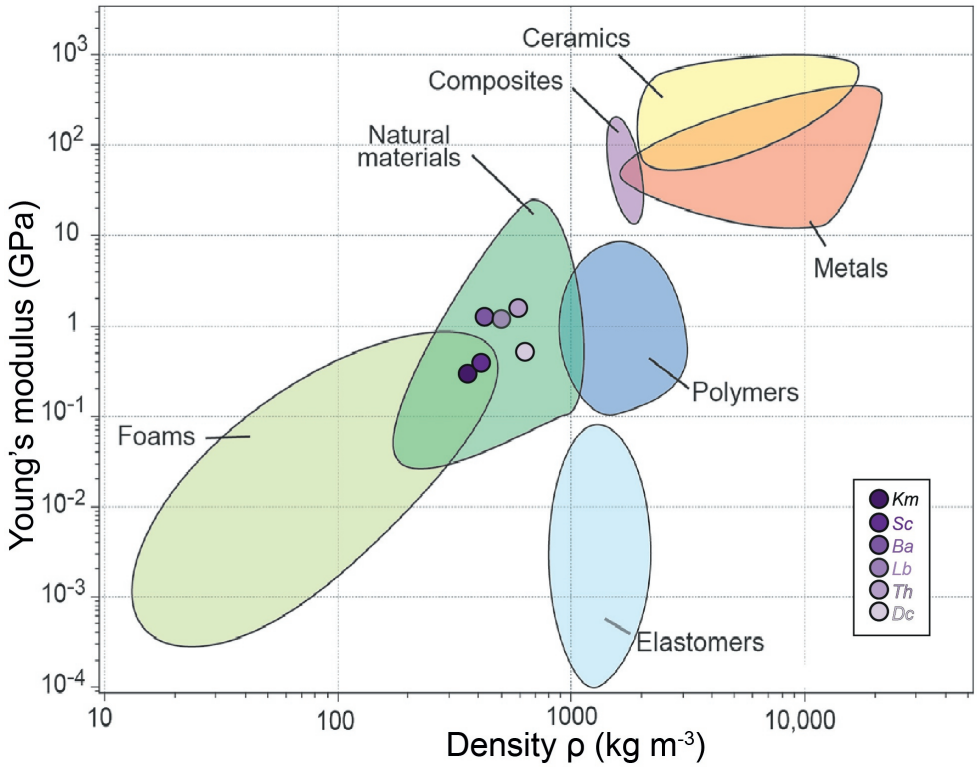

Figure 4 Material family chart of the Young's modulus (GPa) vs density (kg m^{-3}). Results are shown after mechanical analysis of mycelium materials of: *K. mutabilis*, *S. commune, B. adusta*, *L. betulina*, *T. hirsuta* and *D. configrosa*. Figure adapted from Ashby (2005).

The fact that mycelium is a key determinant in the properties of the mycelium composite also raises the question whether different mycelium architecture impacts material properties. *T. hirsute, B. adusta* and *L. betulina* belong to the order Polyporales that are known to have fruiting bodies with trimitic hyphal architecture (Justo & Hibbett, 2011). Trimitic architecture consists of generative, skeletal and binding hyphae of which the two latter are thicker and more highly branched (Pegler, 1996). Vegetative mycelium can consist of generative and/or skeletal hyphae.

Besides architecture of the mycelium, the composition and architecture of the cell walls may also determine mycelium composite properties. So far, both cell wall composition and architecture have not been studied of *T. hirsuta, L. betulina* and *B. adusta.* Their cell walls may differ greatly with respect to the relative presence of chitin, α- and β-glucans and homo- or heteropolymers of mannose, galactose and xylose (Chapter 6).

B. adusta grew faster and produced less total CO_2, while the mechanical properties of its mycelium material were similar to that of *T. hirsuta* and *L. betulina.* Fungi emitting less CO_2 are desirable as they reduce the release of one of the most important greenhouse gases contributing to climate change. Together, *B. adusta* has a high potential for production of mycelium material at industrial scale.

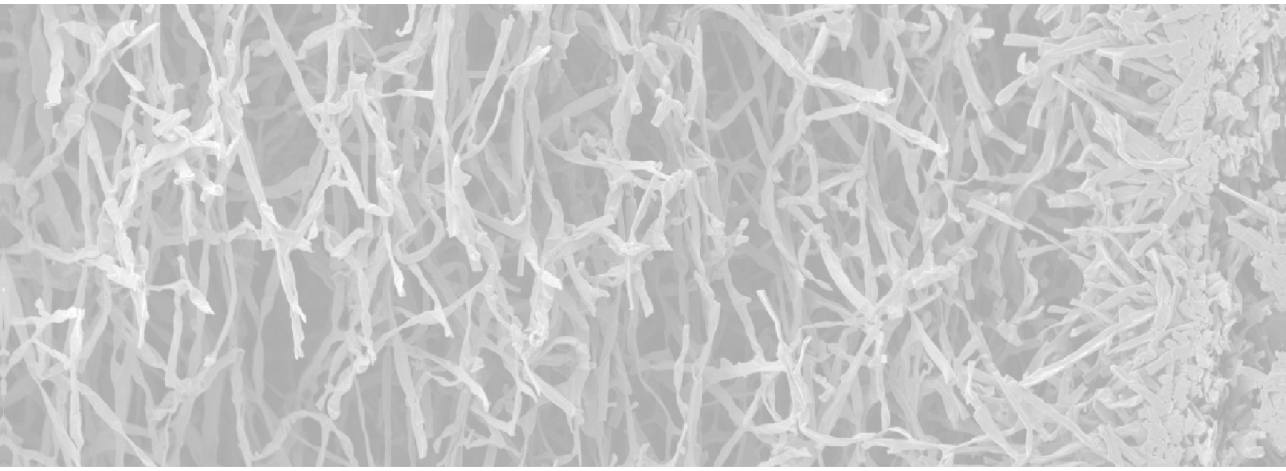

Chapter 4

Hydrophobin gene deletion and environmental growth conditions impact mechanical properties of mycelium by affecting the density of the material

Appels, F. V. W., Dijksterhuis, J., Lukasiewicz, C. E., Jansen, K. M. B., Wösten, H. A. B., & Krijgsheld, P.

This chapter has been published as:

Appels, F. V. W., Dijksterhuis, J., Lukasiewicz, C. E., Jansen, K. M. B., Wösten, H. A. B., & Krijgsheld, P. (2018). Hydrophobin gene deletion and environmental growth conditions impact mechanical properties of mycelium by affecting the density of the material. Scientific Reports, *8*(1), 4703.

Abstract

Filamentous fungi colonize substrates by forming a mycelium. This network of hyphae can be used as a bio-based material. Here, we assessed the impact of environmental growth conditions and deletion of the hydrophobin gene *sc3* on material properties of the mycelium of the mushroom forming fungus *Schizophyllum commune.* Thermogravimetric analysis showed that Δ*sc3* mycelium retained more water with increasing temperature when compared to the wild type. The Young's modulus (E) of the mycelium ranged between 438 and 913 MPa when the wild type strain was grown in the dark or in the light at low or high CO_2 levels. This was accompanied by a maximum tensile strength (σ) of 5.1–9.6 MPa. In contrast, E and σ of the Δ*sc3* strain were 3–4- fold higher with values of 1237–2727 MPa and 15.6–40.4 MPa, respectively. These values correlated with mycelium density, while no differences in chemical composition of the mycelia were observed as shown by ATR-FTIR. Together, genetic modification and environmental growth conditions impact mechanical properties of the mycelium by affecting the density of the mycelium. As a result, mechanical properties of wild type mycelium were similar to those of natural materials, while those of Δ*sc3* were more similar to thermoplastics.

Introduction

The use of bio-based materials is part of the conversion to a circular economy. These materials are derived from molecules or structures of microbes, plants, macro-algae, and animals. Plant-derived thermoplastic starch (Averous, Moro, Dole, & Fringant, 2000), bacterial-derived polyhydroxyalkanoic acid (Babu, O'Connor, & Seeram, 2013), and fungal mycelium (Haneef et al., 2017; Holt et al., 2012; Islam, Tudryn, Bucinell, Schadler, & Picu, 2017; Yang, Zhang, Still, White, & Amstislavski, 2017) are examples of bio-based materials. Fungal mycelia consist of hyphae that grow at their tips and branch subapically. The internal turgor pressure and the rigid cell walls enable hyphae to penetrate organic material such as plant waste. Secreted enzymes degrade polymers in the substrate into molecules that can be taken up to serve as nutrients. Fungal mycelia can cover huge areas, in particular those of mushroom forming fungi. For instance, the mycelium of an *Armillaria* individual had colonized almost 10 km^2 of forest (Ferguson, Dreisbach, Parks, Filip, & Schmitt, 2003).

Schizophyllum commune is a model for mushroom forming fungi (Ohm et al., 2010). Germination of its basidiospores results in a vegetative mycelium that colonizes fallen branches and logs of hardwood. Fusion of two individuals with compatible mating type loci results in a fertile mycelium. Fruiting is induced upon exposure to blue light and ambient CO_2 (i.e. 400 ppm). The outer layer of the *S. commune* cell wall consists of a water-soluble mucilage of β-(1,3)(1,6)-glucan (Sietsma & Wessels, 1977). This so called schizophyllan is also secreted into the culture medium. An α-(1,3)-linked glucan is located beneath the mucilage, while the inner layer of the cell wall consists of chitin cross-linked to a highly branched β-(1,3)(1,6)-glucan (Sietsma & Wessels, 1977, 1981). The SC3 hydrophobin impacts cell wall composition of *S. commune.* In the absence of this cell wall protein the amount of schizophyllan is increased, while the amount of glucan that is cross-linked to chitin is reduced (van Wetter, Wösten, Sietsma, & Wessels, 2000). SC3 also attaches hyphae to hydrophobic surfaces (Wösten, de Vries, & Wessels, 1993), mediates escape of hyphae from the aqueous environment into the air (Wösten et al., 1999), and makes aerial structures hydrophobic (Wösten et al., 1993; Wösten, Asgeirsdóttir, Krook, Drenth, & Wessels, 1994). The latter is illustrated by the fact that wild type mycelium has a water contact angle of 115 degrees, being similar to the highly hydrophobic surface of Teflon, while water immediately soaks into the mycelium of the Δ*sc3* strain (Wösten et al., 1994).

Here, properties of wild type and Δ*sc3* mycelium of *S. commune* was assessed after growth in the light or in the dark at 400 or 70,000 ppm CO_2. Mycelium of strain Δ*sc3* retained more water with increasing temperature when compared to that of the wild type. Both the absence of SC3 and environmental conditions affected mechanical properties of the mycelium, which can be explained by changes in the density in the mycelium. Together, genetic modification and environmental growth conditions can be used to create a palette of mycelium materials.

Materials and Methods

Strains and culture conditions

S. commune wild type strain 4-39 (CBS 341.81) and its derivative Δ*sc3* (van Wetter et al., 2000) were used in this study. A quarter of a 7-day-old colony grown on minimal agar medium (MM) (Dons, de Vries, & Wessels, 1979) was homogenized in 50 mL MM

for 30 s at low speed using a Waring Blender (Waring Laboratory, Torrington, England). The homogenate was grown for 24 h at 200 rpm and 30°C, after which the culture was homogenized. Static liquid cultures were inoculated by taking up 600 mg wet weight mycelial homogenate in a volume of 6 mL MM and spreading it in a 9 cm Petri dish. Cultures were grown at 30°C in the light (2000 Lux from 5 W LED spot lights (Calex, the Netherlands) or in the dark at 400 or 70,000 ppm CO_2. After 3 days, 30 mL MM was applied underneath the mycelial mat (Lugones et al., 2004) and growth was prolonged for 5 days at 30°C.

Complementation of the Δ*sc3* strain

The coding sequence of *sc3* with 995 bp upstream and 301 bp downstream flanking sequences was amplified by PCR using High-Fidelity Phusion polymerase (NEB, Ipswich, USA). The PCR fragment was cloned into plasmid pUC20Nour that consists of a nourseothricin resistance cassette in a pUC20 backbone (van Peer, de Bekker, Vinck, Wösten, & Lugones, 2009). The resulting vector pUC20sc3Nour was introduced into Δ*sc3* as described (van Peer et al., 2009). A first selection was performed using 8 μg mL^{-1} nourseothricin (Jena Biosciences, Jena, Germany) and 500 μg mL^{-1} caffeine (Sigma, St Louis, MO, USA). Nourseothricin resistant colonies were transferred to a 2nd selection plate containing 20 μg mL^{-1} nourseothricin. Colonies were screened by immunodetection using SC3-antiserum (Wösten et al., 1994). To this end, transformants were grown for 3 days at 30°C on perforated polycarbonate (PC) membranes (Maine Manufacturing, Sanford, ME, USA; pore size 0.1 μm) on MM agar. The colonies with the underlying PC membrane were transferred for 1 h to a fresh MM agar plate on which a PVDF membrane was placed. Immunodetection of SC3 on the PVDF membranes was performed as described (Wösten et al., 1994).

Tensile measurements

Mycelium of two liquid static cultures was dried on top of each other at room temperature. Thickness of the mycelium was measured by a high accuracy length gauge (Heidenhain MT1281, Traunreut, Germany). Tensile measurements of 3 mycelium rectangular specimens (18 x 4 mm) of 5 biological replicas were performed using the Dynamic Mechanical Analyzer Q800 (TA Instruments, New Castle, DE, USA) equipped with an 18 N capacity load cell. The Young's modulus (E) was obtained by taking the stress/strain slope in the 0.10% to 0.15% strain range. The maximum

strength (σ) was obtained from force per unit area, while elongation at breaking point (ε) was obtained by determining the strain (in mm) at the moment of breaking.

Thermogravimetric analysis

Thermogravimetric analysis was performed with a TGA Q50 (TA Instruments, New Castle, DE, USA). Measurements were performed with 25–30 mg of mycelium in a platinum pan under a constant flow of nitrogen gas (60 mL min^{-1}). Temperature increased from 20 to 600°C with a rate of 10°C min^{-1}. Each experiment was performed using biological duplicates.

Chemical analysis of mycelial films with ATR-FTIR spectroscopy

Spectra of mycelia were recorded using a PerkinElmer ATR-FTIR spectrometer with a diamond/ZnSe crystal (PerkinElmer, Waltham, MA, USA). Each spectrum was measured between 4000 cm^{-1} to 650 cm^{-1} and compiled from 10 accumulated scans. Four samples were measured per strain per growth condition. Mycelium was placed with their bottom side facing the crystal.

Scanning Electron microscopy

Mycelium of two liquid static cultures was dried on top of each other at room temperature. Small rectangles (3 x 3 mm) were cut with a scalpel and attached with a 2 mm piece of Scotch tape in a 1 cm ø copper cup. After snap-freezing with liquid nitrogen, samples were transferred to a JEOL 5600LV scanning electron microscope (JEOL, Tokyo, Japan) by the use of an Oxford CT1500 Cryostation. Ice was removed from the sample by sublimation at -85°C. Gold was sputter coated for 2 min, after which micrographs were acquired at an acceleration voltage of 5 kV.

Statistical analysis

Statistical analysis was performed with the software package IBM SPSS statistics 22.0 (IBM Corporation, Armonk, New York) using two-tailed independent-samples *t*-Tests and Pearson correlation analysis ($p \leq 0.05$).

Results and Discussion

Environmental conditions and deletion of *sc3* impact the density of mycelium

Mycelium of the wild type and the hydrophobin deletion strain Δ*sc3* was grown as liquid static cultures (see Material and Methods) in the light or in the dark at 400 ppm (low) or 70,000 ppm (high) CO_2. Density of wild type mycelium grown at low CO_2 in the dark or at high CO_2 in the light was similar (819–1026 kg m^{-3}; Figure 1, Table 1). Lower densities were obtained after growing at high CO_2 in the dark (683 kg m^{-3}) and at low CO_2 in the light (515 kg m^{-3}).

Table 1 Young's modulus (E), maximum tensile strength (σ), elongation at breaking (ε), and density of mycelium of wild type and Δ*sc3 S. commune* strains grown in the light or in the dark at 400 or 70,000 ppm CO_2. n=5; average ±SEM.

Strain	Growth condition	E (MPa)	σ (MPa)	ε (%)	Density (kg m^{-3})
Wild type	Dark, low CO_2	749±49	9.6±1.1	1.2±0.1	819±18
	Dark, high CO_2	550±48	6.5±0.3	1.4±0.1	683±17
	Light, low CO_2	438±40	5.1±0.4	1.3±0.1	515±10
	Light, high CO_2	913±69	9.5±0.6	1.3±0.1	1026±46
Δ***sc3***	Dark, low CO_2	2523±184	33.9±2.8	1.7±0.2	2101±18
	Dark, high CO_2	1237±108	15.6±2.3	1.9±0.1	984±36
	Light, low CO_2	1914±156	22.3±1.5	1.8±0.1	1562±56
	Light, high CO_2	2727±95	40.4±2.5	2.6±0.5	1902±38

The relation between mycelium density, CO_2 and light is not clear yet. Possibly, it results from interacting signaling pathways that respond to light and CO_2. Density of Δ*sc3* mycelium resulting from the different growth conditions followed a similar trend as the wild type but was in all conditions 1.4–3 fold higher (Figure 1; Table 1). As expected (Wösten et al., 1999), scanning electron microscopy revealed that Δ*sc3* mycelium lacked the thick layer of aerial hyphae observed in the wild type that is characterized by a low hyphal density (Figure 2).

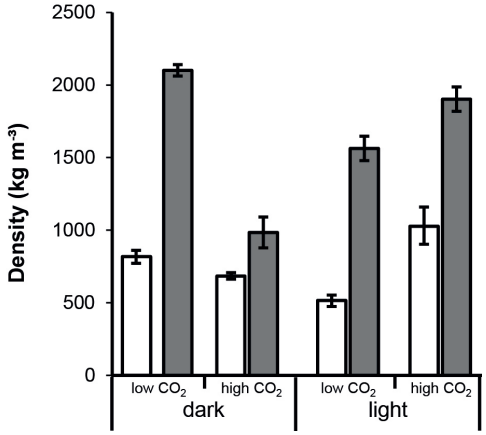

Figure 1 Density of mycelia of liquid static cultures of wild type (non-shaded bars) and Δ*sc3* (grey shaded bars) grown in the dark or light at 400 or 70,000 ppm CO_2.

Lower density of the wild type mycelium is also explained by the fact that hyphae of Δ*sc3*, but not those of wild type, were embedded in a mucilage (Figure 2). This mucilage is most probably schizophyllan that is abundantly released by strain Δ*sc3* (van Wetter et al., 2000).

Environmental conditions and deletion of *sc3* impact mechanical properties of mycelium

Mechanical properties were determined of wild type and Δ*sc3* mycelium grown in liquid static cultures in the light or in the dark at high or low CO_2. The Young's modulus (E) of the wild type strain grown in the light increased from 438 to 913 MPa as a result of increased CO_2 levels (Figure 3A, Table 1).

In contrast, high CO_2 in the dark resulted in a lower E when compared to low CO_2 levels (550 to 749 MPa). Similar results were obtained with the maximum strength (Figure 3B, Table 1). Mycelium of the wild type grown in the dark at high and low CO_2 had a maximum strength (σ) of 6.5 and 9.6 MPa, respectively. These values were 9.5 and 5.1 MPa, respectively, when wild type mycelium was grown in the light. The elongation at breaking of wild type mycelia was between 1.2 and 1.4% and was not affected by the growth conditions (Figure 3C; Table 1).

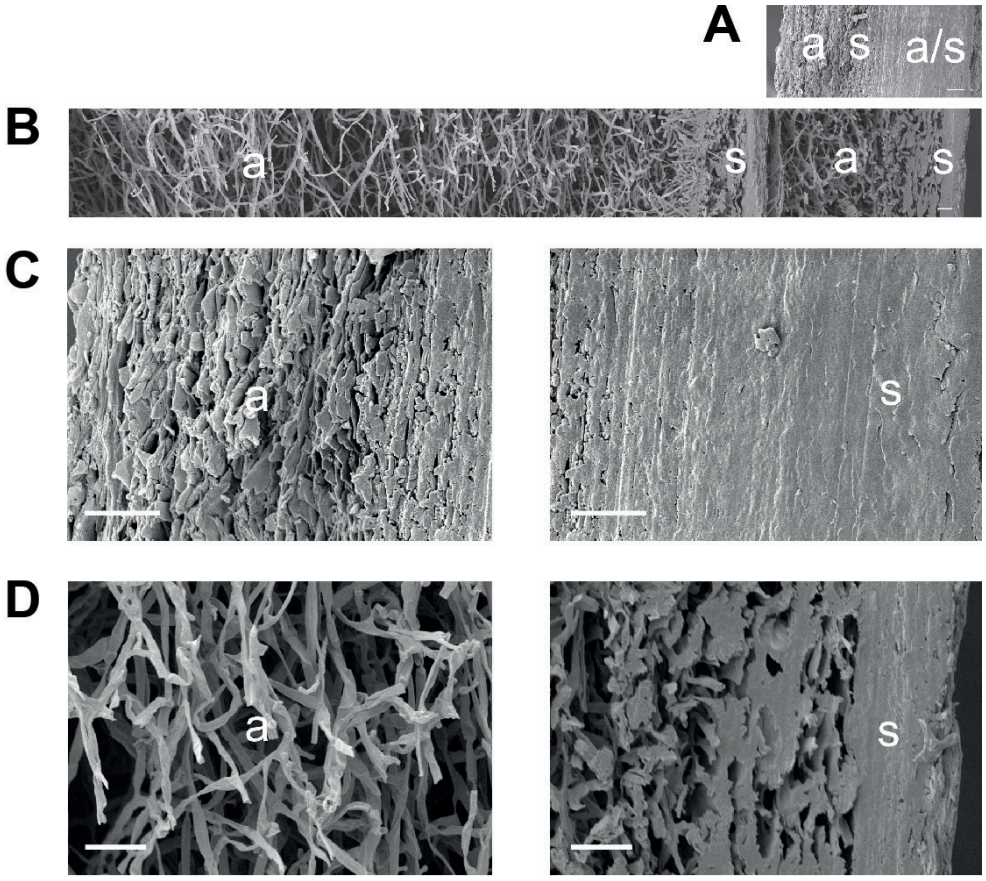

Figure 2 Cryo-SEM microscopy showing an overview (**A, B**) and detailed morphology (**C, D**) of two mycelium layers of *S. commune* Δ*sc3* (**A, C**) and wild type (**B, D**) that had been grown in light and low CO_2 and that had been dried on top of each other (this was required to enable mechanical analysis of strain Δ*sc3*). a indicates air exposed sides of the mycelium during culturing, while s indicates substrate exposed sides. Scale bar represents 10 µm.

Mycelium of Δ*sc3* had a higher E and σ when compared to wild type under all growth conditions (Figure 3AB; Table 1). E of Δ*sc3* grown in the light increased from 1914 MPa to 2727 MPa as a result of increased CO_2 levels (Figure 3A; Table 1). In contrast, an increase in CO_2 in the dark resulted in a decrease of the Young's modulus from 2523 MPa to 1237 MPa. Similar results were obtained with σ (Figure 3B; Table 1). Mycelium of Δ*sc3* grown in the dark at high CO_2 had a σ of 15.6 MPa, while mycelium grown at low CO_2 had a σ of 33.9 MPa. These values were 40.4 and 22.3 MPa, respectively, when mycelium was grown in the light.

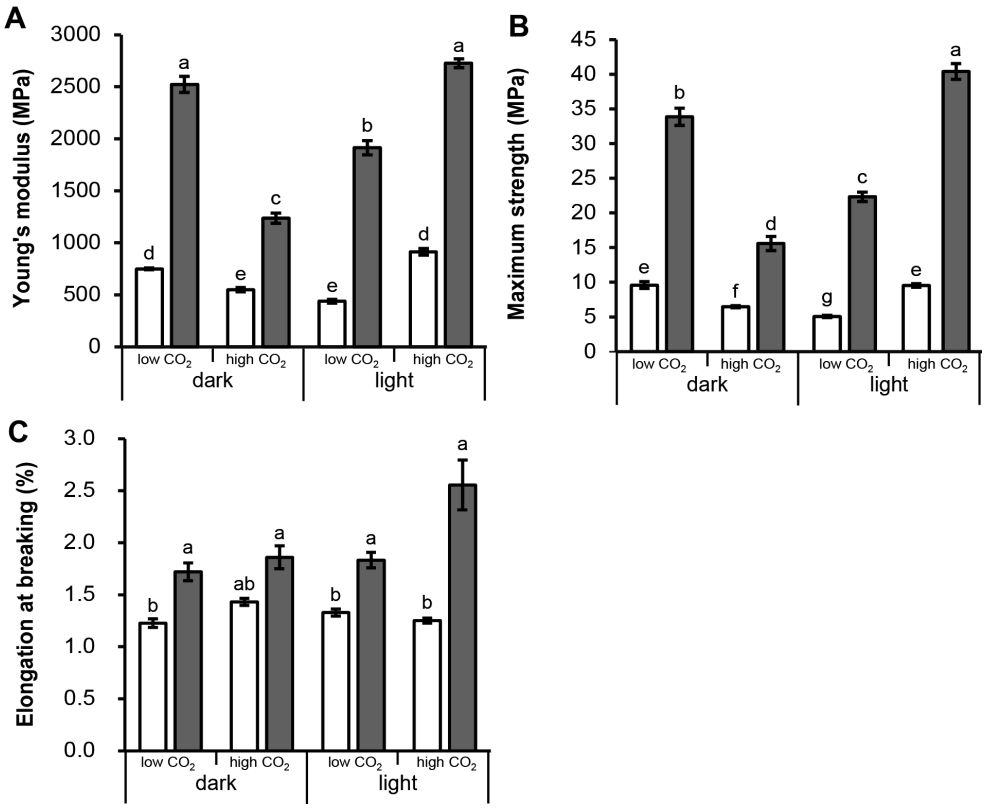

Figure 3 Young's modulus (**A**), maximum tensile strength at breaking (**B**), and elongation at breaking (**C**) of mycelia of liquid static cultures of wild type (non-shaded bars) and Δ*sc3* (grey shaded bars) grown in the dark or light at high or low CO_2. Different letters indicate significant differences (two-tailed independent sample *t*-test, n=15, p<0.05).

Elongation of Δ*sc3* mycelia at breaking was not affected by the environmental conditions (Figure 3C; Table 1), but it was higher than wild type in dark and low CO_2 (1.7 vs 1.2%), light and low CO_2 (1.8 vs 1.3%), and light and high CO_2 (2.6 vs 1.3%).

Reintroducing *sc3* in strain Δ*sc3* restored E, σ, and elongation at breaking to wild type levels (data not shown), showing that the differences in properties between wild type and Δ*sc3* is due to the absence of SC3. E and σ correlated with the density of the mycelium (R^2=0.91 (p<0.01), R^2=0.83 (p<0.01), respectively) as observed with natural composites and polymers (Ashby, 2005). Together, both wild type and Δ*sc3* mycelium behaved as rigid and brittle materials, also indicated by their typical stress strain curves

(data not shown). Notably, E and σ of *S. commune* mycelium were up to 227 and 37-fold stronger when compared to *Pleurotus ostreatus* and *Ganoderma lucidum* (Haneef et al., 2017). However, elongation at breaking was higher for the latter species being up to 13-fold in the case of *G. lucidum.*

Mycelia of wild type and Δ*sc3* have a similar chemical composition as indicated by ATR-FTIR

Chemical composition of the mycelia was determined with attenuated total reflectance Fourier-transform infrared spectroscopy (ATR-FTIR). Spectra of wild type and Δ*sc3* were similar (Figure 4; Table 2) and also did not change with the different environmental conditions (data not shown). As expected (Sietsma & Wessels, 1977), signals originating from lipids and protein were low, while those of carbohydrate were high.

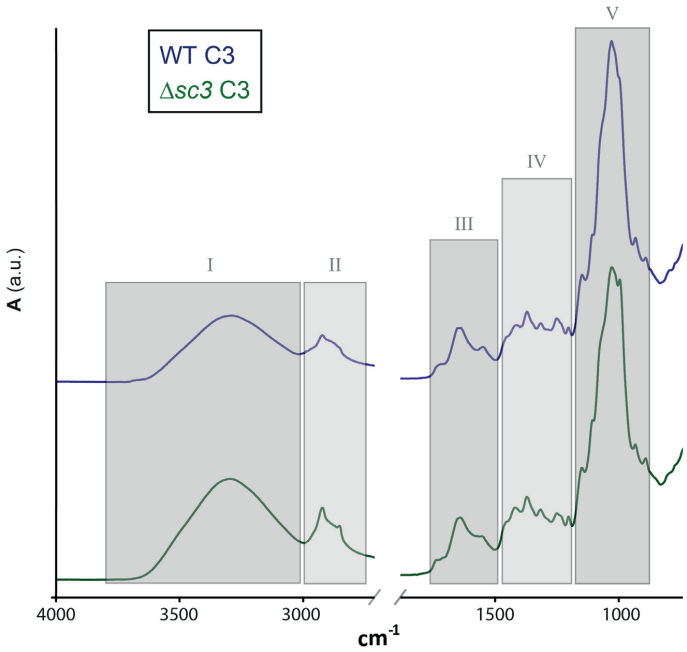

Figure 4 ATR-FTIR spectra of liquid static cultures of *S. commune* wild type and Δ*sc3* grown in light and low CO_2. Similar absorption peaks were observed between strains, indicating that the mycelia had a similar chemical composition. Definition of wavenumber regions I-V can be found in Table 2. Spectra were obtained in quadruple.

Table 2 Wavenumber regions in ATR-FTIR spectral windows and their dominating chemical compounds (linked macromolecules), and functional group assignments. Adapted from Naumann (2009).

Symbol	$\tilde{\nu}$ (cm^{-1})	Macromolecule	Assignment
I	3700-2996	various	O-H, N-H
II	2996-2800	lipid	C-H
III	1800-1485	protein	Amide I + II
IV	1485-1185	Protein, lipid, phosphate compound	CH2, CH3, P=O
V	1185-900	Polysaccharide	C-O-C, C-O-P

Previously, it was shown that Δ*sc3* has an increased amount of schizophyllan and a reduced amount of glucan cross-linked to chitin (van Wetter et al., 2000). ATR-FTIR spectra indicate that the amount of glucan produced by wild type and Δ*sc3* was similar but that the wild type has a higher degree of cross-linking. These results and the correlation between E and σ with density of the mycelium show that differences in mechanical properties between mycelia of wild type and Δ*sc3* grown at different environmental conditions can be explained by the density of the mycelium.

Thermogravimetric analysis of mycelial films

Thermogravimetric analysis revealed that thermal degradation of wild type and Δ*sc3* was most pronounced between ±225 and 300°C (Figure 5), being similar to *P. ostreatus* and *G. lucidum* (Haneef et al., 2017). Notably, weight loss at 100°C differed between wild type and Δ*sc3* irrespective of the growth conditions (7.5% vs 5.0%, respectively, $p < 0.001$, data not shown). This indicates that the absence of SC3 leads to a higher water activity. This is in line with the hydrophilicity of the mycelium of the deletion strain, which is in contrast with the hydrophobic nature of the wild-type hyphae that are in contact with air (Wösten et al., 1993; Wösten et al., 1994).

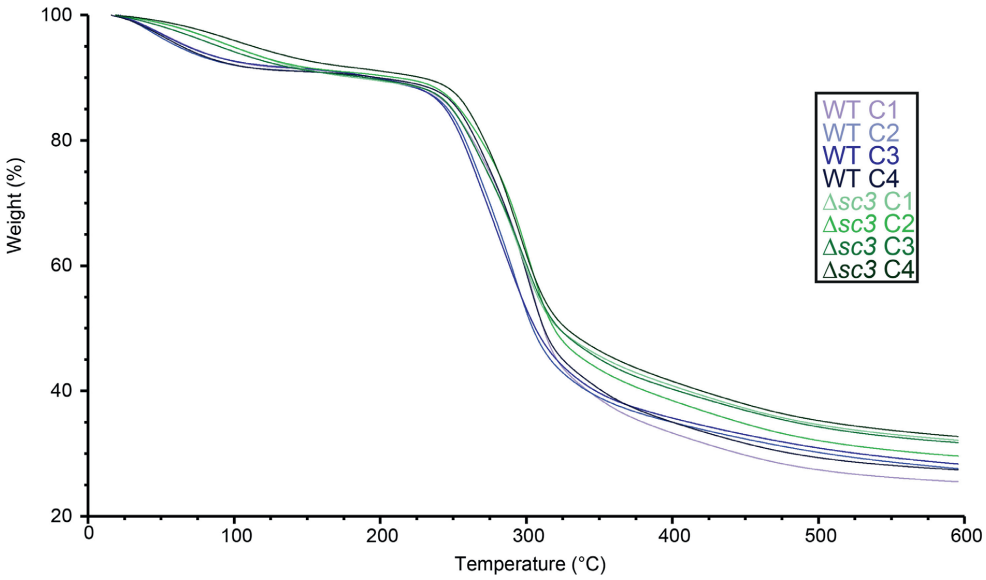

Figure 5 Thermogravimetric analysis of mycelia of *S. commune* wild type and Δ*sc3* grown in the dark at low (C1) and high (C2) CO_2 and in the light at low (C3) and high (C4) CO_2. Experiments were performed in duplicate.

Conclusions

Fungal mycelium offers an attractive bio-based material because of its mechanical properties and by the fact that it grows on low quality waste streams such as straw and sawdust. We here showed that mechanical properties of mycelium of *S. commune* can be changed by adapting environmental conditions and by inactivating the *sc3* hydrophobin gene. E and σ of the deletion strain were 3–4-fold higher when compared to the wild type. Notably, they were up to 227- and 37-fold higher, respectively, when compared to mycelium of *P. ostreatus* and *G. lucidum*. Yet, the latter species formed a more elastic mycelium (Haneef et al., 2017). Both CO_2 and light affected material properties of *S. commune*. For instance, wild type mycelium showed a 1.7-fold higher E in light compared to dark when grown at high CO_2. Conversely, E was 2.1-fold higher when light-grown wild type was cultivated at low and high CO_2. Differences in E and σ between the different strains and culture conditions were shown to be caused by differences in density of the mycelium and not by differences in chemical composition. The mechanical properties of wild type are similar to those of plant materials (e.g. wood, cork, bamboo) and animal material (leather), while those of Δ*sc3* are more similar to thermoplastics (e.g. polyethylene, polypropylene, polyvinyl chloride). This is

mainly caused by increased density and not by increased strength of the material (Figure 6). The palette of fungal materials can be further diversified by treating mycelium chemically or physically.

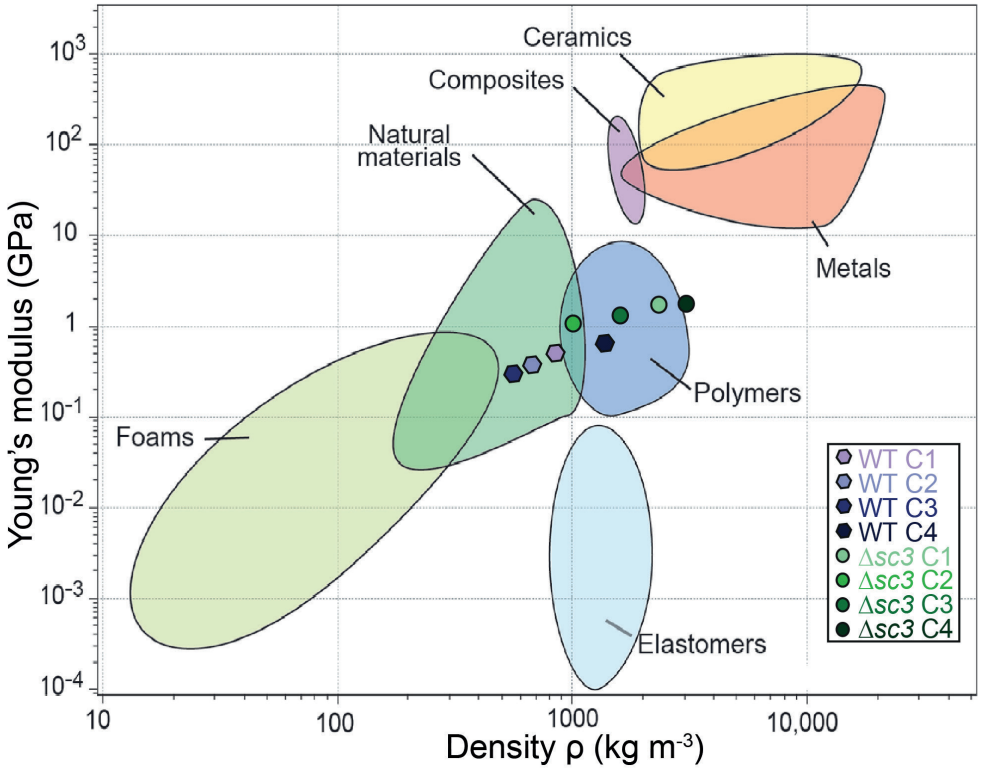

Figure 6 Material family chart of the Young's modulus (E) (GPa) vs density (kg m^{-3}). Mycelium of wild type *S. commune* has properties similar to those of natural materials, while Δ*sc3* mycelium behaves like polymers. Figure adapted from Ashby (2005).

Chapter 5

Mechanical properties of pure mycelium materials resulting from *Schizophyllum commune* liquid shaken cultures

Appels, F. V. W., Dijksterhuis, J., van den Brandhof, J. G., de Kort, G., & Wösten, H. A. B.

Abstract

Fungal mycelium is a promising new class of bio-based materials. So far, pure mycelium materials have been produced using static cultures. Depending on the growth conditions, such mycelium films of *Schizophyllum commune* strain 4-39 have a density of 515–1026 kg m^{-3}, a Young's modulus of 0.438–0.913 GPa, an ultimate tensile strength of 5.1–9.6 MPa, and a maximum strain of 1.2–1.4%. These properties are similar to those found in the natural materials family. We here for the first time assessed properties of mycelium materials resulting from liquid shaken cultures. To this end, *S. commune* 4-39 was grown in defined medium with 20 g L^{-1} glucose. This resulted in a dry weight biomass of 9.1 g L^{-1}, implying a 38% conversion of the carbon source in the medium into mycelium. Drying of the biomass resulted in films with a density of 587 kg m^{-3}, a Young's modulus of 0.468 GPa, an ultimate tensile strength of 5.0 MPa and a strain at breaking of 1.5%. Treating mycelial films with 0–32% glycerol impacted material properties. The largest effect was observed after treatment with 32% of the plasticizing agent. Density and strain at breaking increased to 1435 kg m^{-3} and 29.6%, whereas the Young's modulus and the ultimate tensile strength decreased to respectively 0.003 GPa and 1.8 MPa. Moreover, glycerol treatment changed the surface of mycelium films from hydrophobic to hydrophilic and made the hyphal matrix less permeable for water. Together, liquid shaken cultures of the *S. commune* strain 4-39 result in mycelium materials similar to those of static cultures. Treatment with 8% glycerol and 16–32% glycerol resulted in mycelium materials that are classified within the polymer and the elastomer family of materials, respectively, whereas the non-treated mycelium material is classified within the natural materials family.

Introduction

The use of bio-based materials is part of the transition towards a sustainable economy. Molecules or structures of microbes, algae, plants, and animals are a source for these materials. Thermoplastic starch from plants, polyhydroxyalkanoate (PHA) from bacteria and fungal mycelium are examples of bio-based materials (Appels et al., 2018, 2019; Haneef et al., 2017; Islam, Tudryn, Bucinell, Schadler, & Picu, 2017, 2018; Jones, Huynh, Dekiwadia, Daver, & John, 2017; Keshavarz & Roy, 2010; Curvelo et al., 2001; Chapters 2 & 4). Fungal mycelium consists of hyphae that grow at their tips and that branch subapically. This hyphal network colonizes organic substrates such as

agricultural waste streams. This is accompanied by secretion of enzymes that degrade the organic polymers into molecules that can be taken up by the fungus to serve as nutrients. Mycelium can cover large areas exemplified by an *Armillaria* individual that had colonized almost 10 km^2 of forest (Ferguson, Dreisbach, Parks, Filip, & Schmitt, 2003).

Pure and composite mycelium materials are distinguished (Appels et al., 2018, 2019; Islam et al., 2018; Jones et al., 2017; Chapters 2 & 4). Composite materials are obtained by inactivating the fungus (e.g. by heating) before it has fully degraded the organic substrate. These materials comprise of substrate particles (e.g. sawdust) or fibers (e.g. straw) that are bound together by the mycelial network. Non-post-treated mycelium composites exhibit properties similar to foams such as expanded polystyrene (Appels et al., 2019; Islam et al., 2018; Yang, Zhang, Still, White, & Amstislavski, 2017; Chapter 2). For instance, they have a Young's modulus (E) of 0.14–60 MPa, and a density of 100–390 kg m^{-3}. Their properties depend on the fungus, the substrate and the growth conditions (Appels et al., 2019; Jones et al., 2017; Chapter 2). Post-treatment can change the composite mycelium material properties. For instance, heat pressing results in mycelium materials with a density, elastic modulus and flexural strength similar to that of natural materials like cork (Appels et al., 2018; Chapter 4).

Pure fungal materials are the result of complete degradation of the substrate. Like composite mycelium materials, their properties depend on the substrate, the type of fungus, and its growth conditions (Appels et al., 2018; Haneef et al., 2017; Islam et al., 2017; Przekora, Palka, & Ginalska, 2016; Chapter 4) as well as post-processing. For instance, E of mycelium films of static liquid cultures of *Schizophyllum commune* strain 4-39 ranges between 0.438 GPa and 0.913 GPa when grown at 400 or 70.000 ppm CO_2 (Appels et al., 2018; Chapter 4), while it ranges between 1.237–2.727 GPa in the case of a derived strain in which the hydrophobin gene *sc3* is inactivated (Wösten et al., 1999). This increased strength is caused by the increased density of the mycelium of this deletion strain. Together, mechanical properties of wild type 4-39 and Δ*sc3* mycelium of *S. commune* are similar to those of natural materials (e.g. leather) and polymers (e.g. high density polyethylene) (Ashby, 2005), respectively.

Here, we assessed for the first time the properties of mycelium films resulting from liquid shaken cultures. To this end, *S. commune* 4-39 biomass from liquid shaken cultures was dried and either or not treated with glycerol. Mycelium films of liquid shaken cultures that had not been treated with glycerol had properties similar to those of static cultures. In contrast, glycerol treatment had a large impact by changing the material properties from being similar to natural materials to those of polymers and elastomers. Moreover, glycerol treatment resulted in reduced hydrophobicity and water permeability of the material.

Materials and Methods

Strains and culture conditions

S. commune wild-type strain 4-39 (*MAT*A41*MAT*B41,CBS 341.81) was grown for 5 days at 30 °C in the light in 55 mm diameter Petri dishes containing 10 mL minimal medium (MM) (Dons, de Vries, & Wessels, 1979) solidified with 1.5% agar. The culture was homogenized in 100 mL MM for 30 sec using a Waring Blender (Waring Laboratory, Torrington, England) and grown in a 250 mL Erlenmeyer for 24 h at 200 rpm. Aliquots of this culture (routinely 0.2 g wet weight) were used to inoculate a 2 L Erlenmeyer containing 1.2 L MM. Cultures were grown for 7 days in the dark at 200 rpm. After adding 800 mL of water, the culture was filtered using a Melitta® coffee filter placed in a Büchner funnel (110 mm diameter) that was connected to a vacuum pump (Leybold, Divac 1.2 L, Cologne, Germany). The resulting layer of mycelium was dried after transfer to a flat surface covered with cellophane (Embalru, Nijverdal, Netherlands).

Posttreatment of mycelium materials

Strips of dried mycelium (2x8 cm) were submerged for 24 h in 0–32% aqueous glycerol (Sigma, St Louis, MO, USA) and dried between 2 sheets cellophane at ambient temperature.

Mechanical analysis of mycelium materials

Mycelial films were cut using an ISO 527 type 5A sample cutter attached to a Zwick ZCP 020 manual cutting press (Zwick GmbH, Ulm, Germany). Thickness of the resulting bone shaped samples was measured at 3 points along the axis of the sample

using a digital length gauge device (Heidenhain-Metro MT 1200, Traunreut, Germany). Sample weight was measured after tensile tests performed with a Zwick/Roell Z020 (Zwick GmbH, Ulm, Germany) at room temperature using a preload force of 0.25 N with a 2 mm min^{-1} test speed. Young's modulus (E) was determined at the linear part of the stress/strain curve. The ultimate tensile strength (ε) (in MPa) was obtained from force per unit area, while strain at breaking point (σ) (in %) was obtained by calculating the strain (in mm) at the moment of breaking.

Water contact angle of mycelial films of *S. commune*

Water contact angles were measured with the Drop Shape Analyser DSA 10 Mk2 (KRÜSS, Hamburg, Germany) according to van der Mei et al. (1998). Droplets of 5 µL ultra-pure water were used to measure the contact angle. A baseline was set manually and three technical replicates were measured for each of the 4 biological replicates. The contact angle was measured 10 seconds after placing the droplet.

Analysis of pellet size

The surface area of pellets (n≥49) was determined from photographs using ImageJ v.1.4.7 (Schneider, Rasband, & Eliceiri, 2012).

Statistical analysis

Statistical analysis was performed with the software package IBM SPSS statistics 22.0 (IBM Corporation, Armonk, New York). Differences in pellet size were analysed using a Kruskal-Wallis test ($p \leq 0.05$), while material and mechanical properties of mycelia were analysed by a Welch's t-test followed by a Games-Howell post hoc test ($p \leq 0.05$).

Results

Liquid shaken cultures of *S. commune* 4-39 were grown for 7 days in the dark with 200 or 2000 mg wet weight mycelial homogenate as an inoculum. The surface area of the micro-colonies in these liquid shaken cultures was 11.9 mm^2 and 6.9 mm^2, respectively (Figure 1). Mechanical analysis did not show any statistical significant differences in material properties resulting from these differences in pellet size and hence further experiments were performed using 200 mg inoculum per 1.2 L MM. Total dry weight

biomass was 9.1±0.6 g L^{-1} (N=12, ±s.d.). This implies a 38% conversion of the glucose in the medium into mycelium.

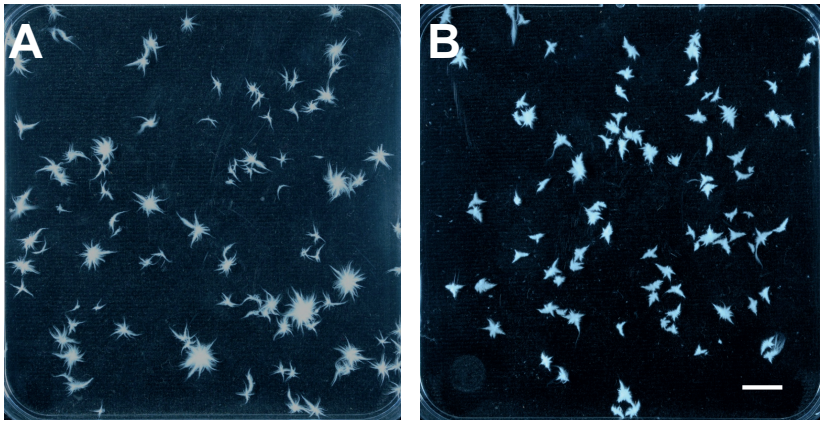

Figure 1 The effect of 200 (**A**) and 2000 (**B**) mg of inoculum on the dimension of pellets in liquid shaken cultures of *S. commune* grown for 6 days at 30ºC and 200 rpm. Scale bar represents 10 mm.

Post-treatment of mycelium

Dried mycelium films were incubated for 24 h in 0–32% glycerol, dried again at room temperature and analysed. Untreated material had a white and brittle appearance. This changed to a brownish, rubbery appearance when mycelium had been treated with ≥8% glycerol (Figure 2). The air voids in untreated mycelium had partly disappeared after treatment with 8% glycerol.

The density of dried mycelium films (587±27 kg m^{-3}) was not statistically different after treatment with water (696±48 kg m^{-3}) or 1% glycerol (769±46 kg m^{-3}) (Table 1). Density did increase after treatment with ≥ 2% glycerol. Densities of 1338±38 kg m^{-3} and 1435±29 kg m^{-3} were observed after treatment with 16 and 32% glycerol, respectively (Table 1). This increased density was not the result of a decreased thickness of the mycelium as was observed in the case of treatment with 2–8% glycerol.

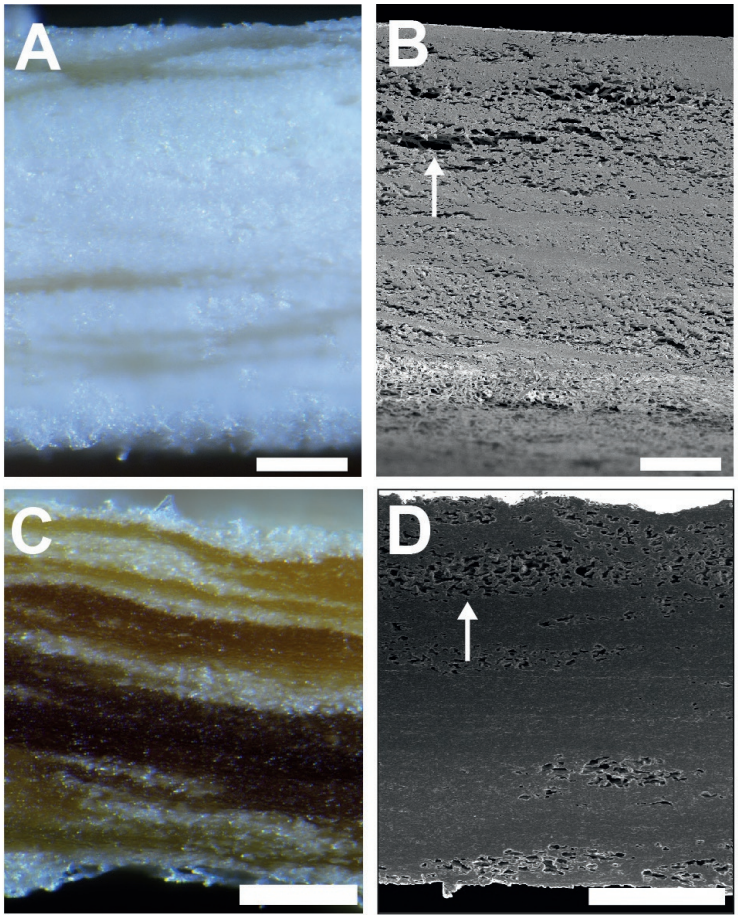

Figure 2 Light microscopy (**A**,**C**) and scanning electron microscopy (**B**,**D**) of untreated mycelium films (**A**,**B**) and films treated with 8% glycerol (**C**,**D**). Scale bars represent 100 µm.

Incubation with 0–2% glycerol resulted in a higher E (1.065±0.163 GPa – 1.048±0.069 GPa) when compared to untreated mycelium (0.468±0.043 GPa), while treatment with 8–32% glycerol resulted in a lower E modulus ranging between 0.124 and 0.003 GPa (Figure 3; Table 1). The ultimate tensile strength (σ) of mycelium treated with water or 1–4% glycerol ranged between 9.6 and 11.2 MPa and was in all cases higher than that of untreated mycelium (5.0±0.5 MPa) (Figure 3; Table 1). In contrast, the ultimate tensile strength of mycelium treated with 8–16% glycerol (6.4±0.7 and 3.6±0.3 MPa, respectively) was not different from the strength of untreated mycelium. Treatment with 32% glycerol resulted in the weakest material showing an ultimate tensile strength of 1.8±0.1 MPa.

Table 1 Thickness (cm), weight (g), density (kg m^{-3}), Young's modulus (E, GPa), ultimate tensile strength (σ, MPa), strain at breaking (ε,%) and water contact angle (WCA) of mycelial films treated with glycerol. Letters following data indicate statistically significant differences to the material specified with that letter (p≤0.05).

	Thickness (cm)	Weight (g)	Density (kg m^{-3})	E (GPa)	σ (MPa)	ε (%)	n	WCA (°)
Control (a)	$0.06\pm0.00^{b-g}$	$0.54\pm0.01^{b-d,g,h}$	$587\pm27^{d-h}$	$0.468\pm0.043^{b-d,f-h}$	$5.0\pm0.5^{b-e,h}$	$1.5\pm0.1^{f-h}$	12	$107\pm3^{f-h}$
H_2O (b)	$0.04\pm0.00^{a,h}$	$0.38\pm0.01^{a,c,e-h}$	$696\pm48^{e-h}$	$1.065\pm0.163^{a,f-h}$	$11.2\pm1.4^{a,g,h}$	$1.2\pm0.1^{e-h}$	16	90 ± 5^{h}
1% glyc (c)	$0.04\pm0.00^{a,h}$	$0.44\pm0.01^{a,b,e-h}$	$769\pm46^{e-h}$	$0.949\pm0.083^{a,f-h}$	$9.6\pm0.8^{a,g,h}$	$1.4\pm0.1^{e-h}$	12	$96\pm1^{f-h}$
2% glyc (d)	$0.03\pm0.00^{a,h}$	$0.45\pm0.02^{a,f-h}$	$994\pm76^{a,g,h}$	$1.048\pm 0.069^{a,e-h}$	$12.3\pm1.2^{a,f-h}$	$2.2\pm0.3^{a,g,h}$	8	90 ± 4^{h}
4% glyc (e)	$0.03\pm0.00^{a,h}$	$0.52\pm0.02^{b,c,g,h}$	$1166\pm74^{a-c}$	$0.688\pm0.059^{d-h}$	$10.1\pm1.0^{a,g,h}$	$3.8\pm0.6^{a-c}$	8	90 ± 4^{h}
8% glyc (f)	$0.03\pm0.00^{a,g,h}$	$0.58\pm0.02^{b-d,g,h}$	$1262\pm37^{a-c,h}$	$0.124\pm0.020^{a-h}$	$6.4\pm0.7^{d,g,h}$	$14.9\pm1.7^{a-c,h}$	12	$70\pm7^{a,c}$
16% glyc (g)	$0.04\pm0.00^{a,f,h}$	$0.81\pm0.03^{a-h}$	$1338\pm38^{a-d}$	$0.021\pm0.004^{a-h}$	$3.6\pm0.3^{b-h}$	$23.7\pm1.7^{a-d}$	8	$72\pm7^{a,c}$
32% glyc (h)	$0.05\pm0.00^{b-g}$	$1.16\pm0.04^{a-h}$	$1435\pm29^{a-d,f}$	$0.003\pm0.000^{a-g}$	$1.8\pm0.1^{a-g}$	$29.6\pm0.9^{a-d,f}$	8	$60\pm4^{a-e}$

Maximum strain did not differ between untreated mycelium films and films treated with 0–1% glycerol with values ranging between 1.2 and 1.5% (Table 1). Higher percentages of glycerol showed an increase in maximum strain up to a maximum strain of 29.6±0.9% at 32% glycerol. Untreated mycelium material was hydrophobic as shown by its water contact angle of 107±3° (Table 1). Glycerol treatment reduced the water contact angle showing hydrophilicity of mycelium (water contact angle <90°) after treatment with ≥8% of the plasticizing agent. Treating mycelium with 32% glycerol resulted in a water contact angle of 60±4°. Water droplets penetrated non-treated mycelium after 5 minutes, while this was not observed when mycelium was treated with 32% glycerol.

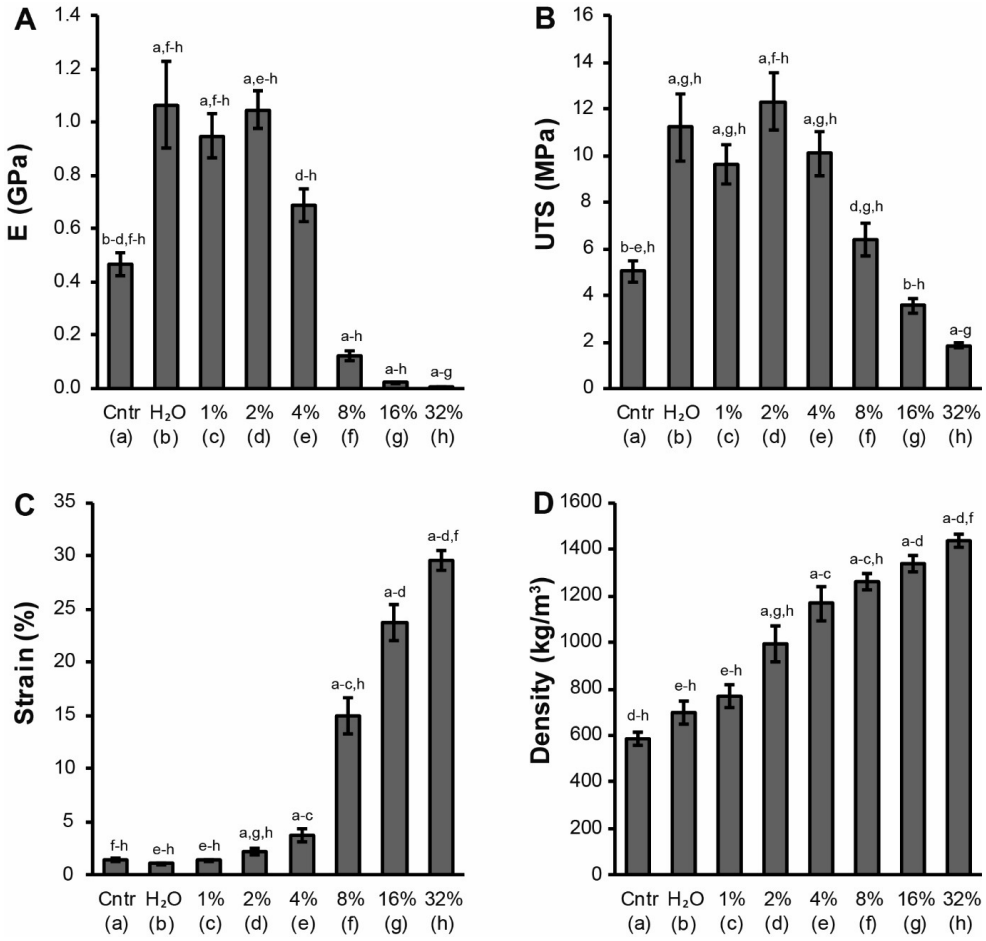

Figure 3 Young's modulus (E) (**A**), ultimate tensile strength (σ) (**B**), strain at breaking (ε) (**C**) and density (**D**) of *S. commune* mycelium films treated with 0–32% glycerol, untreated mycelium films serving as a control. Letters above bars indicate statistically significant differences to the materials specified with that letter ($p \leq 0.05$, $n \geq 8$).

Discussion

Previously, pure mycelium materials were made of static liquid cultures of the wild-type *S. commune* strain 4-39 and the hydrophobin deletion strain Δ*sc3* (Appels et al., 2018; Chapter 2). Density of the resulting wild-type mycelium films was 515–1026 kg m^{-3} depending on the growth conditions. This was accompanied by an E of 0.4–0.9 GPa, a σ of 5.1–9.6 MPa, and a strain at breaking of 1.2–1.4%. Notably, mycelium of the Δ*sc3* strain showed different properties. The E and σ values of this strain were 3–4-

fold higher with values of 1.237–2.727 GPa and 15.6–40.4 MPa, respectively. These values correlated with a 2-fold higher mycelium density, while no differences in chemical composition of the mycelia were observed as shown by ATR-FTIR. Together, materials of the wild type and the Δ*sc3* strain showed similar properties when compared to natural materials and polymers, respectively. Here, we used for the first time liquid shaken cultures and post-treatment with the plasticizing agent glycerol to form mycelium materials. Properties of materials resulting from untreated biomass of liquid shaking cultures were similar to those of static liquid cultures. In contrast, treatment with glycerol impacted the Young's modulus changing the behavior from being similar to natural material like to polymer-, and elastomer-like materials. Thus, we have produced for the first-time mycelium materials that are classified in the latter material group (Figure 4).

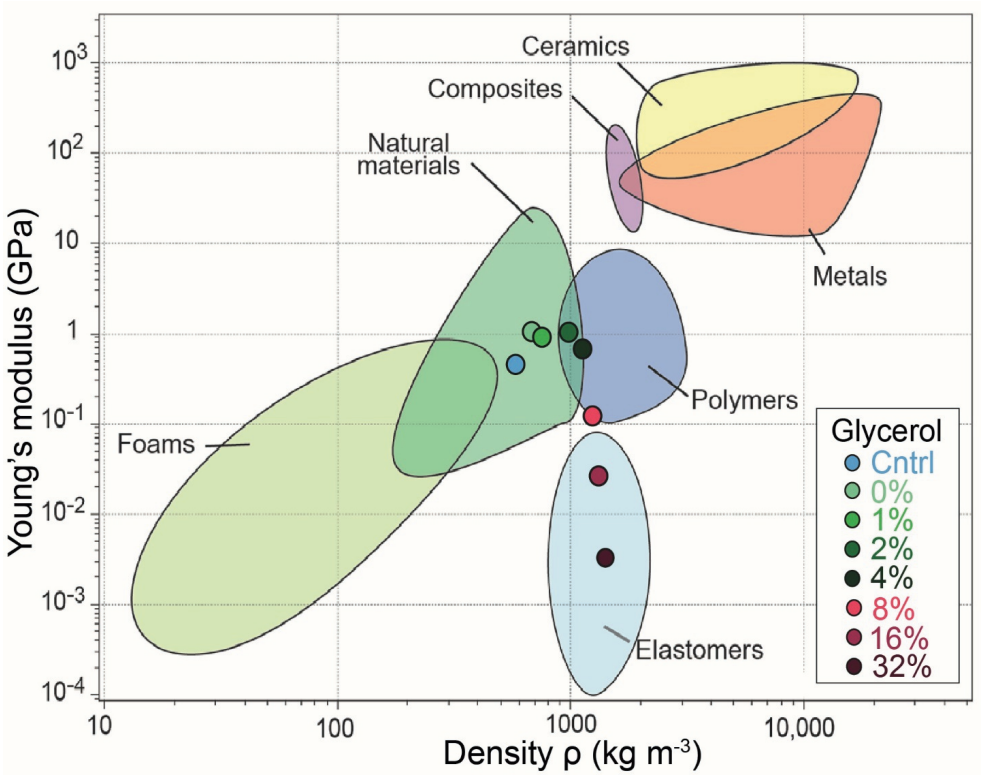

Figure 4 Material family chart of the Young's modulus (E) (GPa) vs density (kg m^{-3}). Mycelium of wild type *S. commune* posttreated or not with different concentrations of the plasticizer glycerol. Figure adapted from Ashby (2005).

Mycelium films treated with 0–2% glycerol were thinner and had a reduced weight when compared to untreated mycelium. The latter can be explained by washing water-soluble proteins and sugars out of the material. The same may occur at higher concentrations of glycerol but here the amount of glycerol penetrating the mycelium compensates for (4–8% glycerol) or is higher (16–32% glycerol) than the removal of water-soluble polymers from the mycelium. Scanning electron microscopy indicates that glycerol fills the air voids that are present in untreated mycelium. The fact that the density of mycelium material treated with 16 or 32% glycerol is higher than that of the plasticizing agent (1338 and 1435 kg m^{-3} versus 1260 kg m^{-3}) implies that glycerol also penetrates the cell walls and the cytoplasm of hyphae. The intra- and extracellular glycerol would also explain why mycelium treated with 8–32% glycerol did not sorb water, while sorption was observed in the case of untreated mycelium despite its highly hydrophobic nature of its surface. This hydrophobicity is explained by the hydrophobin SC3 that coats hyphae with a hydrophobic lining (Wösten, de Vries, & Wessels, 1993; Wösten et al., 1999) and by the presence of air between the hyphae. Treatment with glycerol reduced the water contact angle from 107°±3° to 60±4°. This may be explained by the replacement of the hydrophobic air between the hyphae with the hydrophilic plasticizing agent.

Treatment with glycerol resulted in materials with different mechanical properties. Treatment with 0–2% glycerol resulted in a 2-fold increased E and σ, and a 1.2–1.7-fold increased density when compared to untreated mycelium. In addition, elasticity increased by 50% in the case of 2% glycerol. In contrast, treatment with 8% glycerol resulted in a 2.1-fold increase in density, a 3.8-fold decrease in E, a 1.3-fold increase in σ, and an almost 10-fold increase in elasticity. Treatment with 32% glycerol even showed a 2.4-fold increase in density, a 150-fold lower E, a 2.8-fold lower σ, and a 20-fold higher elasticity when compared to untreated mycelium. The low E together with relatively high density classifies mycelium material treated with 16 or 32% glycerol in the family of elastomers. A decreased E while observing increased density in the case of treatment with ≥8% glycerol contrasts the positive correlation between density and Young's modulus in the case of untreated mycelium (Appels et al., 2018, Chapter 4).

Together, mycelium materials with different density, hydrophilicity, water permeability and mechanical properties can be produced by treating pure mycelial sheets with

glycerol. This widens the spectrum of applications of mycelium materials. For instance, the reduced water sorption of mycelium materials after treatment with glycerol is of interest for outdoor applications.

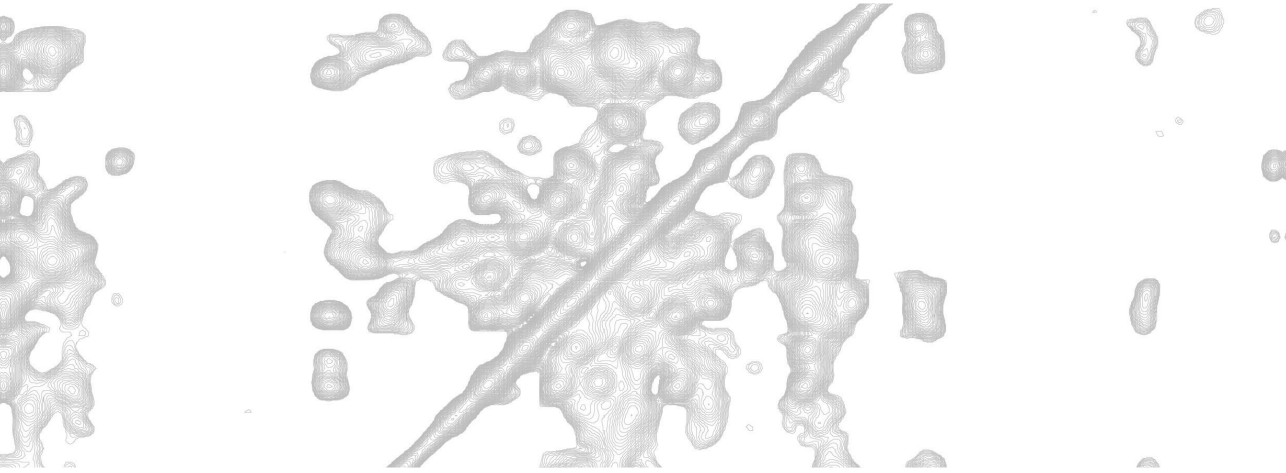

Chapter 6

Characterization of the cell wall of a mushroom forming fungus at atomic resolution using solid-state NMR

Appels, F. V. W., Ehren H. L., Houben, K., Renault, M. A. M., Wösten, H. A. B., & Baldus, M.

Abstract

Fungal cell walls play essential roles in the interaction with the (a)biotic environment and are key to morphogenesis and mechanical strength of hyphae. Here, solid-state NMR (ssNMR) was used for the first time to study the structural organization of the cell wall of a basidiomycete using intact mycelium and samples after destructive treatments. The cell walls of *Schizophyllum commune* consisted of the sugars glucose, N-acetylglucosamine, mannose and fucose. The former two sugars are part of α- and β-glucans and chitin, while the latter two sugars may be part of heteropolysaccharides or homopolymeric fucan and mannan. The mobile fraction of the cell wall showed signals indicative of β-(1,3)-glucan, β-(1,3-1,6)-glucan, α-(1,3)-glucan, α-(1,4)-glucan and homo- or heteropolymeric mannose, while the rigid part of the cell wall gave rise to signals indicative of chitin, β-(1,3)-glucan, β-(1,3)(1,6)-glucan, α-(1,3)-glucan and homo- or heteropolymeric fucose. These findings provide a paradigm shift in the structural organization of the cell wall of the model basidiomycete *S. commune*.

Introduction

The fungal kingdom is diverse with 120.000 identified species and a total predicted number of 3.8 million representatives (Hawksworth & Lücking, 2017). Its two main phyla are the Ascomycota and the Basidiomycota that diverged 500 million years ago (Hibbett et al., 2007). Their representatives degrade dead organic matter, or establish pathogenic or mutual beneficial interactions with plants, animals and microbes. For instance, the mushroom forming fungus *Schizophyllum commune* feeds on fallen branches and timber of deciduous trees and on softwood and grass silage but it can also be an opportunistic pathogen of plants and animals (Ohm et al., 2010).

Cell walls play essential functions in the interaction of fungi with their (a)biotic environment and are key to hyphal morphogenesis and mechanical strength (Gow, Latge, & Munro, 2017). As such, they are of significant interest for the medical, agricultural and biotechnological field as well as for the production of sustainable materials (Gow et al., 2017; Wösten, 2019). Despite their importance, relatively little is known about fungal cell walls. Previous work has shown that the composition of fungal cell walls is dynamic and varies between species, strains, environmental conditions, and developmental stage (Bowman & Free, 2006; Erwig & Gow, 2016). Until recently,

biochemical analysis of fungal cell walls was based on destructive methods using enzymatic and/or chemical treatments. Phosphate buffered saline (PBS) is normally used for gentle washing of cells prior to, e.g., DNA or protein extraction (Andrews & Faller, 1991). More stringent solubilization extraction procedures include SDS (Klis, Groot, & Hellingwerf, 2001) and/or alkali treatment (Sietsma & Wessels, 1977; van Wetter, Wösten, Sietsma, & Wessels, 2000). While these approaches have provided valuable insight into the chemical composition of cell walls, such procedures provide only limited insight into the molecular architecture of intact cell walls. In recent years, solid-state NMR spectroscopy (ssNMR) has made important progress to obtain atomic-level insight into molecular structure and dynamics of complex biomolecular systems including those of cell walls of bacteria (Renault et al., 2012), diatoms (Jantschke et al., 2015) and plants (Dupree et al., 2015). In addition, the intact cell wall structure of the human pathogenic ascomycete *Aspergillus fumigatus* was studied at atomic resolution (Kang et al., 2018). This study indicated that α-(1,3)-glucan has a more important function than previously assumed. It was found to form a dynamic layer together with glycoproteins at the outer part of the cell wall, capping a hydrated matrix of (1,3)-, (1,4)-, and (1,6)-linked β-glucans. In turn, this matrix covers the inner layer of the cell wall consisting of a hydrophobic and rigid scaffold composed of chitin and α-(1,3)-glucan. In contrast, studies in the past indicated that chitin, β-(1,3)-glucan and β-(1,6)-glucan form the rigid part of the *A. fumigatus* cell wall (Bowman & Free, 2006).

In the following solid-state NMR was used to investigate the cell wall of the model species for mushroom formation *S. commune* (Ohm et al., 2010). Comparing ssNMR data obtained on intact preparations with samples after destructive treatments refined our results and allowed us to evaluate previous studies that used enzymatic and chemical treatment. The latter studies had revealed that the cell walls of vegetative hyphae of the basidiomycete *S. commune* consist of glucose (67.6%), N-acetylglucosamine (12.5%), mannose (3.4%), xylose (0.2%), amino acids (6.4%), and lipids (3.0%) (Sietsma & Wessels, 1977). Further work indicated that a water-soluble mucilage of β-(1-3)(1-6)-glucan forms the outer layer of the *S. commune* cell wall (Sietsma & Wessels, 1977). This so called schizophyllan would cover an alkali-soluble α-(1,3)-linked glucan that is partly present in microcrystalline form. The inner layer of the cell wall would consist of randomly oriented chitin microfibrils cross-linked to and

embedded in a highly branched β-(1,3)(1,6)-glucan and would form the alkali-insoluble backbone of the cell wall (Sietsma & Wessels, 1977, 1981; van der Valk et al., 1977).

In the following, it is shown that the mobile phase of the cell wall consists mainly of β-(1,3)-glucan, β-(1,3-1,6)-glucan, α-(1,3)-glucan, α-(1,4)-glucan and mannan residues, while the rigid part consists of chitin, β-(1,3)-glucan, α-(1,3)-glucan and, surprisingly, also fucose. Thus, ssNMR provides new insights in the structural organization of the cell wall of the model basidiomycete *S. commune*.

Materials and Methods

Strain and culture conditions

S. commune wild type strain 4-39 (CBS 341.81) was grown at 30°C for 6 days on a polycarbonate membrane (pore size 0.1 µm; Merckmillipore, Burlington, MA, USA) overlying minimal agar medium (MMA). MMA consisted per liter of 20 g $^{13}C_6$-glucose (Buchem, Netherlands), 0.5 g $MgSO_4$ (Sigma-Aldrich, St Louis, MO, USA), 1.31 g $(^{15}NH_4)_2SO_4$ (Sigma-Aldrich, St Louis, MO, USA), 0.12 mg thiamine-HCl (Sigma-Aldrich, St Louis, MO, USA), 5 mg $FeCl_3$, trace elements (Whitaker, 1951) and 1.5% agar. Cultures were inoculated with mycelium from the periphery of a 7-day-old colony.

Sample preparation

Cultures were harvested from the polycarbonate membranes (see above) and dried at ambient temperature. The mycelium was homogenized twice for 1 minute at 25 Hz in a stainless steel grinder jar containing a metal ball (20 mm diameter) using a Tissuelyser II (Qiagen, Hilden, Germany). The homogenized mycelium was hydrated using ultra-pure water to improve resolution in the spectra of this untreated fraction. Alternatively, the homogenized mycelium was washed twice with PBS buffer (1.15 g $Na_2HPO_4.2H_2O$, 0.2 g KH_2PO_4, 0.2 g KCl, 8 g NaCl per liter, pH 7.4) followed by 3 washes with ultra-pure water. The material was centrifuged for 10 minutes at 6000 *g* (Eppendorf 5920R, Hamburg, Germany) between all washing steps. Part of this fraction was subjected to solid-state NMR (see below), while the rest of the material was extracted 3 times in excess 1% SDS (Sigma-Aldrich, St Louis, MO, USA) for 10 min at 100°C, followed by 3 washes with ultra-pure water. Again, the material was centrifuged for 10 minutes at 6000 *g* between the washing steps. The resulting SDS

extracted cell wall fraction was subsequently incubated in 1 M KOH (Sigma-Aldrich, St Louis, MO, USA) for 20 min at 60°C, after which the pH was set to 5 with acetic acid. The alkali insoluble cell wall fraction was pelleted 15 min at 6000 *g,* washed 2 times with ultra-pure water for 1 min at room temperature by suspending by vortexing. This was followed by a 12-h-washing step with ultra-pure water at 4°C, after which the alkali insoluble cell wall fraction was collected via centrifugation for 15 min at 6000 *g*.

High Performance Liquid Chromatography

Sugar analysis was performed after total hydrolysis of the fungal cell walls with sulphuric acid. To this end, 0.1 g untreated cell wall fraction (see above) was taken up in 2 mL ultra-pure water at 4°C and centrifuged for 15 min at 4000 *g.* The pellet was suspended in 2% SDS, 40 mM ß-mercaptoethanol, 50 mM Tris-HCl, 5 mM EDTA, pH 7.4. After incubating for 10 min at room temperature and centrifugation for 15 min at 4000 *g*, the pellet was resuspended in 1 mL ultra-pure water. After freeze drying, 15 mg of the material was suspended in 225 µL 72% (w/w) sulfuric acid (Sigma-Aldrich, St Louis, MO, USA). After 3 h incubation at room temperature, the sulphuric acid was diluted to 1 M by adding 2.81 mL ultra-pure water. This suspension was incubated for 4 h at 100°C in a water bath. After the suspension was cooled to room temperature, pH was set at 6–8 with 40 g L^{-1} $Ba(OH)_2.8H_2O$ (Sigma-Aldrich, St Louis, MO, USA) and stored for 12 h at 4°C to allow precipitation of $BaSO_4$. After centrifugation for 15 min at 4000 *g*, metabolite concentrations were determined in the supernatant by high-performance liquid chromatography using elution at 60°C with 0.6 mL min^{-1} 5 mM H_2SO_4 and an Aminex HPX-87H column (Biorad) connected to a Waters Alliance e2695 HPLC. Peaks were detected by a refractive-index detector (Waters 2414) and a dual-wavelength absorbance detector (Waters 2489) at 210 nm and 270 nm. Raw data was processed into PeakArea's and concentrations with Empower2 software from Waters.

Solid-State NMR

Magic Angle Spinning (MAS) solid-state NMR (ssNMR) experiments were performed on a Bruker 700 MHz standard bore magnet equipped with an AVANCE-III console using a 3.2 mm MAS Efree HCN triple channel probe or on a 800 MHz wide bore magnet with an AVANCE-III console using a 3.2 mm HNCD MAS probe. Mycelium was filled into standard 3.2 mm MAS rotors. Experiments were recorded at a set

temperature of 260 K and MAS frequencies of either 12 or 13 kHz leading to sample temperatures above 0°C due to frictional heating. ^{1}H, ^{13}C and ^{15}N chemical shifts were referenced externally to histidine and adamantane. ^{1}H and ^{13}C pulses were applied with 70–90 kHz and 45–50 kHz, respectively. Detection of 1D and 2D ^{13}C dipolar based spectra made use of SPINAL 64 proton decoupling (Fung, Khitrin, & Ermolaev, 2000) with field strengths of 70–90 kHz. 10 kHz WALTZ (Shaka, Keeler, & Freeman, 1983) proton decoupling was applied for acquisition of J-based spectra. The 1D spectra were recorded using a 2 sec recycle delay with acquisition times between 8–9 s and 8–17 sec for dipolar based spectra and *J*-based spectra, respectively. Cross-polarization (CP) conditions were optimized using 70–100% ramped ^{1}H pulses, corresponding ^{13}C pulses and contact times between 400 and 1000 µs (Table S1). 1D direct excitation (DE) and CP spectra were processed with line-broadening of 10–30 Hz and 50–100 Hz for the INEPT (Insensitive Nuclei Enhanced by Polarization Transfer (Morris & Freeman, 1979) spectra. The dipolar based 2D ^{13}C–^{13}C Spin diffusion experiments were recorded using a 2 s recycling delay and 10 ms and 4–7 ms acquisition times in the direct dimension (F2) and the indirect dimension (F1), respectively. ^{13}C-^{13}C mixing was propagated through proton driven spin diffusion using Phase-Alternated-Recoupling-Irradiation-Schemes (PARIS) (Weingarth, Bodenhausen, & Tekely, 2010) for 120 ms. The resulting spectra were processed with a 0.25 ϖ shifted sine squared window function in both dimensions. *J*-based INEPT-TOBSY (Total-Through-Bond-Correlation-Spectroscopy) spectra (Andronesi et al., 2004; Baldus & Meier, 1996) were recorded using 6.1 ms mixing time at 145 Hz, 1.5 ms recycle delay and acquisition times of 13–17 ms (F2) and 6-9 ms (F1), respectively. A 0.33 π shifted sine squared window function in both dimensions was used for processing these spectra. Processing of spectra was done with BRUKER Topspin 3.5 and analysis was done with SPARKY (Goddard and Kneller, SPARKY 3, University of California, San Francisco). Chemical shifts described in the literature (Table S2) were used to interpret the ssNMR spectra.

Results

Mycelium of a 6-day-old colony of *S. commune* (Figure 1) was analyzed by ssNMR. Dipolar and *J*-based spectra were recorded of non-treated, PBS-washed, hot-SDS-extracted and alkali-extracted mycelium to probe rigid and mobile components, respectively.

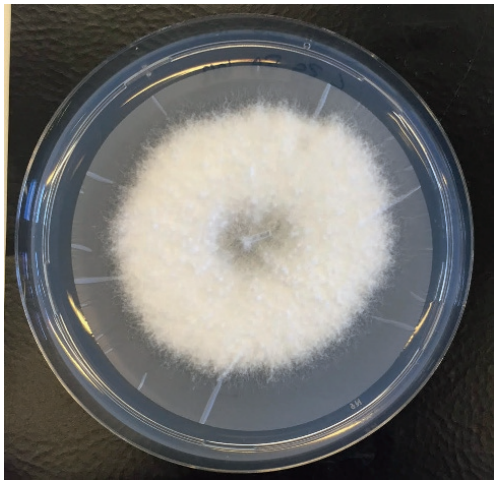

Figure 1 A 6-day-old *S. commune* 4-39 colony grown on a perforated polycarbonate-membrane overlaying solidified minimal medium.

Non-treated homogenized samples represent the whole mycelium. After washing with PBS most of the cytoplasm is removed, while extraction with hot-SDS results in a cell wall fraction. This fraction lacks hot-SDS soluble cell wall molecules including β-(1-3)(1-6)-glucan, while subsequent extraction with alkali has been described to remove α-(1,3)-glucan (Sietsma & Wessels, 1977, 1981) and other alkali-soluble components. 1D ssNMR spectra of the hydrated mycelium showed signals corresponding to sugars, lipids and amino acids (Figure S1). Washing with PBS and extraction with SDS and alkali resulted in a loss of signals in the ^{13}C chemical-shift range between 10–45 ppm in the 1D INEPT spectrum (Figure S1B), indicative of mobile lipids and/or amino acids species (Figure S1B). Loss of signals within this region was also observed in the CP spectra used to probe rigid components (Figure S1C). The spectra also showed a reduction of polysaccharide signals resulting from the washing and extraction steps (Figure S1).

To obtain a more detailed understanding of the molecular composition of the intact cell wall preparation, two-dimensional (2D) ^{13}C-^{13}C *J*-based INEPT-TOBSY (Figure 2A & C) were recorded as well as dipolar-based ^{13}C-^{13}C correlation spectra (Figure 2B). The resulting correlation pattern was analyzed in reference to published literature data (Table S2 and S3). Polysaccharide signals were indicative of β-(1,3)(1,6)-glucan ($B^{a,b,d}$, NRb in Figure 2), α-(1,4)-glucan (A^{a}), α-(1,3)-glucan (A^{b}),chitin (Ch^{a-c}), fucan (F) and mannan ($M^{a,b}$).

Here, $B^{a,b,d}$ is the backbone of β-(1,3)(1,6)-glucan with C6-linked single glucose monomers (NRb). The incomplete spin system A^{b} showed signals indicating presence of either α-(1,3)-glucan or α-(1,6)-glucan. However, as literature describes an important role for α-(1,3)-glucan and not α-(1,6)-glucan in the cell wall of *S. commune* (Sietsma & Wessels, 1977, 1981; van der Valk et al., 1977) it was decided to assign A^{b} as α-(1,3)-glucan. Moreover, spin systems were found suggesting a significant abundance of reducing ends of β-(1,3)-glucan (Rb), reducing ends α-(1,4)-glucan (Ra^{b}), and reducing ends of α-(1,3)-glucan (Ra^{a}).

Next, a series of 2D ^{13}C-^{13}C PARIS spectra (that utilize dipolar transfer and thus report on rigid molecules) was analyzed to examine the effect of washing and extraction on the resulting ssNMR signature. In Figure 3, ssNMR data are compared of hydrated (A), PBS-washed (B), SDS-extracted (C) and alkali-extracted (D) mycelium of *S. commune* recorded with 120 ms mixing time showing major rigid components. Peaks obtained from hydrated mycelium (Figure 3A) corresponded to β-(1,3)-glucan, chitin, and non-reducing ends of β-glucan and α-(1,3)-glucan. Moreover, a spin system was found with a chemical shift of 18.6 ppm indicative of the presence of a methylated hexose like fucose. HPLC confirmed the presence of fucose (Figure S2). The intensity of fucose was however lower than intensities for other sugars.

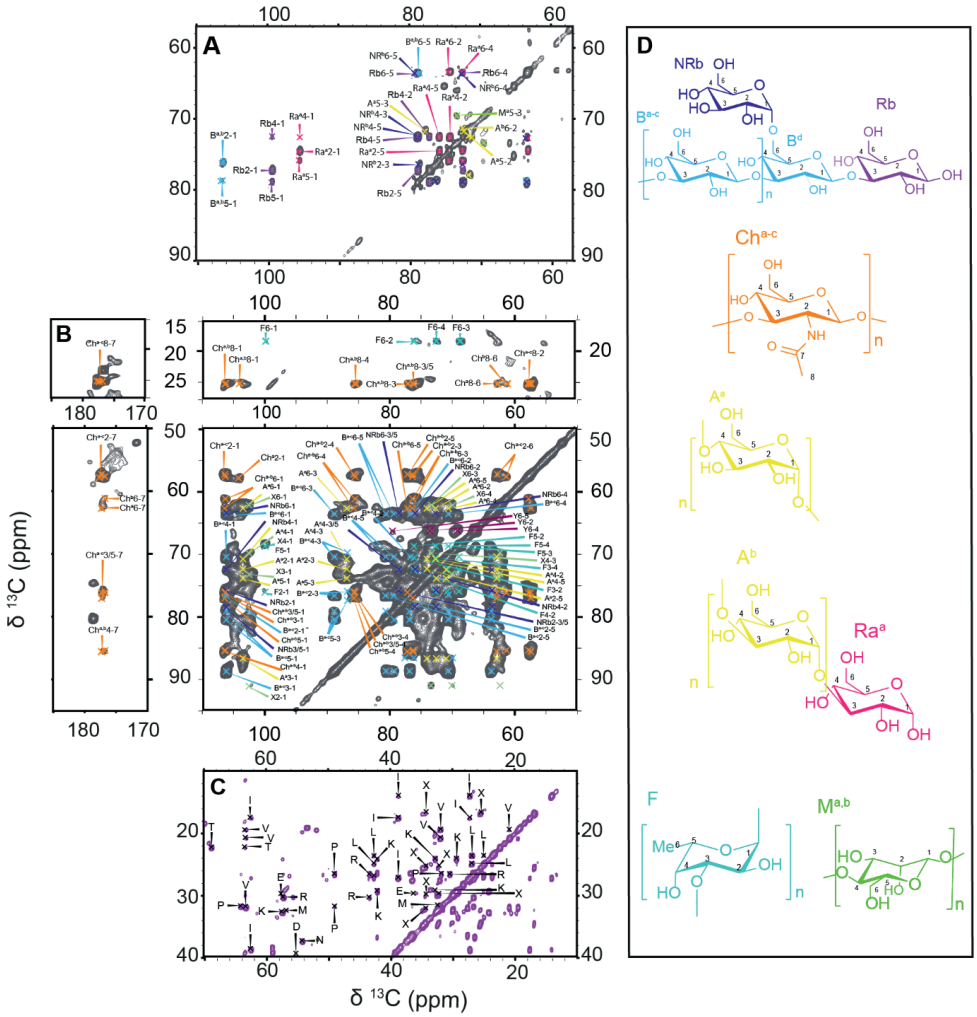

Figure 2 Spectral cutouts of 2D (^{13}C,^{13}C) INEPT (**A**), PARIS (**B**) and INEPT TOBSY (**C**) experiments, revealing different amino acids and polysaccharides (indicated in **D**). (**D**) Molecular structures of β-1,3-glucan ($B^{a,b,d}$, light blue); non-reducing end β-1,3-glucan (NRb, dark blue); reducing end β-1,3-glucan (Rb, purple); chitin (Ch^{a-c}, orange); fucan (F, turquoise); mannan (M, green), α-1,4-glucan (A^a, olive green), α-1,3-glucan (A^b, yellow); reducing end α-1,4-glucan (A^d, brown) and reducing end α-1,3-glucan (Ra^a pink). Chemical shifts belonging to the sugar molecules are shown in Table S2. For increased readability see: Appels, 2020.

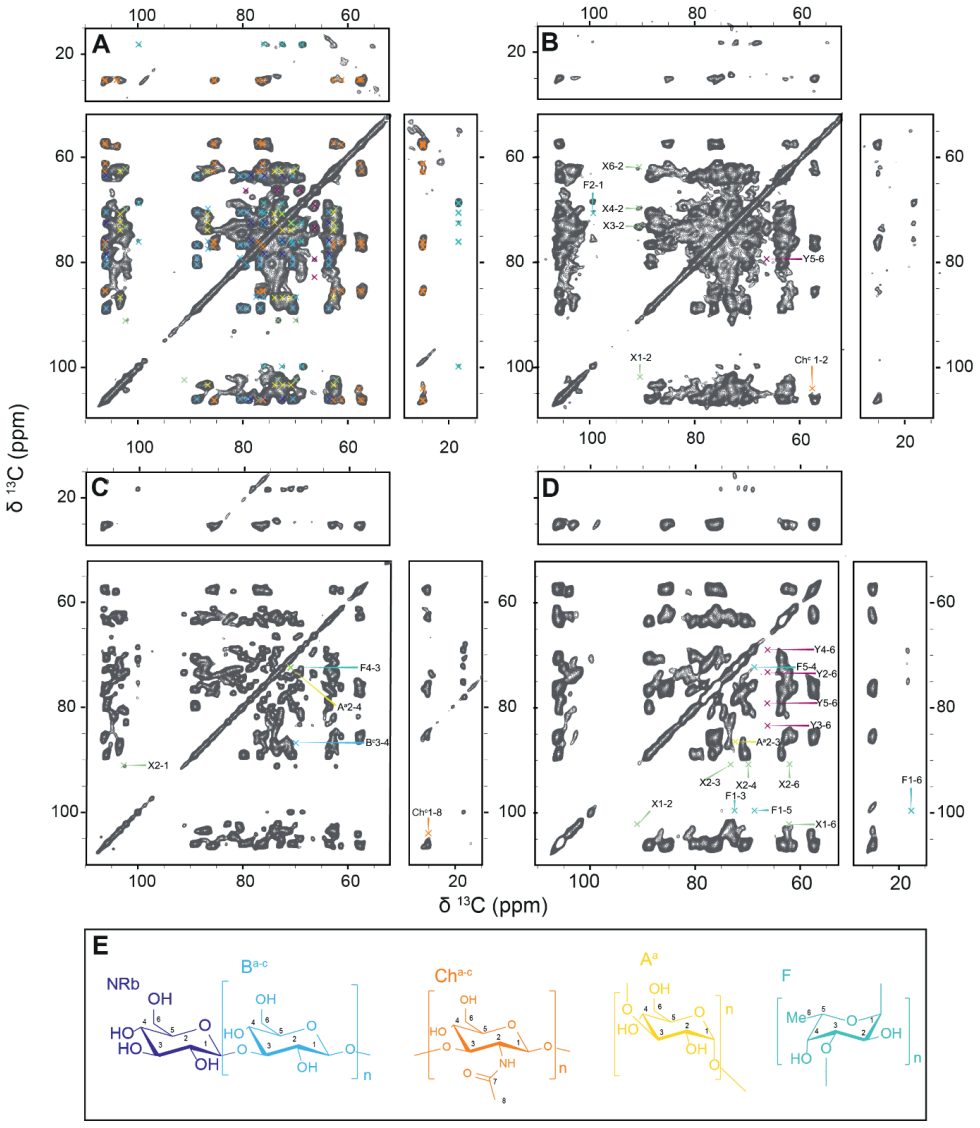

Figure 3 Two-dimensional ^{13}C-^{13}C PARIS spectra of hydrated (**A**), PBS-washed (**B**), SDS-extracted (**C**) and alkali-extracted (**D**) mycelium of *S. commune* recorded with 120 ms mixing time showing major rigid components. Changes in the spectra arising from sequential washing steps are depicted in panel B, C and D. Molecular structures are shown in panel **E**. β-1,3-glucan (B^{a-c}, light blue); non-reducing end β-1,3-glucan (NRb, dark blue); chitin (Ch^{a-c}, orange); fucan (F, turquoise); α-(1,3)-glucan (A^a, yellow). For increased readability see: Appels, 2020.

Peak intensities of the hydrated mycelium suggest that β-(1,3)-glucan is the most abundant sugar in the rigid part of the cell wall followed by a relatively high abundance of chitin (Figure S3). The C1 of β-(1,3)-glucan ranged between 106.0 and 106.4 ppm. Peak doubling was observed for C5 as indicated by peaks observed at 77.4 ppm, 79.2 ppm and 80.5 ppm, suggesting different spatial structures or chemical environments. Three different forms of chitin were identified by the C7 and C8 of N-acetylglucosamine showing chemical shifts ranging between 176.8–177.7 ppm and 24.9–25.0 ppm, respectively. Moreover, chemical shifts of C1 ranged between 104.1–106.3 ppm and those of C6 ranged from 61.2 ppm to 62.7 ppm. These different conformations might be caused by the orientation of the chitin strands or a heteropolymeric nature of the polysaccharide resulting from crosslinks to other sugars such as β-glucan. Furthermore, we could distinguish α-glucan from β-glucan by a downfield shift of C1 from 106.0–106.4 ppm to 103.4 ppm. A downfield shift of C3 from 86.6–88.7 ppm to 78.4 ppm suggests the presence of non-reducing ends of β-glucan. This non-reducing end is most likely the C6-linked monomeric glucose subunit of β-(1,3)(1,6)-glucan.

Washing the hydrated mycelium with PBS resulted in only minor changes of the recorded chemical shifts (Figure 3B, Table 1). In general, less intense cross peaks were observed within the aliphatic region (10–45 ppm, data not shown). On the other hand, additional peaks belonging to fucose and the correlations of an unidentified molecule X became visible. The latter molecule and correlations denoted by Y in Figure 3B that only appeared before washing remain currently unassigned. Extracting the PBS-washed mycelium with SDS removed all protein/lipid signals (data not shown) but enhanced resolution of the spectrum (Figure 3C). The lost signal belonging to X in PBS-washed mycelium was resolved again in the spectrum of SDS extracted material, whereas some signals belonging to β-(1,3)-glucan, α-(1,3)-glucan and fucose were lost when compared to PBS-washed mycelium. Subsequent extraction with alkali further improved resolution of the spectra. Signals belonging to the unidentified molecules X and Y were removed, while decreased signal intensity was found for fucan and α-(1,3)-glucan. Remaining signals belonged to β-(1,3)-glucan, β-(1,3)(1,6)-glucan and chitin.

Table 1 Chemical shifts of molecular moieties found within the recorded spectra based on literature values (see Table S2).

	MOLECULE		C1	C2	C3	C4	C5	C6	C7	C8
INEPT	→3)-β-Glcp-(1→	B^a	105.0	75.3	87.3	70.5	77.9	63.1		
	→3)-β-Glcp-(1→	B^b	105.2	75.5	86.3	70.4	78.0	63.1		
	→3,6)-β-Glcp-(1→	B^d	103.3	72.1				68.2		
	β-Glcp-(1→	NRb	105.4	75.6	78.0	71.9	78.2	63.2		
	→3)-β-Glcp	Rb	98.4	76.8		72.1	78.4	63.2		
	→4)-α-Glcp-(1→	A^a		71.1	77.2	78.0	71.1			
	→3)-α-Glc-(1→	A^b	100.6	72.4		71.1				
	Reducing end α-(1,3)-glucan	Ra^a	90.2	72.5		78.8				
	Reducing end α-1,4-glucan	Ra^b	94.7	74.0	75.4	72.2		63.1		
	Mannan/galactan	M^a		76.1	73.2	79.1	69.7	63.9		
		M^b	102.3	74.4	73.2		69.1			
PARIS	chitin	Ch^a	106.3	57.3	76.2	85.5	77.1	62.7	177.3	24.9
		Ch^b	106.2	57.7	76.2	85.4	76.2	61.2	176.8	25.0
		Ch^c	104.1	57.9					177.7	24.9
	→3)-β-Glcp-(→1	B^a	106,0	76.7	88.7	70.5	80.5	63.6		
		B^b	106,0	76.7	88.7	70.5	79.2	63.6		
		B^c	106.4	76,0	86.6	69.8	77.4	63.1		
	β-Glcp-(1→	NRb	106,0	75.6	78.4	72.4	78.4	63.5		
	→3)-α-Glcp-(1→	A^a	103.4	72.5	86.7	70.5	73.9	62.7		
	→3)-α-Fuc-(1→	F	99.8	70.5	76.0	72.5	68.7	18.2		
		X	102.4	91.0	73.3	69.8		62.2		
		Y		73.2	82.9	69.1	79.5	66.0		

Next, the occurrence of mobile molecular species in different cell preparations was analyzed. In Figure 4, two-dimensional (^{13}C-^{13}C) INEPT-TOBSY spectra are shown that resulted from hydrated (A), PBS-washed cells (B), SDS-extracted (C) and alkali-extracted (D) mycelium. Peaks obtained from hydrated unwashed mycelium were indicative of mobile parts of β-(1,3)-glucan ($B^{a,b}$, Figure 4A), non-reducing ends of β-glucan (NRb; indicative of presence of β-(1,3)(1,6)-glucan), α-(1,4)-glucan (A^a), α-(1,3)-glucan (A^b), reducing ends of α-(1,3)-glucan (Ra^a), reducing ends of α-(1,4)-glucan (Ra^b) and mannan (M^a). β-glucan and α-glucan were distinguished by their different C1 chemical shifts. The C1 chemical shifts for α-(1,3)-glucan were found at

100.6 ppm (A^b), while the C1 shifts for β-glucans ranged between 103.3 ppm (B^d) and 105.2 ppm (B^b). The non-reducing end of β-glucan is indicated by a downfield shift for C3 from 86.3–87.3 ppm for $B^{a,b}$ to 78.0 ppm for NRb. The reducing ends were identified by their relatively low C1 chemical shift; for β-(1,3)-glucan (Rb) 98.4 ppm compared to 105.0–105.2 ppm and for α-(1,4)-glucan (Ra^b) 94.7 ppm instead of 100.6 ppm. A spin system was found that corresponds to mannan (Table 1). The presence of mannan was confirmed by HPLC with a peak at a retention time of 9.681 minutes that corresponds to galactose or mannose (Figure S2).

More intense signals were found for non-reducing ends of glucans after washing mycelium with PBS (Figure 4B). A spin system was found with chemical shifts of C1 of 103.3 ppm, C2 of 72.1 ppm and a strong C6 signal at 68.2 ppm, possibly belonging to a β-(1,3)(1,6)-glucan. Signals belonging to mannan (M^a) showed more intense and new peaks. Due to the absence of a signal corresponding to C1 it is not possible to discriminate between α-, or β-mannan. Signals of some polysaccharides (e.g. $B^{a,b}$) were more pronounced after SDS extraction of PBS-washed mycelium (Figure 4C). In contrast, signals of α-(1,3)-glucan (A^b), mannan (M^a) and reducing ends of β-(1,3)-glucan (Rb) and α-(1,3)-glucan (Ra^a) disappeared. In addition, signals of a new species of mannan (Mb) and the reducing end of α-(1,3)-glucan (Ra^a) became visible. Finally, alkali treatment (Figure 4D) resulted in signals indicating the presence of α-(1,4)-glucan (A^a), two species of β-(1,3)-glucan ($B^{a,b}$) and the non-reducing end of β-(1,3)-glucan. The latter is indicative of the C6 linked glucose subunit of β-(1,3)(1,6)-glucan.

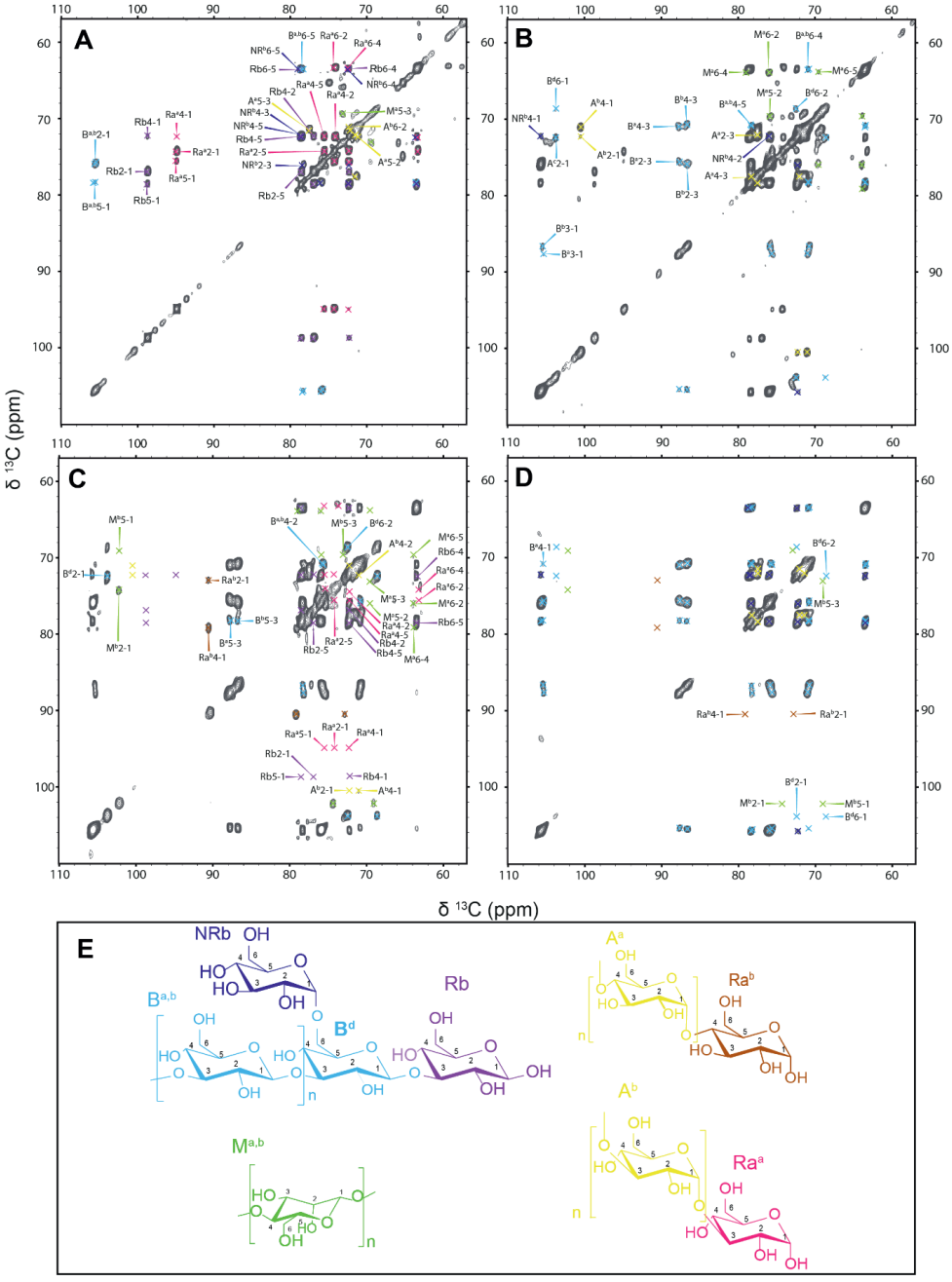
A
B
C
D
E
δ 13C (ppm)
δ 13C (ppm)
NRb OH
Rb
Ba,b
Bd
Ma,b
Aa
Ab
Raa
Rab

Figure 4 (p.90) Two-dimensional (^{13}C-^{13}C) INEPT-TOBSY spectra obtained on hydrated (**A**), PBS-washed (**B**), SDS-extracted (**C**) and alkali-extracted (**D**) mycelium of *S. commune*. Signals appearing as a result of the washing step are annotated in the upper left part of the panels in **B**, **C** and **D**. Signals disappearing after the washing procedure are annotated lower right part of the panel. All chemical shifts belonging to the specific molecule are shown in Table 1. Molecular structure of molecules are shown in panel **E**; β-1,3-glucan ($B^{a,b,d}$, light blue); non-reducing end β-1,3-glucan (NRb, dark blue); reducing end β-1,3-glucan (Rb,purple); mannan ($M^{a,b}$ green), α-1,4-glucan (A^a, olive green), α-1,3-glucan (A^b, yellow); reducing end α-1,4-glucan (Ra^b, brown), reducing end α-1,3-glucan (Ra^a, pink). For increased readability see: Appels, 2020.

Discussion

The phylum Basidiomycota contains 16 classes, 52 orders, 177 families, 1589 genera and more than 30,000 species (Hibbett et al., 2007). Approximately 32% of the described fungal taxa thus belong to this phylum (Dai et al., 2015). The Basidiomycota includes mushroom forming fungi as well as microfungi, such as rusts, smuts and yeasts. The composition and structural organization of the cell walls of basidiomycetes have not been well studied despite their importance for the lifestyle of these fungi and their medical implications. Moreover, it has been well established that fungal cell walls contain molecules with bioactive properties. For instance, schizophyllan (Wasser, 2003) and the hydrophobin SC3 (Akanbi et al., 2013; Wösten & Scholtmeijer, 2015) of *S. commune* have been shown to have anti-tumor activities.

Cell wall composition of the basidiomycete *S. commune* has been previously analysed (Sietsma & Wessels, 1977, 1981; van der Valk et al., 1977). To this end, cell walls were extracted by aqueous SDS and alkali treatment followed by sugar analyses and transmission electron microscopy. This revealed that the cell wall of *S. commune* consists of a water-soluble mucilage of β-(1-3)(1-6)-glucan covering an alkali-soluble α-(1,3)-linked glucan. The most inner layer of the cell wall was found to consist of chitin cross-linked to and embedded in highly branched alkali-insoluble β-(1,3)(1,6)-glucan. To improve our understanding of the basidiomycetous cell wall architecture, ssNMR was used on hydrated mycelium of *S. commune* and compared to spectra after washing the mycelium with PBS followed by subsequent extractions with SDS and alkali. For every treatment the material was studied using ssNMR techniques revealing

molecules that are either rigid or exhibit a significant degree of molecular mobility. Mobile molecules were found to be more impacted by the washing and extraction steps compared to the rigid cellular components. Hydrated mycelium preparations showed intense and well resolved resonances from flexible lipids, polysaccharides and amino acids as detected by J-based ssNMR spectra. On the other hand, rigid cell components revealed with dipolar spectra were largely dominated by polysaccharide signals. Most intense ssNMR signals representing rigid polysaccharides were found for β-(1,3)-glucan followed by a relatively high abundance of chitin. Moreover, a significant abundance of signals of the non-reducing end of β-glucan was found, most likely originating from the C6-linked glucose subunit of β-(1,3)(1,6)-glucan. The previously found signals for β-(1,3)-glucan are therefore thought to belong to the backbone of β-(1,3)(1,6)-glucan. The presence of this polymer would be in accordance to previous findings in literature (Sietsma & Wessels, 1981; Sonnenberg, Sietsma, & Wessels, 1982). Washing the cellular material with PBS and subsequent extraction with SDS and alkali did not lead to major changes of rigid cell wall associated sugars. Instead, lipid/protein signals exhibiting rigid behaviour were reduced, mostly as a result of PBS washing. The loss of protein signal was unexpected as the fungal hydrophobin SC3 is known to form hot-SDS insoluble cell wall bound complexes (de Vries et al., 1993). Possibly, the relative abundance of SC3 compared to cell wall sugars is too small for the ssNMR methods used in our current study. More sophisticated spectral filtering methods may be used in the future to further analyse such species. Interestingly, fucose was identified in the rigid cell wall fraction after alkali extraction. The role of fucose in cell walls of basidiomycetous fungi is rarely described (Bartnicki-Garcia, 1968; Rhode, Cornelius, Rimington, Roets, & Fourie, 1958). To our knowledge, this is the first time that fucose is shown to play a role in the rigid alkali resistant part of the cell wall.

Notably, J-based ssNMR experiments revealed that flexible molecules can be alkali resistant and that an α-glucan, possibly α-1,4-glucan, plays a role in the alkali-resistant core of the cell wall. INEPT spectra of intact hydrated cellular material were dominated by flexible β-glucan and α-glucan signals. Signals were found that indicate the presence of non-reducing ends for β-glucan and are, again, most likely the C6 linked glucose subunit of β-(1,3)(1,6)-glucan. Reducing-ends of α-, and β-glucans were also found. These signals became less pronounced with PBS washing and subsequent

SDS/alkali extraction steps. Most likely washing and extraction methods removed these molecules. However, it is also possible that spectra are increasingly dominated by other polysaccharides due to increased mobility of these molecules. Increased mobility could be the result of increased water accessibility of glucan layers resulting from loosening by the harsher extraction methods.

Signals belonging to the mannan species M^a increased mostly after PBS washing. This increase could be the result of increased mobility of mannan or increased visibility in the spectrum due to removal of PBS soluble cell components. A different mannan species (M^b) became visible after SDS extraction while signals from the mannan species M^a were lost. Glycosyl-linkage analysis should identify the mannan species in the future.

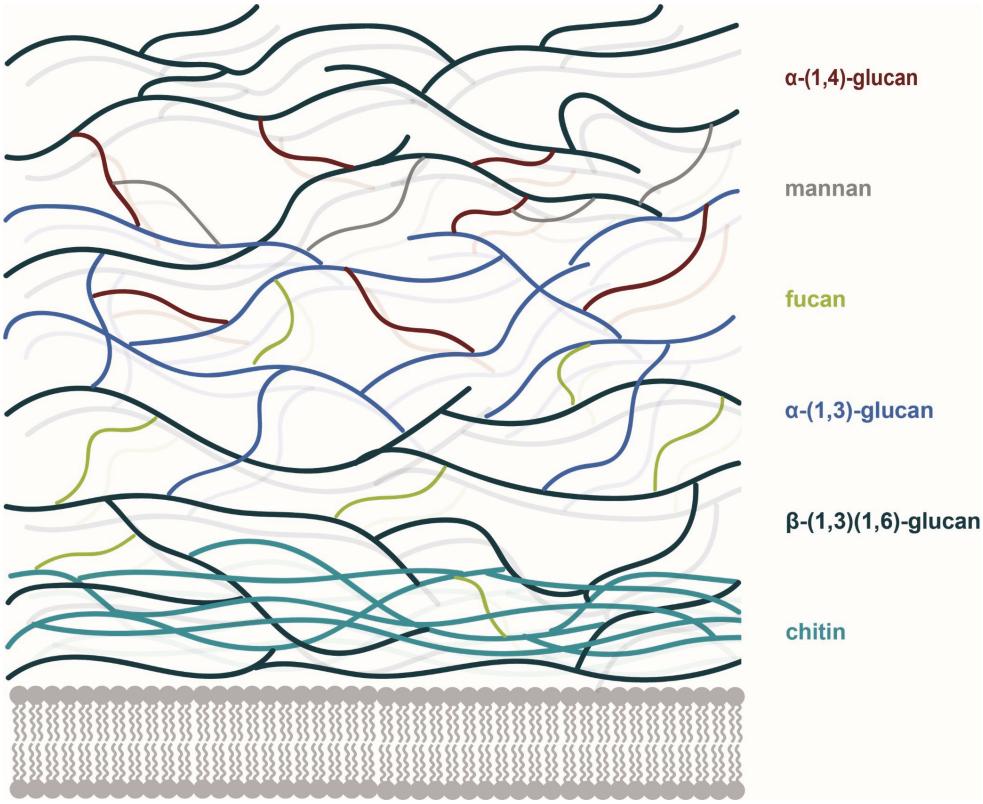

Figure 5 Model of the *S. commune* cell wall structure focusing on sugar composition. Adapted from Kang et al., 2018.

Taken together, our current study demonstrates the use of ssNMR to probe rigid and mobile species in intact molecule cell species. The ssNMR experiments on *S. commune* cell preparations after different extraction methods allowed us to identify further molecular species. Compared to previous studies, our data suggest that the rigid part of the cell wall of the model basidiomycete *S. commune* not only contains chitin and β-(1,3)(1,6)-glucan but also α-(1,3)-glucan and homo- or heteropolymeric fucose. Moreover, signals are found indicative of an alkali-resistant α-(1,4)-glucan. When combined with earlier work and recent results obtained with the human pathogenic ascomycete *Aspergillus fumigatus*, a new model of the cell wall architecture of *S. commune* emerges (Figure 5).

In this model, β-(1,3)(1,6)-glucan forms the outer cell wall layer covering alkali soluble α-(1,3)-glucan. The latter covers the alkali-resistant backbone composed of β-(1,3)(1,6)-glucan and chitin. We now have added α-(1,4)-glucan and the homo- or heteropolymeric fucan and mannan in the cell wall model. Their flexibility or rigidity, as indicated by ssNMR do not provide localization of these molecules in the cellular architecture. Therefore, these polymers have been presented throughout the cell wall in the model. Future studies, for example using ssNMR methods that probe structure and macromolecular arrangements (Weingarth & Baldus, 2013) will further refine the molecular view of the *S. commune* cell wall.

Supplementary information

Table S1 Measuring conditions for the recorded 1D and 2D spectra.

Sample	1H pulse (kHz)	13C pulse (kHz)	Dec. SPINAL64 (kHz)	CP contact time (µs)	13C CP-field (kHz)	1H CP-field (kHz)	1D DE	1D CP	1D INEPT	2D PARIS	2D INEPT
Hyd.	71	46	71	400	42	63	512	512	512	128	16
PBS	83	50	83	600	47	83	64	64	64	48	128
SDS	87	50	87	1000	44	70	128	128	128	96	64
Alk.	71	50	71	800	45	87	32	256	128	176	16

Table S2 Chemical shifts of different sugars according to literature.

	C1	C2	C3	C4	C5	C6	C7	C8	References
β-1,3-glucan[a]	103.3	73.9	86.3	68.7	76.2	61.1			Chakraborty et al 2006
β-1,3-glucan[b]	102.7	72.7	86.0	68.3	76.2	60.9			Alquini et al 2004
β-1,3-glucan[c]	105.3	75.9	87.0	70.8	78.3	63.4			Fontaine 2000
Reducing end β-1,3-glucan	98.4	76.5	87.4	70.9	78.3	63.5			Fontaine 2000
Non-reducing end β-1,3-glucan[a]	104.4	75.2	77.8	71.8	78.1	62.9			Dong et al 2009
Non-reducing end β-1,3-glucan[b]	103.1	73.8	76.5	70.3	76.3	61.0			Chang and Lu 2004
Non-reducing end β-1,3-glucan[c]	105.5	76.2	78.3	72.3	78.7	63.4			Fontaine 2000
α-1,3-glucan[a]	101.0	71.4	83.2	70.3	73.5	61.3			Bock et al 1983
α-1,3-glucan[b]	97.0	70.3	80.1	69.8	73.4	61.8			Mondal et al
Reducing end α-1, glucan	99.7	71.8	72.8	70.0	71.3	60.8			Smiderle et al 2010
α-1,6-glucan[a]	100.2	72.0	72.7	73.9	75.9	68.1			Luo et al 2008
α-1,6-glucan[b]	101.1	72.1	74.0	70.6	71.3	67.6			McIntyre and Vogel 1993
α-1,4-glucan[a]	99.8	71.5	75.3	78.7	71.2	60.1			Gonzaga et al 2005
α-1,4-glucan[b]	100.7	72.1	74.2	77.7	72.1	61.5			McIntyre and Vogel 1993
Mannan[a]	102.0	76.3	72.5	81.4	70.3	62.4			Marchessault et al 1990
Mannan[b]	102.4	75	72.5	83	70.9	62.9			Marchessault et al 1990
Mannan[c]	101.7	69.9	72.1	81	75.9	61.9			Petkowicz et al 2001
β-1,3-galactan	105.7	72.4	82.2	70.2	76.6	62.5			Bilan et al 2010
β-1,6-galactan	105	72.3	74.2	70.2	75.2	71.5			Bilan et al 2010
Chitin[a]	104.2	55.2	74.8	84.1	74.8	60.9	173.1	22.5	Jang et al 2004
Chitin[b]	104.0	54.6	73	82.8	75.4	60.5	172.6	22.5	Jang et al 2004
Chitin[c]	104.3	55.3	73.5	83.2	75.9	61.1	175.8-173.5	22.9	Kameda et al 2004
α-1,3-fucan	97.2	68.1	76.3	70	68.1	16.8			Bilan et al 2010

Table S3 Chemical shifts (ppm) of peaks shown in Figure S1.

	a	b	c	d	e	f	g	h	i	j	k	l	m	n	o	p	q
Figure 2A	16,7	17,9	23,1	25,3	27,4	29,8	32,3	34,5	36,2	74,1	75,8	87,6	94,8	98,6	174,7	176,6	178,4
Figure 2B	16,8	25,4	27,5	Na	29,8	32,3	34,5	36,2	65,3	74,2	77,0	94,9	98,6	Na	130,5	132,2	
Figure 2C	16,9	23,1	24,9	32,6	35,2	42,0	57,6	66,2	76,0	78,3	80,3	88,52	105,9	176,7			

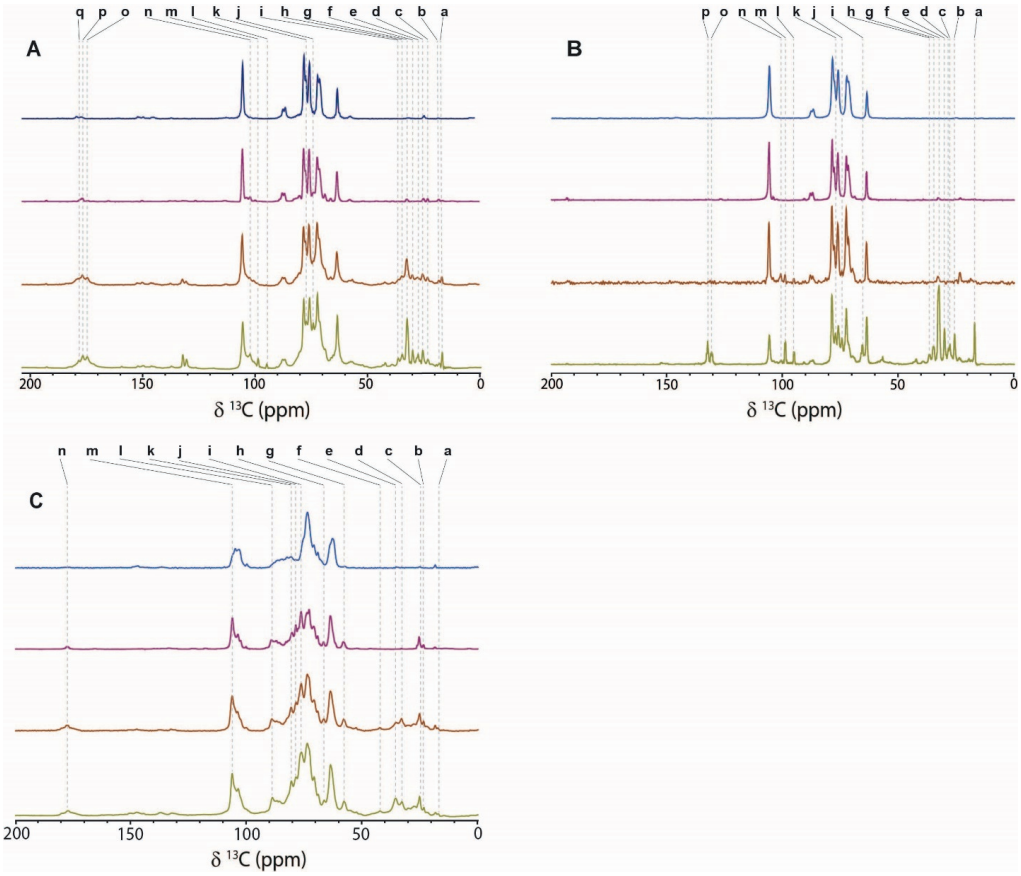

Figure S1 One-dimensional solid-state ^{13}C NMR spectra of non-treated (green), PBS-washed (orange), SDS-extracted (pink) and alkali-extracted (blue) *S. commune* mycelium recorded with direct excitation (**A**), INEPT (**B**) and CP magnetization transfer steps (**C**). Peak annotations (a–q) correspond to lipids and amino acids (±10–45 ppm) and polysaccharides (±60–178 ppm) and peptide signals. Their ^{13}C chemical shifts are reported in Table S3.

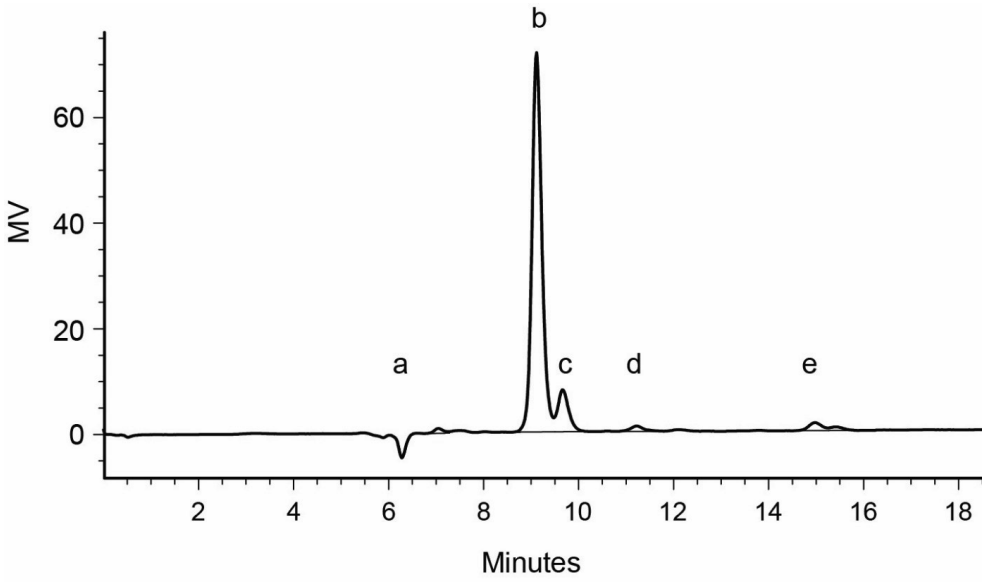

Figure S2 HPLC analysis of the sugars contained in the *S. commune* mycelium. a) 9.299 min, negative peak representing an artefact of the eluent. This is also the retention time of chitin that is now invisible. b) 9.133 minutes, glucose; c) 9.681 minutes, mannose and/or galactose; d) 11.241 minutes, fucose; e) 14.994 min, acetic acid possibly arising from sulfuric acid hydrolysis of acetyl group from chitin.

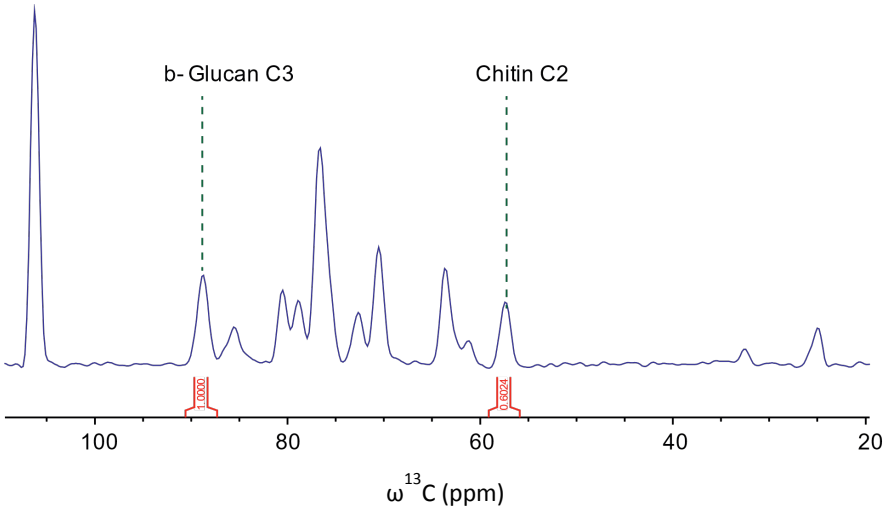

Figure S3 1D slice extracted from the two-dimensional (^{13}C-^{13}C)-PARIS ssNMR showing isolated ^{13}C signals from β-(1,3)-glucan (C3 resonance) and chitin (C2 resonance) of the hydrated cell wall. A semi-quantitative analysis was performed by calculating the ratio of the peak intensities (Imax), i.e. Imax C2/ Imax C3=0.60.

Metals
Polymers
ams

Chapter 7

Summary and General Discussion

Introduction

The linear “take-produce-consume-discard” model that is the standardly used in our economy assumes abundance of resources and unlimited waste disposal (Jurgilevich et al., 2016). The intrinsic unsustainability of this model necessitates development of sustainable, circular alternatives. Renewable feedstocks and biodegradability are two important factors in circular production. To this end, industries like those from the construction and textile sectors have gained interest in bio-based materials. Such materials can result from whole organisms (e.g. wood) or from extraction/purification of its components (e.g. starch). Fungal mycelium is an upcoming resource used in the production of bio-based materials.

Fungi are omnipresent microorganisms with an important role in nature and for mankind (Baxi et al., 2016). The two major phyla are the Ascomycota, including most yeast- and mold-like fungi, and the Basidiomycota, including most mushroom forming fungi. For their growth, fungi degrade dead organic matter or establish a symbiotic relationship with plants, animals or microbes. Filamentous fungi colonize substrates by means of mm- to cm-long hyphae generally having a diameter between 1-10 µm. These hyphae grow at their tip and branch subapically forming a 3D network that is called mycelium. This mycelium can vary in size ranging from sub-millimeter to kilometer dimensions (Ferguson, Dreisbach, Parks, Filip, & Schmitt, 2003; Smith, Bruhn, & Anderson, 1992). Members of the mushroom forming fungi have specialized in lignocellulose degradation, such as agricultural waste streams like straw and sawdust. These fungi can upgrade these waste streams by transforming them into materials.

Cell walls of fungi are important for the interaction of fungi with their (a)biotic environment, are essential for morphogenesis and provide mechanical strength of hyphae (Gow, Latgé, & Munro, 2017). The latter suggests an important role of cell walls in determining mycelium material properties. Fungal cell wall composition is dynamic and varies between species, strains, environmental conditions, and developmental stage (Bowman & Free, 2006; Erwig & Gow, 2016).

Mycelium-based materials can be made of pure mycelium or consist of a combination of mycelium and another material such as the substrate. Pure mycelium can be used as leather or textile replacement, while composite materials have been developed for use as packaging, insulation and construction materials. Pure mycelium can be obtained by growth on a solid substrate (Haneef et al., 2017) or by growth in static liquid (Chapter 4) or liquid shaken (Chapter 5) cultures. To this end, the fungal skin covering the solid substrate is harvested, while the fungus is allowed to fully degrade its carbon source in the liquid cultures. Composite materials can be made by mixing additional materials with pure mycelium or by inactivating fungal growth on a solid substrate before its full degradation. In the latter case, hyphae have bound organic fibers during colonizing of the substrate (Jones et al., 2018).

Material properties are defined as the set of attributes of a material. Density (ρ, kg m^{-3}) and price (\$ kg^{-3}) are examples of general properties, while examples of mechanical properties are the Young's modulus (E, GPa), ultimate tensile strength (σ, MPa) and elongation at breaking (ε,%) (Ashby, 2005). The Young's modulus is a measure of rigidity defined by the amount of stress (in Pa) causing a specific strain (in %) and should not be confused with strength. The ultimate tensile strength is the amount of stress in longitudinal direction a material can withstand before breaking. The elongation at breaking is the proportional deformation determined by the change in length divided by its original length.

The properties of pure mycelium materials are the outcome of the substrate, species or strain, its growth conditions (Appels et al., 2018; Haneef et al., 2017; Chapter 4) as well as its post-processing. Post-processing can consist of physical, chemical, and/or biological treatments. Heat pressing and adding plasticizing agents are examples of a physical and a chemical treatment, respectively, while selective degradation of components of a mycelium material by microorganisms is an example of a biological treatment.

The aim of this thesis was to improve knowledge on mycelium-based materials. This was achieved by systematic studies on the impact of fungal strains, substrates, growth conditions, and physical and chemical treatments on material properties of pure and composite mycelium materials.

Pure mycelium materials

Pure mycelium materials were produced with mycelium grown in static and liquid cultures (Chapter 4 & 5). Dried and untreated mycelium films produced with both types of cultures showed similar material properties regarding Youngs modulus, ultimate tensile strength and elongation at breaking. These properties were similar to materials that are classified in the group of natural materials (Figure 1).

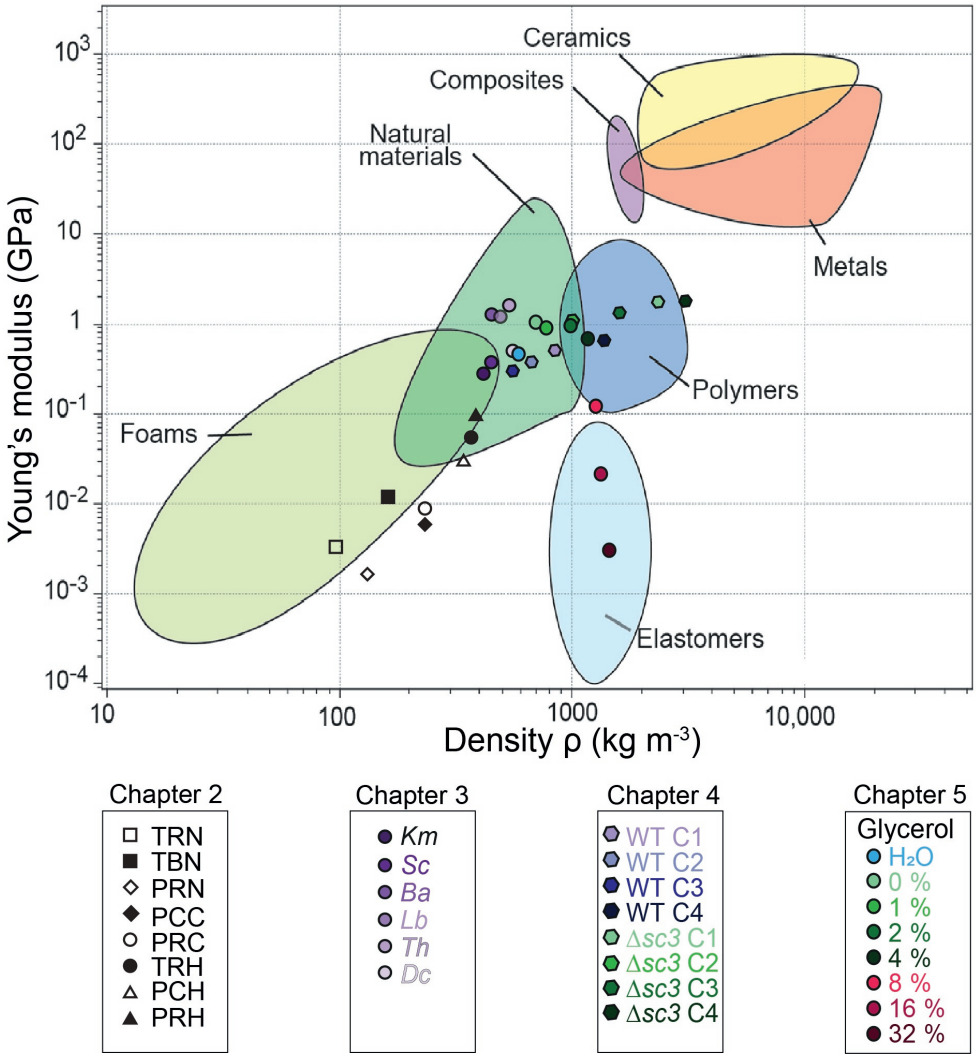

Figure 1 Relation between the Young's modulus (GPa) and density (kg m^{-3}) of material families (Ashby, 2005).

However, the macrostructure of pure mycelium materials produced with mycelium from static and liquid cultures was different. The mycelium of the static liquid culture consists in part of submerged mycelium and a part that grows in the air. The former dries up very dense having almost no air voids with an appearance resembling that of paper. The aerial mycelium, however, is less dense and has a cotton like appearance. Mycelium obtained from shaking liquid cultures had a more homogeneous appearance after drying, being most similar to the submerged part of the dried mycelium from liquid static cultures. Still, some air voids were observed after drying mycelium from liquid shaking cultures. Such air voids are an added value in the production of insulation or sound absorbing materials but comes at the expense of rigidity.

Static liquid cultures of homokaryotic sterile wild-type *Schizophyllum commune* and the *sc3* hydrophobin gene deletion strain (Δ*sc3* strain) were grown in the light or the dark at low or high CO_2 (Chapter 4). Light and ambient CO_2 initiate fructification in many fertile heterokaryotic strains of mushroom forming fungi. Changing growth conditions from ambient CO_2 (400 ppm) to high CO_2 (i.e. 70.000 ppm) in the dark resulted in mycelium films with decreased E. In contrast, change of growth from ambient to high CO_2 in the light increased E. Deletion of *sc3* resulted in a >2-fold increase of material rigidity compared to wild-type *S. commune* irrespective of the environmental growth conditions. Initially, it was hypothesized that these differences were caused by differences in the chemical composition of the cell wall as described by van Wetter and colleagues (2000). However, chemical analysis by ATR-FTIR did not show large differences in macromolecular composition of the material of the wild-type and the Δ*sc3* strain. Scanning electron microscopy did show differences between the mycelium films of these strains. The material of the Δ*sc3* strain was more homogeneous and densely packed compared to the wild-type S*. commune* material. Indeed, the density of the material appeared higher when produced with the deletion strain. This density increase correlated with increased rigidity and ultimate tensile strength of the mycelium-based material.

Growth of static liquid cultures is labour intensive and challenging to upscale. As an alternative, liquid shaken cultures were used to produce fungal biomass (Chapter 5). Growing for 7 days resulted in a conversion of 38% of the glucose in the medium into fungal biomass. For comparison, a study by Wu et al. (2003) to increase fungal

biomass formation in liquid shaken cultures of *Pleurotus tuber-regium* showed a highest conversion rate of glucose to biomass of 31.8% after 20 days of growth (Wu, Cheung, Wong, & Huang, 2003). The untreated mycelium sheets produced with liquid shaking cultures had brittle behaviour (like dried clay) and were therefore post-processed with the plasticizing agent glycerol. Adding a series of glycerol concentrations to the mycelium sheets drastically increased elasticity, reduced ultimate tensile strength and increased elongation at breaking. This shift in material properties from being brittle to ductile was reflected by a shift from being a natural-like material to a polymer-like material (concentrations of glycerol up to 8%) or even an elastomer-like material (concentration of glycerol ≥16%) (Figure 1). Examples of these two material groups are plastics and rubbers, respectively. Together, different growth methods, genetic modification, culture conditions and post-processing resulted in a range of mycelium materials with properties placing them in the groups of natural materials, polymer-like materials, and elastomers.

As mentioned above, fungal strains, environmental growth conditions, the substrate and processing determine the properties of the mycelium material. Changes in density is one of the mechanisms by which material properties change. The chemical composition may be another mechanism. The cell wall is a major part of the hyphae making up 15–25% of the mycelium biomass (Nevalainen, Te'o, Penttilä, & Pakula, 2005) and provides mechanical strength to hyphae. Thus, the cell wall composition may affect mechanical properties of mycelium materials as well. Therefore, a non-destructive method called solid-state NMR was used to analyse the architecture of the *S. commune* cell wall (Chapter 6). By growing on a membrane, mycelium could be easily separated from the solidified minimal medium underlying the membrane. Unwashed homogenized mycelium was studied, as well as homogenized mycelium that was washed with PBS either or not followed by extraction with hot SDS and alkali. Both flexible and rigid components of the cell wall were studied by ssNMR using literature values to assign peaks. Evidence is presented that the flexible part of the cell wall consists of β-(1,3-1,6)-glucan, α-(1,3)-glucan, α-(1,4)-glucan and homo- or heteropolymeric mannose. Signals observed in the rigid part of the cell wall indicate presence of chitin, β-(1,3)(1,6)-glucan, α-(1,3)-glucan and homo- or heteropolymeric fucose. The exact location of the flexible and rigid sugar moieties remains to be elucidated.

Previously, destructive techniques were used to analyze cell wall composition of *S. commune* (Sietsma & Wessels, 1977, 1979, 1981). To this end, cell wall fractions were obtained by hot water extraction, SDS extraction and alkali treatments. Fractions were subsequently processed by chemical or enzymatic treatment to allow monomeric sugar analysis. From these data it was concluded that the cell wall of *S. commune* consists of a water-soluble mucilage of β-(1-3)(1-6)-glucan covering an alkali-soluble α-(1,3)-linked glucan while the most inner layer of the cell wall consists of chitin embedded in and crosslinked to highly branched alkali-insoluble β-(1,3)(1,6)-glucan. Use of ssNMR enabled to study intact polymers within previously mentioned cell wall fractions and to discriminate between dynamic and rigid cell wall components. The data presented in Chapter 6 thus give a better reflection of the architecture of the cell wall of *S. commune* and actually have changed our view of this complex organelle. Studying the cell wall of the human pathogen *Aspergillus fumigatus* with ssNMR also resulted in a dramatic change in our understanding of its composition (Kang *et al.,* 2018). It was shown that α-(1,3)-glucan also plays a major role in the rigid core of the *A. fumigatus* cell wall, while previous studies indicated that the rigid core of the cell wall was mainly composed of β-(1,3)(1,6)-glucan and chitin (Latgé, 2007).

Composite mycelium materials

Composite mycelium materials were produced by growing fungi in a solid substrate and stopping growth before the substrate was fully degraded (Chapters 2 & 3). During colonization, the fungus binds the substrate particles acting as a glue. Chapter 2 focussed on composite materials produced by the basidiomycetes *Pleurotus ostreatus* and *Trametes versicolor* (Chapter 2). These fungi were grown on beech sawdust, rapeseed straw and cotton waste. The combination of fungus and substrate impacted material properties. For example, *T. versicolor* on beech sawdust resulted in highest elastic modulus while ultimate tensile strength was comparable to *T. versicolor* grown on rapeseed straw. Yet, pressing and not the type of fungus or substrate had the largest influence on the mechanical performance of the materials. Cold pressing *P. ostreatus* grown on straw or cotton increased density 2-fold compared to non-pressing. Heat pressing *T. versicolor* on straw and *P. ostreatus* on cotton and straw resulted in a >3-fold increase of density. Heat-pressing improved homogeneity, rigidity and

ultimate tensile strength of the materials. This caused the performance of the materials to shift from being foam-like (e.g. styrofoam) to natural-like (e.g. cork).

There was no overall relation between water absorption and the type of fungus, substrate, or pressing condition used to produce the material. Exposure to 60% relative humidity (RH) resulted in thickness increase for *P. ostreatus* grown on rapeseed straw that was not- or cold-pressed. Similar results were found for *P. ostreatus* grown on cotton with no further pressing. Exposure to 80% RH resulted in weight increase of *P. ostreatus* grown on rapeseed straw that was cold- or hot-pressed. Exposure to 80% RH increased thickness only for hot-pressed *T. versicolor* grown on rapeseed straw. These findings are important to consider when applying these materials e.g. as insulation panels when sandwiched between other materials. Weight increase after placing the material on water varied between 43% for not-pressed *T. versicolor* grown on beech sawdust and up to 508% for not-pressed *P. ostreatus* grown on cotton. These findings imply the necessity for a coating when used in humid environments; preferably biodegradable bio-based coatings like PLA or PHA (Iwata, 2015).

Screening wild-type strains is a powerful tool in the search for novel bio-based materials. Nine wood-degrading fungi were isolated from a forest near Utrecht Science Park (Chapter 3). A new method was developed to quantify growth within the substrate based on CO_2 production as a proxy for mycelium activity. Visual inspection of fungal growth at the surface of the substrate correlated with CO_2 release. The latter showed that some species (*S. commune* and *Bjerkandera adusta*) are fast colonizers of the substrate but enter the stationary phase relatively fast. Possibly these species have more difficulties reaching and or degrading less accessible polysaccharides. Other species (*Trametes hirsuta* and *Lenzites betulina*) had a longer lag phase but grew exponentially for a longer time thus producing overall more CO_2. Visual inspection showed that these species indeed had produced a denser mycelium within the substrate when compared to the fast colonizing strains.

Six out of the nine natural isolates were heat pressed and mechanically analyzed after a 4-week growth period. The material properties of these mycelium materials places are comparable to natural materials. Interestingly, the materials that were most rigid and strong originated from the three strains with the highest cumulative CO_2 production

(*T. hirsuta*, *L. betulina* and *B. adusta*). Future studies should assess the impact of prolonged growth periods on various substrates. Prolonged growth will increase fungal biomass, while degradation of the fibers in the substrate will be increased.

Together, also in the case of the composite materials the type of fungus, substrate, environmental growth conditions and processing determine the properties of the mycelium material. *B. adusta* has been shown to have a high potential to use for the production of composite mycelium materials because of its relatively fast growth, low CO_2 production, and its material performance.

Conclusions

A range of materials have been produced with material properties ranging from being foam-like, to natural-like to polymer-like to elastomer-like considering the Young's moduli and densities. Growth of fungi within sawdust or straw resulted in a foam-like material. Properties changed to natural-like when heat-pressing was applied. Dried pure mycelium was shown to have properties similar to that of natural materials. By changing environmental growth conditions material properties changed towards being more comparable to polymers. Genetic modification resulted in more rigid and stronger materials placing them within the polymer family. Applying plasticizing agents to pure mycelium obtained from liquid shaken cultures drastically decreased rigidity and ultimate tensile strength while increasing the elongation at breaking, giving it elastomer-like properties.

At this moment, pure mycelium materials have been produced that could replace materials with a negative footprint such as textiles and leather. Composite materials have been produced with properties ranging from foam-like to natural material-like. The foam like materials have also proven to be highly performative in acoustic absorbance (Jones, Huynh, Dekiwadia, Daver, & John, 2017; Pelletier et al., 2013). Natural material-like materials could replace particle boards such as oriented strand board (OSB) and medium density fiber board (MDF), often containing toxic compounds such as formaldehyde (Boran, Usta, & Gümükaya, 2011). Moreover, fungi can be used to produce functional materials. For instance, fungi that enhance plant growth by supplying nutrients can be used to grow plant pots using agricultural waste as

substrate. Seedlings can directly be planted in the soil within these pots, creating a growth stimulating environment for the plant. Moreover, mycelium composite materials can have great insulation properties (Yang, Zhang, Still, White, & Amstislavski, 2017). When placed in the interior of buildings, the open structure of the mycelium has as added value with its exceptional sound absorbing qualities (Pelletier et al., 2013).

More research is needed to enhance durability of these materials when used in our daily lives. This research should focus on species, growth conditions, substrates and post-processing techniques. Collaboration with experts in the field of chemistry, material science, design and product development will lead to enhanced applicability of fungal materials. This should make it possible to replace more and more unsustainable materials like conventional plastics and rubber.

References

Albertsson, A. C., & Hakkarainen, M. (2017). Designed to degrade. *Science*, *358*(6365), 872–873. https://doi.org/10.1126/science.aap8115

Álvarez-Chávez, C. R., Edwards, S., Moure-Eraso, R., & Geiser, K. (2012). Sustainability of bio-based plastics: General comparative analysis and recommendations for improvement. *Journal of Cleaner Production*, *23*(1), 47–56. https://doi.org/10.1016/j.jclepro.2011.10.003

Andrews, N. C., & Faller, D. V. (1991). A rapid micropreparation technique for extraction of DNA-binding proteins from limiting numbers of mammalian cells. *Nucleic Acids Research*, *19*(9), 2499.

Andronesi, O. C., Pfeifer, J. R., Al-Momani, L., Özdirekcan, S., Rijkers, D. T. S., Angerstein, B., … Baldus, M. (2004). Probing membrane protein orientation and structure using fast magic-angle-spinning solid-state NMR. *Journal of Biomolecular NMR*, *30*(3), 253–265. https://doi.org/10.1007/s10858-004-3452-3

Appels, F. V. W., Dijksterhuis, J., Lukasiewicz, C. E., Jansen, K. M. B., Wösten, H. A. B., & Krijgsheld, P. (2018). Hydrophobin gene deletion and environmental growth conditions impact mechanical properties of mycelium by affecting the density of the material. *Scientific Reports*, *8*(1), 4703. https://doi.org/10.1038/s41598-018-23171-2

Appels, F. V. W., Camere, S., Montalti, M., Karana, E., Jansen, K. M. B., Dijksterhuis, J., … Wösten, H. A. B. (2019). Fabrication factors influencing mechanical, moisture- and water-related properties of mycelium-based composites. *Materials and Design*, *161*, 64–71. https://doi.org/10.1016/j.matdes.2018.11.027

Appels, F. V. W., (2020) *The use of fungal mycelium for the production of bio-based materials* (online version of this thesis, Utrecht University)

Arrieta, M. P., Fortunati, E., Dominici, F., López, J., & Kenny, J. M. (2015). Bionanocomposite films based on plasticized PLA–PHB/cellulose nanocrystal blends. *Carbohydrate Polymers*, *121*, 265–275. https://doi.org/10.1016/J.CARBPOL.2014.12.056

Ashby, M. (2012). *Materials and the Environment: Eco-informed Material Choice*. 2nd Edition. Elsevier Butterworth-Heinemann, Burlington, MA. https://doi.org/10.1016/C2010-0-66554-0

Ashby, M. F., Shercliff, H., & Cebon, D. (2010). Materials: engineering, science, processing and design. *Materials Today*, *13*(3), 67. https://doi.org/10.1016/s1369-7021(10)70042-0

Ashby, M. F., & Johnson, K. (2014). *Materials and Design: The Art and Science of Material Selection in Product Design*. 3rd Edition. Burlington, MA, Elsevier

Butterworth-Heinemann. https://doi.org/10.1016/C2011-0-05518-7

Ashby, M. F. (2005). *Materials Selection in Mechanical Design*. 3rd Edition., Burlington, MA, Elsevier Butterworth-Heinemann.

Asif, M., Muneer, T., & Kelley, R. (2007). Life cycle assessment: A case study of a dwelling home in Scotland. *Building and Environment*, *42*(3), 1391–1394. https://doi.org/10.1016/j.buildenv.2005.11.023

Averous, L., Moro, L., Dole, P., & Fringant, C. (2000). Properties of thermoplastic blends: Starch-polycaprolactone. *Polymer*, *41*(11), 4157–4167. https://doi.org/10.1016/S0032-3861(99)00636-9

Azeredo, H. M. C., & Waldron, K. W. (2016). Crosslinking in polysaccharide and protein films and coatings for food contact - A review. *Trends in Food Science and Technology*, *52*, 109–122. https://doi.org/10.1016/j.tifs.2016.04.008

Babu, R. P., O'Connor, K., & Seeram, R. (2013). Current progress on bio-based polymers and their future trends. *Progress in Biomaterials*, *2*(1), 8. https://doi.org/10.1186/2194-0517-2-8

Baldus, M., & Meier, B. H. (1996). Total Correlation Spectroscopy in the Solid State. The Use of Scalar Couplings to Determine the Through-Bond Connectivity. *Journal of Magnetic Resonance, Series A*, *121*(1), 65–69. https://doi.org/10.1006/JMRA.1996.0137

Bartnicki-Garcia, S. (1968). Cell Wall Chemistry, Morphogenesis, and Taxonomy of Fungi. *Annual Review of Microbiology*, *22*(1), 87–108. https://doi.org/10.1146/annurev.mi.22.100168.000511

Baxi, S. N., Portnoy, J. M., Larenas-Linnemann, D., Phipatanakul, W., Barnes, C., Baxi, S., … Williams, P. B. (2016). Exposure and Health Effects of Fungi on Humans. *The Journal of Allergy and Clinical Immunology: In Practice*, *4*(3), 396–404. https://doi.org/10.1016/J.JAIP.2016.01.008

Berends, E., Scholtmeijer, K., Wösten, H. A. B., Bosch, D., & Lugones, L. G. (2009). The use of mushroom-forming fungi for the production of N-glycosylated therapeutic proteins. *Trends in Microbiology*, *17*(10), 439–443. https://doi.org/10.1016/j.tim.2009.07.002

Beyer, M. K., & Clausen-Schaumann, H. (2005). Mechanochemistry: The mechanical activation of covalent bonds. *Chemical Reviews*. *105*(8), 2921–2948. https://doi.org/10.1021/cr030697h

Bhattacharya, A., Rawlins, J., & Ray, P. (2009). *Polymer Grafting and Crosslinking*. Hoboken, NJ, John Wiley. https://doi.org/10.1002/9780470414811

Boran, S., Usta, M., & Gümükaya, E. (2011). Decreasing formaldehyde emission from

medium density fiberboard panels produced by adding different amine compounds to urea formaldehyde resin. *International Journal of Adhesion and Adhesives*, *31*(7), 674–678. https://doi.org/10.1016/j.ijadhadh.2011.06.011

Bowman, S. M., & Free, S. J. (2006, August). The structure and synthesis of the fungal cell wall. *BioEssays*, Vol. 28, pp. 799–808. https://doi.org/10.1002/bies.20441

Chen, G.Q. (2010). *Biofunctionalization of Polymers and Their Applications*. Berlin, Heidelberg, Springer. https://doi.org/10.1007/10_2010_89

Cowie, J. M. G., & Caleria, A. (2007). *Polymers: chemistry and physics of modern materials.* 3rd Edition. Boca Raton, FL, CRC Press. https://doi.org/10.1201/9781420009873

Crini, G. (2005). Recent developments in polysaccharide-based materials used as adsorbents in wastewater treatment. *Progress in Polymer Science*, *30*(1), 38–70. https://doi.org/10.1016/J.PROGPOLYMSCI.2004.11.002

Crook, E. M., & Johnston, I. R. (1962). The qualitative analysis of the cell walls of selected species of fungi. *Biochemical Journal, 83*(2), 325.

Curvelo, A. A. S., De Carvalho, A. J. F., & Afnelli, J. A. M. (2001). Thermoplastic starch-cellulosic fibers composites: preliminary results. *Carbohydrate Polymers, 45*(2), 183-188. https://doi.org/10.1016/S0144-8617(00)00314-3

Dai, Y.C., Cui, B.K., Si, J., He, S.H., Hyde, K. D., Yuan, H.S., … Zhou, L.W. (2015). Dynamics of the worldwide number of fungi with emphasis on fungal diversity in China. *Mycological Progress*, *14*(8), 62. https://doi.org/10.1007/s11557-015-1084-5

De Vocht, M. L., Scholtmeijer, K., Van Der Vegte, E. W., De Vries, O. M. H., Sonveaux, N., Wösten, H. A. B., … Robillard, G. T. (1998). Structural characterization of the hydrophobin SC3, as a monomer and after self-assembly at hydrophobic/hydrophilic interfaces. *Biophysical Journal*, *74*(4), 2059–2068. https://doi.org/10.1016/S0006-3495(98)77912-3

Dons, J. J. M., De Vries, O. M. H., & Wessels, J. G. H. (1979). Characterization of the genome of the basidiomycete *Schizophyllum commune*. *BBA Section Nucleic Acids And Protein Synthesis*, *563*(1), 100–112. https://doi.org/10.1016/0005-2787(79)90011-X

Dupree, R., Simmons, T. J., Mortimer, J. C., Patel, D., Iuga, D., Brown, S. P., & Dupree, P. (2015). Probing the molecular architecture of *Arabidopsis thaliana* secondary cell walls using two- and three-dimensional 13C solid state nuclear magnetic resonance spectroscopy. *Biochemistry*, *54*(14), 2335–2345. https://doi.org/10.1021/bi501552k

Eichner, K., & Karel, M. (1972). The influence of water content and water activity on

the sugar-amino browning reaction in model systems under various conditions. *Journal of Agricultural and Food Chemistry*, *20*(2), 218–223. https://doi.org/10.1021/jf60180a025

Erwig, L. P., & Gow, N. A. R. (2016). Interactions of fungal pathogens with phagocytes. *Nature Reviews Microbiology*, *14*(3), 163–176. https://doi.org/10.1038/nrmicro.2015.21

Ferguson, B. A., Dreisbach, T. A., Parks, C. G., Filip, G. M., & Schmitt, C. L. (2003). Coarse-scale population structure of pathogenic Armillaria species in a mixed-conifer forest in the Blue Mountains of northeast Oregon. *Canadian Journal of Forest Research*, *33*(4), 612–623. https://doi.org/10.1139/x03-065

Floudas, D., Binder, M., Riley, R., Barry, K., Blanchette, R. A., Henrissat, B., … Hibbett, D. S. (2012). The paleozoic origin of enzymatic lignin decomposition reconstructed from 31 fungal genomes. *Science*, *336*(6089), 1715–1719. https://doi.org/10.1126/science.1221748

Fung, B. M., Khitrin, A. K., & Ermolaev, K. (2000). An Improved Broadband Decoupling Sequence for Liquid Crystals and Solids. *Journal of Magnetic Resonance*, *142*(1), 97–101. https://doi.org/10.1006/JMRE.1999.1896

Garrison, T., Murawski, A., Quirino, R., Garrison, T. F., Murawski, A., & Quirino, R. L. (2016). Bio-Based Polymers with Potential for Biodegradability. *Polymers*, *8*(7), 262. https://doi.org/10.3390/polym8070262

Geiser, K. (2001). *Materials matter*. Cambridge, MA, MIT Press.

Geng, Y., Fu, J., Sarkis, J., & Xue, B. (2012). Towards a national circular economy indicator system in China: An evaluation and critical analysis. *Journal of Cleaner Production*, *23*(1), 216–224. https://doi.org/10.1016/j.jclepro.2011.07.005

Geyer, R., Jambeck, J. R., & Law, K. L. (2017). Production, use, and fate of all plastics ever made. *Science Advances*, *3*(7), e1700782. https://doi.org/10.1126/sciadv.1700782

Gow, N. A. R., Latge, J.P., & Munro, C. A. (2017). The Fungal Cell Wall: Structure, Biosynthesis, and Function. *Microbiology Spectrum*, *5*(3). https://doi.org/10.1128/microbiolspec.funk-0035-2016

Grimm, D., & Wösten, H. A. B. (2018). Mushroom cultivation in the circular economy. *Applied Microbiology and Biotechnology*, *102*(18), 7795–7803. https://doi.org/10.1007/s00253-018-9226-8

Haneef, M., Ceseracciu, L., Canale, C., Bayer, I. S., Heredia-Guerrero, J. A., & Athanassiou, A. (2017). Advanced Materials from Fungal Mycelium: Fabrication and Tuning of Physical Properties. *Scientific Reports*, *7*(1), 41292. https://doi.org/10.1038/srep41292

Harding, K. G., Dennis, J. S., von Blottnitz, H., & Harrison, S. T. L. (2007).

Environmental analysis of plastic production processes: Comparing petroleum-based polypropylene and polyethylene with biologically-based poly-β-hydroxybutyric acid using life cycle analysis. *Journal of Biotechnology*, *130*(1), 57–66. https://doi.org/10.1016/j.jbiotec.2007.02.012

Hawksworth, D. L., & Lücking, R. (2017). Fungal Diversity Revisited: 2.2 to 3.8 Million Species. *The Fungal Kingdom*, *5*(4), 79–95). https://doi.org/10.1128/microbiolspec.funk-0052-2016

Hermabessiere, L., Dehaut, A., Paul-Pont, I., Lacroix, C., Jezequel, R., Soudant, P., & Duflos, G. (2017). Occurrence and effects of plastic additives on marine environments and organisms: A review. *Chemosphere*, *182*, 781–793. https://doi.org/10.1016/j.chemosphere.2017.05.096

Hibbett, D. S., Binder, M., Bischoff, J. F., Blackwell, M., Cannon, P. F., Eriksson, O. E., … Zhang, N. (2007). A higher-level phylogenetic classification of the Fungi. *Mycological Research*, *111*(5), 509–547. https://doi.org/10.1016/J.MYCRES.2007.03.004

Hislop, H., & Hill, J. (2011). Reinventing the wheel: A circular economy for resource security. *Green Alliance*, 1–29.

Holt, G. A., Mcintyre, G., Flagg, D., Bayer, E., Wanjura, J. D., & Pelletier, M. G. (2012). Fungal mycelium and cotton plant materials in the manufacture of biodegradable molded packaging material: evaluation study of select blends of cotton byproducts. *Journal of Biobased Materials and Bioenergy*, *6*, 431–439. https://doi.org/10.1166/jbmb.2012.1241

Hopewell, J., Dvorak, R., & Kosior, E. (2009). Plastics recycling: Challenges and opportunities. *Philosophical Transactions of the Royal Society B: Biological Sciences*, *364*(1526), 2115–2126. https://doi.org/10.1098/rstb.2008.0311

Huysman, S., De Schaepmeester, J., Ragaert, K., Dewulf, J., & De Meester, S. (2017). Performance indicators for a circular economy: A case study on post-industrial plastic waste. *Resources, Conservation and Recycling*, *120*, 46–54. https://doi.org/10.1016/j.resconrec.2017.01.013

Islam, M. R., Tudryn, G., Bucinell, R., Schadler, L., & Picu, R. C. (2017). Morphology and mechanics of fungal mycelium. *Scientific Reports*, *7*(1). https://doi.org/10.1038/s41598-017-13295-2

Islam, M. R., Tudryn, G., Bucinell, R., Schadler, L., & Picu, R. C. (2018). Mechanical behavior of mycelium-based particulate composites. *Journal of Materials Science*, *53*(24), 16371–16382. https://doi.org/10.1007/s10853-018-2797-z

Iwata, T. (2015). Biodegradable and bio-based polymers: Future prospects of eco-friendly plastics. *Angewandte Chemie International Edition*, *54*(11), 3210–3215. https://doi.org/10.1002/anie.201410770

Jansen, M. L. A., Bracher, J. M., Papapetridis, I., Verhoeven, M. D., de Bruijn, H., de Waal, P. P., … Pronk, J. T. (2017). Saccharomyces cerevisiae strains for second-generation ethanol production: from academic exploration to industrial implementation. *FEMS Yeast Research*, *17*(5). https://doi.org/10.1093/femsyr/fox044

Jantschke, A., Koers, E., Mance, D., Weingarth, M., Brunner, E., & Baldus, M. (2015). Insight into the Supramolecular Architecture of Intact Diatom Biosilica from DNP-Supported Solid-State NMR Spectroscopy. *Angewandte Chemie - International Edition*, *54*(50), 15069–15073. https://doi.org/10.1002/anie.201507327

Johnson, E. A. (2013). Biotechnology of non-Saccharomyces yeasts - The ascomycetes. *Applied Microbiology and Biotechnology*, *97*(2), 503–517. https://doi.org/10.1007/s00253-012-4497-y

Jones, M., Huynh, T., Dekiwadia, C., Daver, F., & John, S. (2017). Mycelium composites: A review of engineering characteristics and growth kinetics. *Journal of Bionanoscience*, *11*(4), 241–257. https://doi.org/10.1166/jbns.2017.1440

Jones, M., Bhat, T., Huynh, T., Kandare, E., Yuen, R., Wang, C. H., & John, S. (2018). Waste-derived low-cost mycelium composite construction materials with improved fire safety. *Fire and Materials*. *42*(7), 816–825. https://doi.org/10.1002/fam.2637

Jousse, F., Jongen, T., Agterof, W., Russell, S., & Braat, P. (2002). Simplified kinetic scheme of flavor formation by the Maillard reaction. *Journal of Food Science*, *67*(7), 2534–2542. https://doi.org/10.1111/j.1365-2621.2002.tb08772.x

Justo, A., & Hibbett, D. S. (2011). Phylogenetic classification of *Trametes* (basidiomycota, polyporales) based on a five-marker dataset. *Taxon*, *60*(6), 1567–1583. https://doi.org/10.1002/tax.606003

Kale, G., Auras, R., Singh, S. P., & Narayan, R. (2007). Biodegradability of polylactide bottles in real and simulated composting conditions. *Polymer Testing*, *26*(8), 1049–1061. https://doi.org/10.1016/j.polymertesting.2007.07.006

Kang, X., Kirui, A., Muszyński, A., Widanage, M. C. D., Chen, A., Azadi, P., … Wang, T. (2018). Molecular architecture of fungal cell walls revealed by solid-state NMR. *Nature Communications*, *9*(1), 2747. https://doi.org/10.1038/s41467-018-05199-0

Keshavarz, T., & Roy, I. (2010). Polyhydroxyalkanoates: bioplastics with a green agenda. *Current Opinion in Microbiology*, *13*(3), 321–326. https://doi.org/10.1016/j.mib.2010.02.006

Klis, F. M., Groot, P. De, & Hellingwerf, K. (2001). Molecular organization of the cell wall of *Candida albicans. Medical Mycology*, *39*(1), 1–8. https://doi.org/10.1080/mmy.39.1.1.8-0

Kothe, E. (2001). Mating-type genes for basidiomycete strain improvement in mushroom farming. *Applied Microbiology and Biotechnology*, *56*, 602–612. https://doi.org/10.1007/s002530100763

Kues, U., & Liu, Y. (2000). Fruiting body production in basidiomycetes. *Applied Microbiology and Biotechnology*, *54*(2), 141–152. https://doi.org/10.1007/s002530000396

Latgé, J. P. (2007). The cell wall: A carbohydrate armour for the fungal cell. *Molecular Microbiology*, *66*(2), 279–290. https://doi.org/10.1111/j.1365-2958.2007.05872.x

López-Nava, J. A., Méndez González, J., Ruelas Chacón, X., & Nájera Luna, J. A. (2016). Assessment of edible fungi and films bio-based material simulating expanded polystyrene. *Materials and Manufacturing Processes*, *31*(8), 1085–1090. https://doi.org/10.1080/10426914.2015.1070420

Lugones, L. G., De Jong, J. F., De Vries, O. M. H., Jalving, R., Dijksterhuis, J., & Wösten, H. A. B. (2004). The SC15 protein of *Schizophyllum commune* mediates formation of aerial hyphae and attachment in the absence of the SC3 hydrophobin. *Molecular Microbiology*, *53*(2), 707–716. https://doi.org/10.1111/j.1365-2958.2004.04187.x

Martins, S. I. F. ., Jongen, W. M. ., & van Boekel, M. A. J. . (2001). A review of Maillard reaction in food and implications to kinetic modelling. *Trends in Food Science & Technology*, *11*, 364–373. https://doi.org/10.1016/S0924-2244(01)00022-X

Melero, J. A., Iglesias, J., & Garcia, A. (2012). Biomass as renewable feedstock in standard refinery units. Feasibility, opportunities and challenges. *Energy and Environmental Science*, *5*(6), 7393–7420. https://doi.org/10.1039/c2ee21231e

Mohanty, A. K., Misra, M., & Drzal, L. T. (2002). Sustainable Bio-Composites from Renewable Resources: Opportunities and Challenges in the Green Materials World. *Journal of Polymers and the Environment*, *10*(1), 19–26. https://doi.org/10.1023/A:1021013921916

Morris, G. A., & Freeman, R. (1979, January). Enhancement of Nuclear Magnetic Resonance Signals by Polarization Transfer. *Journal of the American Chemical Society*, *101*(3), 760–762. https://doi.org/10.1021/ja00497a058

Naumann, A. (2009). A novel procedure for strain classification of fungal mycelium by cluster and artificial neural network analysis of Fourier transform infrared (FTIR) spectra. *Analyst*, *134*(6), 1215–1223. https://doi.org/10.1039/b821286d

Nevalainen, K. H., Te'o, V. S., Penttilä, M., & Pakula, T. (2005). Heterologous gene expression in filamentous fungi: A holistic view. In *Applied Mycology and Biotechnology*, *5*, 211–237. https://doi.org/10.1016/S1874-5334(05)80011-5

Oerke, E. C. (2006). Crop losses to pests. *The Journal of Agricultural Science, 144*(1), 31–43. https://doi.org/10.1017/S0021859605005708

Ohm, R. A., De Jong, J. F., Lugones, L. G., Aerts, A., Kothe, E., Stajich, J. E., … Wösten, H. A. B. (2010). Genome sequence of the model mushroom *Schizophyllum commune*. *Nature Biotechnology*, *28*(9), 957–963. https://doi.org/10.1038/nbt.1643

Ohm, R. A., Riley, R., Salamov, A., Min, B., Choi, I. G., & Grigoriev, I. V. (2014). Genomics of wood-degrading fungi. *Fungal Genetics and Biology*, *72*, 82–90. https://doi.org/10.1016/j.fgb.2014.05.001

Parisi, M. L., Fatarella, E., Spinelli, D., Pogni, R., & Basosi, R. (2015). Environmental impact assessment of an eco-efficient production for coloured textiles. *Journal of Cleaner Production*, *108*, 514–524. https://doi.org/10.1016/j.jclepro.2015.06.032

Paul, E. A. (2015). *Soil microbiology, ecology, and biochemistry*. Cambridge, MA, Elsevier Academic Press.

Pegler, D. N. (1996). Hyphal analysis of basidiomata. *Mycological Research*, *100*(2), 129–142. https://doi.org/10.1016/S0953-7562(96)80111-0

Pelletier, M. G., Holt, G. A., Wanjura, J. D., Lara, A. J., Tapia-Carillo, A., McIntyre, G., & Bayer, E. (2013). An evaluation study of pressure-compressed acoustic absorbers grown on agricultural by-products. *Industrial Crops and Products*, *95*, 342–347. https://doi.org/10.1016/j.indcrop.2016.10.042

Powrie, W. D., Wu, C. H., & Molund, V. P. (1986). Browning reaction systems as sources of mutagens and antimutagens. *Environmental Health Perspectives*, *67*, 47–54. https://doi.org/10.1289/ehp.866747

Przekora, A., Palka, K., & Ginalska, G. (2016). Biomedical potential of chitosan/HA and chitosan/β-1,3-glucan/HA biomaterials as scaffolds for bone regeneration — A comparative study. *Materials Science & Engineering*, *58*, 891–899. https://doi.org/10.1016/j.msec.2015.09.046

Renault, M., Tommassen-van Boxtel, R., Bos, M. P., Post, J. A., Tommassen, J., & Baldus, M. (2012). Cellular solid-state nuclear magnetic resonance spectroscopy. *Proceedings of the National Academy of Sciences*, *109*(13), 4863–4868. https://doi.org/10.1073/PNAS.1116478109

Revel, M., Châtel, A., & Mouneyrac, C. (2018). Micro(nano)plastics: A threat to human health? *Current Opinion in Environmental Science & Health*, *1*, 17–23. https://doi.org/10.1016/J.COESH.2017.10.003

Riley, R., Salamov, A. A., Brown, D. W., Nagy, L. G., Floudas, D., Held, B. W., … Grigoriev, I. V. (2014). Extensive sampling of basidiomycete genomes demonstrates inadequacy of the white-rot/brown-rot paradigm for wood decay fungi. *Proceedings of the National Academy of Sciences of the United States of America*, *111*(27), 9923–9928. https://doi.org/10.1073/pnas.1400592111

Sánchez, C. (2008). Lignocellulosic residues: Biodegradation and bioconversion by fungi. *Biotechnology Advances*, *27*, 185–194. https://doi.org/10.1016/j.biotechadv.2008.11.001

Sannigrahi, P., Pu, Y., & Ragauskas, A. (2010). Cellulosic biorefineries-unleashing lignin opportunities. *Current Opinion in Environmental Sustainability*, *2*, 383–393. https://doi.org/10.1016/j.cosust.2010.09.004

Sarrouh, B., Santos, T. M., Miyoshi, A., Dias, R., & Azevedo, V. (2012). Up-to-date insight on industrial enzymes applications and global market. *Journal of Bioprocessing & Biotechniques S*, *4*(002). https://doi.org/10.4172/2155-9821.S4-002

Schneider, C. A., Rasband, W. S., & Eliceiri, K. W. (2012). NIH Image to ImageJ: 25 years of image analysis. *Nature Methods*, *9*(7), 671–675. https://doi.org/10.1038/nmeth.2089

Shaka, A., Keeler, J., & Freeman, R. (1983). Evaluation of a new broadband decoupling sequence: WALTZ-16. *Journal of Magnetic Resonance (1969)*, *53*(2), 313–340. https://doi.org/10.1016/0022-2364(83)90035-5

Sietsma, J. H., Rast, D., & Wessels, J. G. H. (1977). The effect of carbon dioxide on fruiting and on the degradation of a cell-wall glucan in *Schizophyllum commune*. *Journal of General Microbiology*, *102*(2), 385–389. https://doi.org/10.1099/00221287-102-2-385

Sietsma, J. H., & Wessels, J. G. H. (1977). Chemical analysis of the hyphal walls of *Schizophyllum commune*. *BBA - General Subjects*, *496*(1), 225–239. https://doi.org/10.1016/0304-4165(77)90131-3

Sietsma, J. H., & Wessels, J. G. H. (1979). Evidence for covalent linkages between chitin and β-glucan in a fungal wall. *Microbiology*, *114*(1), 99–108.

Sietsma, J. H., & Wessels, J. G. H. (1981). Solubility of (1-3)-β-D/(1-6)-β-D-glucan in fungal walls: Importance of presumed linkage between glucan and chitin. *Microbiology*. *125*(1), 209-212.

Smith, M. L., Bruhn, J. N., & Anderson, J. B. (1992) The fungus *Armillaria bulbosa* is among the largest and oldest living organisms. *Nature, 356*(6368), 428.

Song, J. H., Murphy, R. J., Narayan, R., & Davies, G. B. H. (2009). Biodegradable and compostable alternatives to conventional plastics. *Philosophical Transactions of the Royal Society B: Biological Sciences*, *364*(1526), 2127–2139. https://doi.org/10.1098/rstb.2008.0289

Sonnenberg, A. S. M., Sietsma, J. H., & Wessels, J. G. H. (1982). Biosynthesis of alkali-insoluble cell-wall glucan in *Schizophyllum commune* protoplasts. *Microbiology*, *128*(11), 2667–2674. https://doi.org/10.1099/00221287-128-11-2667

Editiorial Nature Microbiology. (2017). *Nature Microbiology*, *2*(8), 17120. https://doi.org/10.1038/nmicrobiol.2017.120

Thompson, R. C., Moore, C. J., Saal, F. S. V., & Swan, S. H. (2009). Plastics, the environment and human health: Current consensus and future trends. *Philosophical Transactions of the Royal Society B: Biological Sciences*, *364*(1526), 2153–2166. https://doi.org/10.1098/rstb.2009.0053

Tokiwa, Y., Calabia, B., Ugwu, C., Aiba, S., Tokiwa, Y., Calabia, B. P., … Aiba, S. (2009). Biodegradability of Plastics. *International Journal of Molecular Sciences*, *10*(9), 3722–3742. https://doi.org/10.3390/ijms10093722

Van Boekel, M. A. J. S. (2006). Formation of flavour compounds in the Maillard reaction. *Biotechnology Advances*, *24*(2), 230–233. https://doi.org/10.1016/j.biotechadv.2005.11.004

van der Mei, H. C., Bos, R., & Busscher, H. J. (1998). A reference guide to microbial cell surface hydrophobicity based on contact angles. *Colloids and Surfaces B: Biointerfaces*, *11*(4), 213–221. https://doi.org/10.1016/S0927-7765(98)00037-X

van der Valk, P., Marchant, R., & Wessels, J. G. H.(1977). Ultrastructural localization of polysaccharides in the wall and septum of the basidiomycete *Schizophyllum commune*. *Experimental Mycology*, *1*(1), 69-82.

van Peer, A. F., De Bekker, C., Vinck, A., Wösten, H. A. B., & Lugones, L. G. (2009). Phleomycin increases transformation efficiency and promotes single integrations in *Schizophyllum commune*. *Applied and Environmental Microbiology*, *75*(5), 1243–1247. https://doi.org/10.1128/AEM.02162-08

van Wetter, M. A., Wösten, H. A. B., Sietsma, J. H., & Wessels, J. G. H. (2000). Hydrophobin gene expression affects hyphal wall composition in *Schizophyllum commune*. *Fungal Genetics and Biology*, *31*(2), 99–104. https://doi.org/10.1006/fgbi.2000.1231

Vert, M., Doi, Y., Hellwich, K.H., Hess, M., Hodge, P., Kubisa, P., … Schué, F. (2012). Terminology for biorelated polymers and applications (IUPAC Recommendations 2012). *Pure and Applied Chemistry*, *84*(2), 377–410. https://doi.org/10.1351/PAC-REC-10-12-04

Vezzoli, C. (2013). The “Material” Side of Design for Sustainability. In: *Materials Experience: Fundamentals of Materials and Design*, 105–121. https://doi.org/10.1016/B978-0-08-099359-1.00008-4

Vieira, M. G. A., Da Silva, M. A., Dos Santos, L. O., & Beppu, M. M. (2011). Natural-based plasticizers and biopolymer films: A review. *European Polymer Journal*, *47*(3), 254–263. https://doi.org/10.1016/j.eurpolymj.2010.12.011

Wasser, S. (2003). Medicinal mushrooms as a source of antitumor and immunomodulating polysaccharides. *Applied Microbiology and Biotechnology*, *60*(3), 258–274. https://doi.org/10.1007/s00253-002-1076-7

Weingarth, M., & Baldus, M. (2013). Solid-State NMR-Based Approaches for Supramolecular Structure Elucidation. *Accounts of Chemical Research*, *46*(9), 2037–2046. https://doi.org/10.1021/ar300316e

Weingarth, M., Bodenhausen, G., & Tekely, P. (2010). Broadband magnetization transfer using moderate radio-frequency fields for NMR with very high static fields and spinning speeds. *Chemical Physics Letters*, *488*(1–3), 10–16. https://doi.org/10.1016/J.CPLETT.2010.01.072

Wösten, H. A. B., de Vries, O. M. H., & Wessels, J. G. H. (1993). Interfacial Self-Assembly of a Fungal Hydrophobin into a Hydrophobic Rodlet Layer. *The Plant Cell*, *5*(11), 1567. https://doi.org/10.2307/3869739

Wösten, H A B. (2019). Filamentous fungi for the production of enzymes, chemicals and materials. *Current Opinion in Biotechnology*, Vol. 59, pp. 65–70. https://doi.org/10.1016/j.copbio.2019.02.010

Wösten, H. A. B., Asgeirsdóttir, S. A., Krook, J. H., Drenth, J., & Wessels, J. G. H. (1994). The fungal hydrophobin Sc3p self-assembles at the surface of aerial hyphae as a protein membrane constituting the hydrophobic rodlet layer. *European Journal of Cell Biology*, *63*(1), 122–129. Retrieved from https://europepmc.org/abstract/med/8005099

Wösten, H. A. B., Schuren, F. H., & Wessels, J. G. H. (1994). Interfacial self-assembly of a hydrophobin into an amphipathic protein membrane mediates fungal attachment to hydrophobic surfaces. *The EMBO Journal*, *13*(24), 5848–5854. https://doi.org/10.1002/j.1460-2075.1994.tb06929.x

Wösten, Han A. B., & Scholtmeijer, K. (2015). Applications of hydrophobins: current state and perspectives. *Applied Microbiology and Biotechnology*, Vol. 99, pp. 1587–1597. https://doi.org/10.1007/s00253-014-6319-x

Wösten, H. A. B.(2001). Hydrophobins: multipurpose proteins. *Annual Reviews in Microbiology*, *55*(1), 625-646. https://doi.org/10.1146/annurev.micro.55.1.625

Wösten, H. A. B., Van Wetter, M. A., Lugones, L. G., Van der Mei, H. C., Busscher, H. J., & Wessels, J. G. H. (1999). How a fungus escapes the water to grow into the air. *Current Biology*, *9*(2), 85–88. https://doi.org/10.1016/S0960-9822(99)80019-0

Wu, J. Z., Cheung, P. C. K., Wong, K. H., & Huang, N. L. (2003). Studies on submerged fermentation of *Pleurotus tuber-regium* (Fr.) Singer - Part 1: Physical and chemical factors affecting the rate of mycelial growth and bioconversion efficiency. *Food Chemistry*, *81*(3), 389–393. https://doi.org/10.1016/S0308-8146(02)00457-0

Yang, Q., Dou, F., Liang, B., & Shen, Q. (2005). Studies of cross-linking reaction on chitosan fiber with glyoxal. *Carbohydrate Polymers*, *59*(2), 205–210. https://doi.org/10.1016/j.carbpol.2004.09.013

Yang, Z., Zhang, F., Still, B., White, M., & Amstislavski, P. (2017). Physical and mechanical properties of fungal mycelium-based biofoam. *Journal of Materials in Civil Engineering*, *29*(7), 04017030. https://doi.org/10.1061/(asce)mt.1943-5533.0001866

Zabalza Bribián, I., Aranda Usón, A., & Scarpellini, S. (2009). Life cycle assessment in buildings: State-of-the-art and simplified LCA methodology as a complement for building certification. *Building and Environment*, *44*(12), 2510–2520. https://doi.org/10.1016/j.buildenv.2009.05.001

Zhang, M., Cui, S. W., Cheung, P. C. K., & Wang, Q. (2007). Antitumor polysaccharides from mushrooms: a review on their isolation process, structural characteristics and antitumor activity. *Trends in Food Science & Technology*, *18*(1), 4–19. https://doi.org/10.1016/J.TIFS.2006.07.013

Ziegler, A. R., Bajwa, S. G., Holt, G. A., McIntyre, G., & Bajwa, D. S. (2016). Evaluation of physico-mechanical properties of mycelium reinforced green biocomposites made from cellulosic fibers. *Applied Engineering in Agriculture*, *32*(6), 931–938. https://doi.org/10.13031/aea.32.11830

Nederlandse Samenvatting en Discussie

Het lineaire consumptiepatroon waarop onze economie grotendeels is gebaseerd veronderstelt een overvloed aan grondstoffen en onbeperkte capaciteit voor afvalverwijdering. De intrinsieke niet-duurzaamheid van dit model vereist de ontwikkeling van duurzame, circulaire alternatieven. Hernieuwbare grondstoffen en biologische afbreekbaarheid zijn twee belangrijke factoren bij circulaire productie. Mycelium van schimmels is een voorbeeld van een hernieuwbare grondstof die gebruikt kan worden bij de productie van biobased materialen.

Schimmels komen overal voor en hebben een belangrijke rol in de natuur en voor de mensheid. Voor hun groei breken deze micro-organismen dood organisch materiaal af of hebben ze een symbiotische relatie met planten, dieren of andere microben. Filamenteuze schimmels koloniseren substraten door middel van mm- tot cm-lange hyfen met een diameter tussen 1-10 µm. Deze hyfen groeien aan hun top en vertakken meer naar achteren waardoor een 3D-netwerk wordt gevormd dat mycelium wordt genoemd. Dit mycelium varieert in grootte van sub-millimeter tot kilometer-afmetingen. Sommige paddenstoelvormende schimmels hebben zich gespecialiseerd in de afbraak van plantaardig afval zoals de agrarische afvalstromen stro en zaagsel. Deze schimmels kunnen deze afvalstromen upgraden door ze te koloniseren en er zodoende een materiaal van te vormen.

Mycelium gebaseerde materialen kunnen bestaan uit puur mycelium of uit een composiet welke gevormd wordt door een combinatie van mycelium en een ander materiaal zoals stro. Puur mycelium kan worden gebruikt als vervanging van leer of textiel, terwijl mycelium composieten zijn ontwikkeld voor gebruik als verpakking, isolatie en bouwmaterialen.

Het doel van dit proefschrift was om de kennis over materialen op basis van mycelium te verbeteren. Dit werd bereikt door het bestuderen van de impact van schimmelsoorten, substraten, groeiomstandigheden, genetische modificatie en fysische en chemische behandelingen op materiaaleigenschappen van pure en composiet myceliummaterialen.

Pure mycelium-materialen

Pure myceliummaterialen werden geproduceerd door schimmels in stilstaand of geschudde vloeistof te kweken (Hoofdstuk 4 & 5). Gedroogde films van dit materiaal vertoonden vergelijkbare eigenschappen met betrekking tot elasticiteit, ultieme treksterkte en rek bij breuk en waren vergelijkbaar met materialen uit de groep van natuurlijke materialen zoals leer.

Stilstaande vloeibare cultures van de paddenstoelvormende schimmel het waaiertje (*Schizophyllum commune)* en de *sc3*-hydrofobine deletiestam werden in het licht of in het donker gekweekt (Hoofdstuk 4). Het veranderen van groei in atmosferische concentraties CO_2 (400 ppm) naar hoog CO_2 (70.000 ppm) in het donker resulteerde in mycelium films met verhoogde elasticiteit. De elasticiteit nam echter af wanneer CO_2 concentraties toenamen wanneer het mycelium in het licht werd gegroeid. Deletie van sc3 resulteerde daarbij in een >2-voudige toename van materiaalstijfheid in vergelijking met wildtype *S. commune*, ongeacht de groeiomstandigheden. Aanvankelijk werd verondersteld dat deze verschillen werden veroorzaakt door verschillen in de chemische samenstelling van de celwand, echter, onderzoek toonde aan dat het de dichtheid was die correleerde met de elasticiteit en sterkte van het materiaal.

De groei van stilstaande vloeibare culturen is arbeidsintensief en moeilijk om op te schalen. Als alternatief werden vloeibare schudculturen gebruikt om biomassa te produceren (Hoofdstuk 5). Het onbehandelde mycelium uit vloeibare schudculturen was bros en werd daarom behandeld met de weekmaker glycerol. Dit leidde tot verhoging van de elasticiteit, verminderde treksterkte en verhoogde rek bij breuk. De elasticiteit en dichtheid kwamen overeen met die van polymeer-achtige materialen zoals plastics (concentratie van glycerol tot 8%) of zelfs van elastomeren zoals rubber (concentratie van glycerol ≥16%). Door verschillende groeimethoden, kweekomstandigheden en nabewerking te variëren of genetische modificatie toe te passen werden dus een reeks myceliummaterialen verkregen met eigenschappen die vergelijkbaar zijn met natuurlijke materialen, polymeerachtige materialen en elastomeren.

De celwand van filamenteuze schimmels zorgt voor mechanische sterkte en bescherming tegen (a)biotische factoren. Studies hebben aangetoond dat de celwand tot wel 25% van het drooggewicht van een schimmel kan uitmaken. Het feit dat de celwand de mechanische sterkte bepaalt van de schimmeldraden impliceert dat het ook van belang is voor de materiaaleigenschappen van myceliummateriaal. Om de chemische samenstelling van de celwand van *S. commune* te bepalen werd gebruik gemaakt van solid-state Nuclear Magnetic Resonance (ssNMR). Hiermee is het mogelijk om te kijken naar zowel flexibele als rigide celwandcomponenten in een intact systeem zoals mycelium. Dit intacte materiaal werd vervolgens een aantal keer geëxtraheerd om een dieper inzicht in de architectuur van de celwand te krijgen. Het onderzoek heeft sterke aanwijzingen gegeven dat het flexibele deel van de celwand bestaat uit β-(1,3)-glucaan, β-(1,3-1,6)-glucaan, α-(1,4)-glucaan en homo- of heteropolymere mannose, terwijl het rigide deel bestaat uit chitine, β-(1,3)-glucaan, β-(1,3)(1,6)-glucaan, α-(1,3)-glucaan en homo- of heteropolymere fucose. Deze resultaten geven een nieuw inzicht in de celwandsamenstelling van het waaiertje en zijn de basis voor het begrip tussen samenstelling en materiaaleigenschappen van het mycelium.

Composiet mycelium-materialen

Hoofdstuk 2 concentreerde zich op composietmaterialen geproduceerd door *Pleurotus ostreatus* (de osterzwam) en *Trametes versicolor* (het elfenbankje). Deze schimmels werden gekweekt op beukenzaagsel, koolzaadstro en katoenafval. De combinatie van schimmel en substraat beïnvloedde de materiaaleigenschappen. Bijvoorbeeld, materiaal resulterend van groei van *T. versicolor* op beukenzaagsel was het minst elastisch terwijl de ultieme treksterkte vergelijkbaar was met dezelfde schimmel gegroeid op koolzaadstro. Het persen met hitte had de grootste invloed op de mechanische prestaties van de materialen en resulteerde in een >3-voudige toename van de dichtheid voor *T. versicolor* gegroeid op koolzaadstro en *P. ostreatus* gegroeid op koolzaadstro en katoenafval. Door met hitte te persen verbeterde homogeniteit, stijfheid en ultieme treksterkte van de materialen. Hierdoor verschoven de prestaties van de materialen van schuimachtig (denk aan piepschuim) naar natuurlijk (denk aan kurk).

Er was geen verband tussen waterabsorptie en het type schimmel, substraat of manier van persen om een materiaal te produceren. Na het plaatsen van verschillende materialen op water varieerde gewichtstoename tussen 43% voor niet geperste *T. versicolor* op beukenzaagsel tot 508% voor niet-geperst *P. ostreatus* gegroeid op katoen. Deze bevindingen impliceren de noodzaak van een coating bij gebruik in een vochtige omgeving.

Negen soorten hout-afbrekende schimmels werden geïsoleerd uit de natuur nabij Utrecht Science Park om vervolgens te screenen op groei voor de ontwikkeling van biobased materialen. Om groei te kwantificeren werd een methode ontwikkeld gebruikmakend van CO_2-productie als proxy voor de activiteit van mycelium. Visuele inspectie van schimmelgroei aan de oppervlakte van de culturen correleerde met CO_2-productie. Sommige soorten (*S. commune* en *Bjerkandera adusta*) bleken relatief snel het substraat te koloniseren, echter leek groei ook snel af te nemen. Andere soorten (*Trametes hirsuta* en *Lenzites betulina*) hadden meer tijd nodig te hebben om in hun exponentiele groeifase te komen, echter deze schimmels produceerden uiteindelijk meer CO_2. Visuele inspectie toonde aan dat deze soorten inderdaad een hogere dichtheid mycelium in het substraat hadden geproduceerd in vergelijking met de snel koloniserende stammen.

Zes van de negen natuurlijke isolaten werden met hitte geperst na een groeiperiode van 4 weken, waarna de mechanische eigenschappen werden geanalyseerd. De meest rigide en sterke materialen waren afkomstig van de stammen die ook de meeste CO_2 produceerden (*T. hirsuta*, *L. betulina* en *B. adusta*). Hiervan is *B. adusta* uiteindelijk het meest interessant voor het produceren van materialen vanwege de snelheid van kolonisatie en de laagste CO_2 productie. Samengevat bepalen, ook in het geval van de composietmaterialen, het type schimmel, substraat, groeiomstandigheden en behandeling de eigenschappen van het myceliummateriaal.

Conclusies

Schimmels kunnen worden gebruikt om materialen te maken die bij kunnen dragen aan de transitie naar een duurzame economie. We hebben materialen geproduceerd van puur mycelium die materialen kunnen vervangen die een negatieve voetafdruk op

onze aarde hebben, zoals leer en textiel. Daarnaast zijn er composietmaterialen geproduceerd met eigenschappen die vergelijkbaar zijn met schuimen en natuurlijke materialen. De schuimachtige materialen kunnen dienen als isolatiemateriaal. Natuurlijke materiaalachtige materialen kunnen spaanplaten vervangen, zoals *oriented strand board* (OSB) en *medium-density fiberboard* (MDF), die vaak giftige stoffen bevatten zoals formaldehyde.

Naast deze alledaagse materialen kunnen schimmels worden gebruikt om functionele materialen te produceren. Schimmels die bijvoorbeeld plantengroei bevorderen kunnen worden gebruikt om plantenpotten te maken. Zaailingen kunnen met deze ‘slimme’ pot worden gepland, waardoor een groeistimulerende omgeving voor de plant wordt gecreëerd. Een ander voorbeeld van een slimme toepassing is het gebruiken van composiet materialen als isolatiemateriaal. Wanneer geplaatst in het interieur van gebouwen, heeft de open structuur van het mycelium als toegevoegde waarde vanwege zijn uitzonderlijke geluidsabsorberende eigenschappen.

Meer onderzoek is nodig om toepassing van deze materialen mogelijk te maken in ons dagelijks leven. Dit onderzoek moet gericht zijn op soorten, groeiomstandigheden, substraten en nabewerkingstechnieken. Samenwerking met experts op het gebied van chemie, materiaalkunde, ontwerp en productontwikkeling zal leiden tot verbeterde toepasbaarheid van schimmelmaterialen. Dit zal het mogelijk moeten maken om steeds meer niet-duurzame materialen zoals conventionele kunststoffen en rubbers te vervangen of zelfs materialen te ontwikkelen met eigenschappen die nu nog niet beschikbaar zijn.

Curriculum vitae

Freek V.W. Appels

Freek Appels was born on September 15th, 1989 in Veldhoven, The Netherlands. He followed his secondary education at the Koning Willem II College in Tilburg, The Netherlands. September 2010, he started his Bachelor Biology at Utrecht University, followed by a Master in Environmental Biology at the same University. As part of his studies, Freek completed two research internships at Utrecht University. During his first internship Freek studied the hormonal crosstalk between plants and fungi in the Plant-Microbe Interactions group of the Department of Biology under the supervision of Dr. A. Martínez-Medina and Dr. S.C.M. van Wees. Freek studied the use of fungal mycelium for the production of bio-based materials during his second internship in the Molecular Microbiology group under the supervision of Dr. P. Krijgsheld and Prof. Dr. H.A.B. Wösten. Freek obtained his MSc diploma August 2015 and started his PhD project on mycelium materials September 2015, supervised by Prof. Dr. H.A.B. Wösten. Freek was a member of the PhD council of the Institute of Environmental Biology in the period 2016–2019 and is a board member of the Dutch Biotechnology Association (NBV) since 2017. Freek has now a postdoctoral researcher position in the group of Prof. Dr. H.A.B. Wösten where he continues developing bio-based fungal materials.

List of publications

Martínez-Medina, A., **Appels, F. V. W.**, & van Wees, S. C. M. (2017). Impact of salicylic acid-and jasmonic acid-regulated defences on root colonization by *Trichoderma harzianum* T-78. *Plant signaling & behavior*, *12*(8), e1345404.

Appels, F. V. W., Dijksterhuis, J., Lukasiewicz, C. E., Jansen, K. M., Wösten, H. A. B., & Krijgsheld, P. (2018). Hydrophobin gene deletion and environmental growth conditions impact mechanical properties of mycelium by affecting the density of the material. *Scientific reports*, *8*(1), 4703.

Appels, F. V. W., Camere, S., Montalti, M., Karana, E., Jansen, K. M., Dijksterhuis, J., ... & Wösten, H. A. B. (2019). Fabrication factors influencing mechanical, moisture-and water-related properties of mycelium-based composites. *Materials & Design*, *161*, 64-71.

Acknowledgements

Een promotietraject uitvoeren duurt in theorie 4 jaar. In deze 4 jaar word je geacht onderzoek te doen naar een bepaald onderwerp. Bevindingen dienen op een wetenschappelijk verantwoorde manier te worden gecommuniceerd naar derden. Dit geschiedt normaliter via een bundel van bevindingen. De bundel van deze bevindingen vormt samen met een inleiding en een discussie het proefschrift. De thesis. Het meest gelezen onderdeel van theses zijn echter niet de wetenschappelijke bevindingen maar de acknowledgements. Het deel waar een ieder zoekt naar zijn of haar naam alvorens te lezen wat er over anderen geschreven is. Dit gegeven wil ik nemen als leidraad voor het schrijven van dit laatst geschreven onderdeel van mijn thesis. Namelijk; het laat de menselijkheid zien van ons zijn. In de essentie niet de onderzoekende die wilt weten uit welke moleculen een schimmel bestaat, maar de persoon die gedijt door liefde en erkenning. Niet 8 uur maar 24 uur per dag. Het is tijd om geen verhalen over ß-1,3-glucan te prediken maar verhalen die blijk geven van liefde en vriendschap. Want dat is waar het om gaat. Ama et Fac Quod Vis. En ja **Brigit**; het is een vrijdag.

Han, bedankt. Ik had me geen betere patron durven wensen. Ik heb diepgaande respect voor de manier waarop jij omgaat met jouw medemens. De rust en warmte die straal je uit, ondanks de enorme hoeveelheid werk die je verricht. Je houdt dit bij jezelf en verwacht dit niet van anderen. Het maakt het lastig om nee tegen je te zeggen, enfin. Je bent iemand waarbij het fijn is om in de buurt te zijn, ook als het over werk gaat. Het is een voorrecht om jou als baas te hebben gehad. Door jouw colleges van eukaryote microbiologie ben ik mijn bachelorstage gaan doen bij microbiologie. Kijk waar we nu staan. Dankjewel voor de academische opvoeding. Nog meer bedankt voor de rest (zoals de medefinanciering van de wijnavonden). Ik zal je missen.

Die bachelor stage deed ik onder LGL. **Luis**, ook jou vind ik een erg bijzonder persoon (in de positieve zin van het woord). En ook dat heeft te maken met de manier hoe je met andere mensen om gaat. Ik heb je nog nooit onderscheidt zien maken tussen student, medewerker, schoonmaker et cetera. Je luistert en staat open voor ideeën van een ieder. Ik heb genoten van onze amicale gesprekken. De professionele

gesprekken waren wat moeilijker om van te genieten maar dat maakt niet uit. Jij kon op die manier wel je gedachten ordenen.

Dankjewel **Pauline** voor het begeleiden van mij vanaf den beginne. Het is altijd weer leuk om even bij te praten. Echter, we zien elkaar niet meer zoveel.
Wieke bedankt voor alle krantenknipsels en andere meebrengsels. Je bent de meest attente persoon die ik ken op het lab. Alhoewel **Inge**, jij komt erbij in de buurt. Inge het was op het begin even wennen vanuit Heineken om hier bij micro te beginnen. Ik durf te zeggen dat ik een erg bijzondere vriendschappelijke band met je op heb mogen bouwen de afgelopen jaren. Dank voor je luisterend oor en je gaat het rocken de rest van je PhD. **Maarten** ook jij bedankt voor al je hulp. Als ik advies nodig had over figuren of een script dan stond je er meteen; super! **Ioana** I want to thank you for your company the last years. Multzumesc for mirroring my behavior from time to time and always being upright. You are the most honest person I met in the lab over the years. Besides, thank you for loving my daughter Sam so much. I know you want to eat her up; please do not. Peter-Jan. **Petertje** petertje petertje. What shall I write about you. What can I write about you. Maybe nothing. Thanks for the laughs. Thanks for the Jiskefet moments. You are a good scientist and a good person, believe in yourself.

Ivan Amigo. Gracias por mi apprendros espagnol con un vraimente Colombiano! Gracias por la circles with fingers. Los conversationes. Tengo un mico en mi cuello. Gracias por todos. Ik kan ook gewoon in het Nederlands praten aangezien jij gewoon een Nederlander bent. Zo ook jij Natalia. **DJ Escobar**. Thanks for all the invitations to your parties.

Martin succes met het nieuwe project! Het lijkt erop dat je vol enthousiasme aan de slag gaat, mooi om te zien dat het in goede handen achter blijft. Houdt vol. **Jun**, ni hao ma, fe yong how. 很抱歉吃了你所有的糖果. The same goes for you **Xiahao**. You are funny. Always lauging. Keep up the yellow jersey. **Maryam**, also you are so friendly. Always smiling. گذارم می احترام دادید انجام که هایی انتخاب برای شما به من .کنید می گریه داخل وقتی حتی .هستید فارسی شما .میشی خوب.. **Juan** el Mexicano, gracias por el fungi muy bien.
Esther, ouwe fietskameraad. Ik hoop dat je niet te hard aan je FTP werkt. Het voelt het alsof jij wat dat betreft meer aan het groeien bent dan ik. Laten we nog een keer samen gaan fietsen. Dan nemen we ook **Koen** de champignonman mee. **Robert-Jan**

ook jij bedankt voor je extreem vriendelijke persoonlijkheid. En bedankt voor de wine tastings en het gedurende deze aangename bijeenkomsten overbrengen van de nodige knowhow. Het is altijd een plezier om met je te converseren. Brigit. **Brie**. Lachende Brigit met haar afvalwater. Mooi om te zien hoe jij bent gegroeid vanuit je master naar een coördinerend orgaan binnen microbiologie. Van brie met de bril naar bij **Eric**. Rustig Eric. Zo kan ik niet met je werken. Succes met je PhD. Dankjewel voor mij opvangen in Berlijn. **David** je bent al een tijdje weg toch was je er al die tijd. Ik hoop dat het je goed gaat. **Hans**, **Margot** en **Robin** ook jullie bedankt. De samenwerking was niet heel intens toch hebben wij ook zo onze momenten mogen beleven. Mooi om te zien **Robin** hoe hard jouw groep groeit en de kwaliteit van de wetenschap aldaar. Dank voor je increasingly tasty IPAs.

Van schimmels naar bacteriën. **Jésus** (muchos buenos) en **Eline**, succes met de bacvacs! Ik hoop ooit wat van jullie creatie geïnjecteerd te krijgen (of mijn ongeboren kind, ik weet niet wanneer jullie spul precies toegediend dient te worden). **Jan** en **Ria**, we hebben het een aantal keer gezellig gehad tijdens kerstdiners. Dank voor de wijn!

De rest van het lab, Ria Kas bedankt. Alle studenten die ik heb mogen begeleiden; **Pieter, Denise, Franco, Amy, Anne, Edwin, Jeroen, Sigrid, Jara, Vadim, Ward, Anwen, Anik** and all other students. I have learned bigtime from supervising all of you and all-in different ways

People from the PhD council, **Laura, Gilles, Tom, Simone, Marciel.** Also **Saskia** from PMI, you kind of launched me into science. It is nice to see that there are such nice people around.

Niet te vergeten zijn natuurlijk de mensen die van onschatbare waarde zijn, van de ‘keuken’. **Nadia**, والنادر الخاص ولطفك اللطيفة المحادثات على شكرا. **Mohammed**, **Erwin**, **Jan** en **Nebal** dank voor al jullie hulp!

Fungal pleasure. **Thies**, **Aurin**, **Jordi** and **Brand**. You guys shined light over the beginning of my PhD. And then you left (except you Aurin, you stayed). We have had awesome times… It was sad to see you leave. But luckily we are still together. With **Jerre** nowadays. But as people go people come. So there was **Jordi** again. Jordi,

special thanks to you for being back. I really appreciate our valuable contact. You have been important to me the last period.

Les connaisseurs de vin(o). Guys. Grazie mille por tutti! **Antonio**, **Auke** (and **Robert-Jan** and **Koen** but you were mentioned already). The wine evenings we have outside of the lab are great. Even greater for the Dutch economy. I think I am getting spoiled with the wines. But that is ok.

The people from NMR, first of all **Helena**. Helena we have been partners in crime. We laughed and we fought. It took some time (and still does) but in the end I think we can be proud. The hours that I spent on those NMR figures is crazy. Let' s wrap this up. Also **Klaartje**, **Marie** and **Marc**, thanks for all the help!

Maurizio grazie di tutto. Nonostante tutte le folle, sei sempre super gentile. All'inizio a volte pensavo che non fosse possibile, ma lo è davvero. Mi piace molto lavorare con te e sono anche contento della piacevole e calda connessione che siamo riusciti a costruire. E grazie per l'aiuto con la tesi sui funghi alla fine. Grazie.

Onderstaande drie groepen bevatten veel mensen die mijn leven hebben verrijkt over de jaren. Ik hoop dat een ieder zich aangesproken voelt die tot een van dezen behoort.

Vrienden van Biologie
Vrienden van Fietsen
Vrienden van Tilburg
Vrienden

Jan Verhallen †
Simone
Walter en Anton
Bertje Kocx
Flix
Flo
Tom
Niels

Conrad
Luuk
Daan

Love you all. Het kan niet op.

Fara SUPER bedankt voor het ontwerp van de cover. Ik ben er erg blij mee. Ik kan er naar blijven kijken en nieuwe dingen in blijven zien. Daarnaast ook voor al het andere. **Theo**, samen met Fara staan jullie altijd voor ons klaar, zo ervaar ik dat echt. En ook jullie **Frank** en **Shirin** en **Kian** natuurlijk! Ik voel me erg welkom bij jullie.

Papa, ik ben eindelijk klaar met studeren! Ik weet dat je trots bent. We hebben leuke momenten gehad hier in de kroeg in Utrecht, dat er vele keren bij mogen komen! **Pascale**, **Fiore** en **Sam** (leuke naam), kus voor jullie!

Mama, **Walter**, **Janneke**, **Jos**, **Dax**, **Bart**, **Daan** en **Inge**. Moeilijk. Ik ga onderaan beginnen.

Daan. Hermano. Brother. Broer(tje). Ich liebe dich. Thanks voor het checken van de spelling van dit stuk. You are getting old. Staying young. Je bent een prachtig mens. Je bent een prachtig koppel. Met **Inge**. Samen de wereld tegemoet. Goed om je in de familie te hebben Inge. Binnenkort trouwen. Fantastisch. Prachtig.

Bart. Hermano. Frère. Broer. Me gustas tu. Woorden schieten te kort. See you in Canada.

Janneke. Hermana. 姐姐. I love you. Je bent belangrijk voor me. Ook jij een prachtig mens. Dank voor je oor. Dank voor je raad. Heb jezelf lief. Met je prachtige zoon. En je prachtige man. **Jos**, ook goed om jou in de familie te hebben ouwe crosser. Last but not least; **Dax**!

Walter. Walther. **Waltherus**. Postzegelfanaat. Dankjewel voor alles Walter. Vroeger en nu. Het vissen en je liefde voor mama. Ik wilde zeggen: ‘Zullen we eens weer gaan

vissen?”. Ik denk dat ik het sneu vind tegenwoordig. Misschien moeten we gewoon nog een keer op wintersport. Het is goed om je om ons heen te hebben.

Mama. Mijn rots in de branding. Tranen in mijn ogen. Dankjewel voor alles. Dankjewel voor jouw zijn. Dankjewel voor het baren van mij. Dankjewel voor al jouw warme appeltaarten. Dankjewel voor al jouw warme knuffels. Dankjewel voor de warme bijzondere gesprekken die we hebben. Dankjewel voor mij altijd te laten zijn. Dankjewel voor jouw oneindige vertrouwen. De zielsverwantschap voorbij. Je bent geweldig. Ik hou van jou. Die ster en terug.

Lieve **Lis**. Wat een tijd hebben wij achter de rug. Van de Back & Fourth naar poepluiers. Lizzy ik ben zo blij met je. Zowel door het zijn van mijn vrouw (ja vrouw ja!) als door het zijn van de moeder van Sam (wat je verdomd goed doet; mag gezegd worden). Ik voel me sterk met jou aan mijn zij. Ik ontwikkel me in het samen zijn met jou. Wij ontwikkelen ons in ons samenzijn. Jouw steun. Jouw liefde. De meest bijzondere periode van mijn leven zijn wij aan het delen. De laatste periode van mijn promotietraject heeft in het teken gestaan van ons. Dit was belangrijker dan het werk dat in dit boekje beschreven staat. Next level. Je bent een prachtig mens. Dankjewel voor alles. Maar dan ook alles. Ik ben je zo dankbaar! Ik kan niet wachten op de toekomst. Ik hou van je. Die andere ster en terug.

Sam. Sam Fara. Sammie. Het is onvoorstelbaar hoeveel ik in de 6 maanden van jouw bestaan heb geleerd. Je laat me meer tot de kern van ons bestaan komen. Samen zijn en lief hebben. Niet rennen maar zitten. Je brengt rust. Ik heb je vanmorgen voor het eerst zelf om zien rollen. Groots. Dit soort dingen. Je brengt me de wereld. Next level. Het is fantastisch om jou te leren kennen. Ik hou van je. Die ster en terug.

I feel rich having all of you in my life.

With love.

Freek